KUVEMPU UNIVERSITY

"SYNTHESIS AND CHARACTERIZATION OF CERTAIN OXIDE AND OXYFLUORIDE GLASSES DOPED WITH RARE-EARTH IONS"

A Thesis Submitted to the Kuvempu University for the award of degree of

DOCTOR OF PHILOSOPHY

IN

PHYSICS

By

Mr. Basavaraj Gurav. M.Sc.,

Research Guide

Dr. Devidas G B.
M.Sc., M.Phil. Ph.D.
Associate Professor
Department of PG Studies and Research in Physics,
Kuvempu University

Department of PG Studies and Research in Physics,
Kuvempu University,
Jnana Sahyadri, Shankarghatta, - 577451,
Shivamogga District, Karnataka, INDIA.

2023

KUVEMPU UNIVERSITY

“SYNTHESIS AND CHARACTERIZATION OF CERTAIN OXIDE AND OXYFLUORIDE GLASSES DOPED WITH RARE-EARTH IONS”

A Thesis Submitted to the Kuvempu University for the award of degree of

DOCTOR OF PHILOSOPHY

IN

PHYSICS

By

Mr. Basavaraj Gurav. M.Sc.,

Research Guide

Dr. Devidas G B.
M.Sc., M.Phil. Ph.D.

Associate Professor

Department of PG Studies and Research in Physics,

Kuvempu University

Department of PG Studies and Research in Physics,

Kuvempu University,

Jnana Sahyadri, Shankarghatta, - 577451,

Shivamogga District, Karnataka, INDIA.

2023

Dedicated to my Mother

"Annapurna Gurav"

A Mother is more precious and valuable than all the riches in the world

Mr. Basavaraj Gurav
M.Sc.
Research Scholar
Reg No 584/2-4-2019
Department of PG Studies and
Research in Physics,
Jnana Sahyadri, Shankarghatta-577451,
Shivamogga, Karnataka, India.

DECLARATION

I hereby declare that the thesis entitled **"SYNTHESIS AND CHARACTERIZATIONS OF CERTAIN OXIDE AND OXYFLUORIDE GLASSES DOPED WITH RARE EARTH IONS"** submitted to the Kuvempu University, Jnana Sahyadri for the award of degree of **Doctor of Philosophy in Physics** is the result of original research work carried out by me in the Department of PG Studies and Research in Physics, Jnana Sahyadri, Shankarghatta. Under the constant support immense guidance of **Dr. Devidas G. B.** Associate Professor, Department of PG Studies and Research in Physics, Jnana Sahyadri, Shankarghatta.

I further declare that this work or any part of it has not been submitted to any other University /Institute or elsewhere by me or others for any degree or diploma

Basavaraj Gurav

Date: 17-04-2023

Place: Shankarghatta

Kuvempu University

Dr. Devidas G B.
M.Sc.M.Phil., Ph.D.
Associate Professor,
and Research Guide

Dept. of PG Studies and Research in Physics
Jnana Sahyadri, Shankarghatta-577451,
Shivamogga(D), Karnataka, India.
Mobile: 9902846372
E-mail: devidasgb02@gmail.com

CERTIFICATE

This is to certified that the thesis entitled **"SYNTHESIS AND CHARACTERIZATIONS OF CERTAIN OXIDE AND OXYFLUORIDE GLASSES DOPED WITH RARE-EARTH IONS"** submitted to the Kuvempu University, Jnana Sahyadri for the award of degree of **Doctor of Philosophy in Physics** is a Bonafide record of the research work done by **Mr. Basavaraj Gurav** in the Department of PG Studies and Research in Physics, under my supervision and guidance. I also certify that the thesis presents his independent, original investigations without forming previously part of the material for the award of any degree or diploma by any University or Examining body.

Dr. Devidas G B.
Dr. DEVIDAS G.B
M.Sc., M.Phil, Ph.
Associate Professor
Department of Physics,
Kuvempu University,
SHANKARAGHATTA - 577 451.
Shivamogga Dist. Karnataka. (Indi

Date: 17-04-2023

Place: Shankarghatta

Acknowledgements

It's my great pleasure and esteem gratitude to thank my beloved teacher and research supervisor **Dr. Devidas G B.** Associate Professor, Department of PG Studies and Research in Physics, Kuvempu University, Jnana Sahyadri, Shankarghatta for providing me an opportunity to work in his guidance and support in my research. I always feel happy and it's my privilege to work with him for my Ph.D. work, which inspired me with his everlasting, enthusiasm towards research.

Special mention thanks to **Prof B.P.Veerbadrappa,** Vice-chancellor, Kuvempu University, Jnana Sahyadri, Shankarghatta, Shivamogga. For their constant support and encouragement.

I express my sincere gratitude towards **Dr. Ashok R L,** Professor and Chairman. PG Studies and Research in Physics, Kuvempu, University, Jnana Sahyadri Shankarghatta for giving the necessary clearance to carry out my research work in the institution.

I also express my gratitude towards **Dr. Sudha** Professor, PG Studies and Research in Physics, Kuvempu University, Jnana Sahyadri, Shankarghatta for their constant encouragement and moral support during my research work.

I express my gratitude **Prof N.H. Ayachit** Former Registrar KLE-CET Hubli for his inspiration to complete my Ph.D. programme.

I would like to thank **Barrister Amarsimha Patil,** Fellow of the Cambridge University Commonwealth Society London. For their encouragement, support, and legal suggestion to complete my Ph.D. programme.

I am thankful to the **Government of Karnataka,** OBC Department, for the financial support during my research work.

I am Extremely thankful to Dr. Harish C Barshilia, Chief Scientist, Head of Surface Engineering division, National Aeronautical laboratory (SED-NAL), Bangalore, for their support to carry out characterization.

My special thanks to **Dr. R. Rajaramkrishna** National College, Bangalore for their kind support in analysis of characterized data.

I express my regards to our research group **Mr. Ashok Dinkar, Shreekant Biradar, Abhiram, Shivanand, Ravikumar, Dr. Nagaraj O, all my research friends** for their input valuable suggestion with me during these years.

My sincere thanks to **non-teaching staff,** Department of Physics, Kuvempu University, jnana Sahyadri Shankarghatta.

With great pleasure, I express my deepest gratitude my beloved parents **Smt. Annapurna and Late. Sri Bhimappa Gurav** for their affection, care, interest, moral support, kind cooperation and constant encouragement to bring me to this position beyond their capacity. Words are not sufficient to describe my gratitude for her remarkable support given by my mother, I thank God for given wonderful mother to me. I remember the support of my younger brother **Mr. Yankappa Gurav** for his sacrifice and for helping me grow during the most formative years of my educational life.

I once again thank one and all who helped me directly and indirectly to complete my doctoral research work.

Above all, I would like to express my humble gratitude to God, the almighty for showing me the right path throught, I owe all my success to God.

Basavaraj Gurav ......✍

LIST OF ABBREVIATIONS

%	-	Percentage
et al.	-	And others (co-authors)
^{o}C	-	Degree Celsius
Fig.	-	Figure
hrs	-	Hour(s)
NBO	-	Non-bridging oxygen
K	-	Kelvin
RT	-	Room temperature
Tg	-	Glass transition Temperature
Mt	-	Melting temperature
RI	-	Refractive index
ASTM	-	American standard of testing materials
TTT	-	Time-temperature transition
RE's	-	Rare-earths
UV-VIS-NIR	-	Ultra -violet/visible/Near infrared
XRD	-	X-ray diffraction
FTIR	-	Fourier Transform Infra-red spectroscopy
PL	-	Photoluminescence spectroscopy
J-O	-	Judd-Ofelt
PPM	-	Parts per million
CCT	-	Corelated color temperature
CIE	-	International Commission on Illusion
Y/B	-	Yellow to Blue
WLED's	-	White light emitting diodes

LIST OF TABLES

LIST OF FIGURES

CONTENTS

PREFACE

The present Ph.D. thesis entitled "synthesis and characterizations of certain oxide and oxyfluoride glasses doped with rare - earth ions" focuses on the preparations, characterizations and concentrates dependent photoluminescence properties in the UV-visible NIR regions. Although oxide and oxyfluoride borate glasses have been widely studied, still there is need for the identifications of new glass host for NIR emitting solid state device application. The main objective of the present work is to demonstrate different spectroscopic properties of certain oxide and oxyfluoride glasses doped with rare earth ions for solid state device applications. The work is divided in to Six chapters as fallows

Chapter 1: In this chapter, concerns the background studies of glasses, classifications of glasses and different properties of glasses. Literature survey of previously reported results on rare earth ion doped oxide and oxyfluoride glasses. its objective of the work are discussed in brief.

Chapter 2 : This chapter consist brief about oxide and oxyfluoride glasses and dopants such as Nd^{3+}, $Dy^{3+,}$ $Sm^{3+,}$ followed by melt quenching technique for the preparation of $Nd^{3+,}$ Dy^{3+} doped oxide and oxyfluoride glasses and instruments used for characterization of glass samples.

Chapter 3 : In this chapter we prepared first series of Nd^{3+} doped oxide glasses with different concentrations x=0.1,0.3, and 0.5 The oxide glass samples were prepared by melt quenching technique. The synthesized glass samples were characterized by the powder XRD, FTIR, UV-Visible Spectroscopy and Photoluminescence studies. The non-crystallinity of the prepared glasses was confirmed by XRD studies. The analysis of FTIR spectra can reveal information on the rotation and vibration of different molecules within the glass matrix. The optical properties of prepared glasses were done by UV-visible spectroscopy. The absorbance studies of borate glasses doped with different concentrations of Nd_2O_3 were carried out. The optical band gap was calculated direct and indirect band gap values respectively. Emission intensity is enhanced Two-fold times decreases because of concentrations quenching. The estimated out comes strongly support the use of these glasses in NIR emitting solid-state device applications.

Chapter 4 : This chapter deals with the study of photoluminescence interaction of alkali fluoride over alkali oxide in Nd^{3+} doped of different concentrations. The glass samples were prepared by melt quenching technique. The prepared samples were characterized by the powder XRD, UV-visible spectral studies, photoluminescence studies, Judd-Ofelt analysis and radiative properties studies. The amorphous nature of glasses is confirmed by XRD studies the physical properties of prepared glass samples were studied. The optical properties of prepared glasses were done by UV-visible spectroscopy; we have studied UV-Visible NIR absorption spectrum of prepared glasses. The luminescence studied carried out by the photoemission spectra of prepared glass. The J-O parameters are studied and analysed in details in this chapter. The estimated outcomes strongly support the use of these oxyfluoride glasses in NIR solid state device applications. The results obtain from various technique of the synthesized glasses discussed and analysed

Chapter 5A : This chapter deals with third series of Dy^{3+} doped of various concentrations x=0.1, 0.3, 0.5 and 1.0 glasses. The glass samples were prepared by melt quenching technique and were characterized by the Powder XRD, UV-Visible spectra, FTIR, analysis Photoluminescence studies, Judd-Oflet analysis and Radiative properties. The non-crystallinity nature of glasses is confirmed by XRD studied and the physical properties of prepared samples were studied. The optical properties of prepared glass samples were studied by UV-Visible spectroscopy the luminescence studies were carried out by the photoemission spectra of prepared glasses.

Chapter 5B: This chapter deals with the study of Barium oxide and oxyfluoride glasses Dy^{3+} ions for WLED's applications. The glass samples were prepared by melt quenching technique. The prepared samples were characterized by the powder XRD, UV-visible spectral studies, photoluminescence studies, The amorphous nature of glasses is confirmed by XRD studies, physical, optical, structural and photoluminescence properties studies were analysed for oxide and oxyfluoride glasses for use in solid state white light emitting device applications..

Chapter 6 : summarizes the results and conclusion that are drawn from the present investigations of Nd^{3+}, Dy^{3+} doped oxide and oxyfluoride glasses along with the comparison of results reported in the literature from the systematic analysis of the both the present as well as earlier studies reported, its suggest that there is a scope for the further extension of work better understanding and these materials to develop the photonic/solid state device applications.

Some of the results of the above investigations have been presented at the national and international conferences / seminar and also published in national / international journals.

Motivation of Research:

Different alkali and alkaline earth metals modified with Ln^{+3}:oxyfluoride glasses were prepared and analysed their optical and photoluminescence properties. The work comprises to reduce the OH vibration and increase the emission intensity of alkali fluoride doped glasses, fluoride content introduced in the glass matrices to reduce the phonon energy of the glasses which enhances the oscillator strength, stimulated emission cross-section and emission intensity of the glass.

Problem Statement

The oxide glasses have been gained interest in the recent past and have been reported many literatures in the oxide glasses. There is fever research which focuses on the fluoride doped glasses. The addition of fluoride is proven to decrease the phonon energy and increase the luminescence intensity of the glasses and prove to be potential in the field of solid state display device applications.

1. INTRODUCTION

Glass is an amorphous solid. When a substance lacks long-range order, it is referred to as amorphous. One of the main goals of study over the years has been to correlate attributes with structure. There have been a number of books **[1-6]** which give the historical background and recent development in glass research. A glass has been defined in a number of ways. Following are these definitions in time order: [1930] Glass is amorphous, i.e., structure less solid **[7].**

1. [1938] Glass is an inorganic substance that is continuous with and analogous to its liquid state, substance due to a reversible change in viscosity during cooling, has reached such a high degree of viscosity that it may be treated as rigid for all practical purposes. **[1].**

2. [1949] Glass is an inorganic product of fusion that is cooled to a stiff form without crystallization, according to the American standard of testing materials (ASTM). **[8].**

3. [1960] secrist and Mackenzie defined that glass is a non-crystalline solid **[9].**

4. [1968] A glass is an amorphous solid which exhibits a glass transition **[6].** Heat capacity, thermal expansivity and other thermodynamic parameters change more or less abruptly during the glass transition.

In numerous glass systems, glass formation has been studied. Glasses can generally be made of materials that are covalent, ionic, metallic, Van-der Waals or hydrogen linked (table 1.1). As opposed to crystalline solids, there is no need for exact stoichiometry. Glasses can be created utilizing a wide number of methods and compositions. Rawson**[3].** For example, has given the compositional range for a number of oxide and oxyfluoride glasses.

Table 1.1 nature of chemical bonding in various glasses

Bonding style	**Examples**
Covalent	Oxides glasses (Borate, Silicate, Phosphate, Vanadate etc.,) B_2O_3, SiO_2, GeO_2, K_2O-B_2O_3, Na_2O- SiO2 etc.
Ionic	Nitrates, halides, sulphate, carbonates etc., KNO_3 – Ca $(NO_3)_{3,}$ Cd (NO_3)- $KnO_{3,}$ $ZnSO_4$- K_2SO_4, Li SO_4
Hydrate ionic	Aqueous solution of salts Ca $(NO_3)_{2.}$ $4H_2O$, Fe (Cl_2) $3.6H_2O$
Metallic	Rapidly quenched alloys, Au-La, Cu-Zr, Nb-Rb, Ni-B etc.
Van der Waals	Organic liquids (glucose, toluene, Anethole etc.) Or molecules

1.1 THEORIES OF GLASS FORMATION

The various models which have been developed to explain glass formation these fall into two categories –(a) Those draw attention to certain characteristics of the structure of the glass-forming material such as the atomic constituents' geometrical arrangement, the type and strength of interatomic bonds, etc. (b) those who referred dynamics of crystallization below the melting point into account. Both are necessary to comprehend the issue. Uhlmann **[10]** has reviewed these approaches. In the fallowing section, we summarize the various models of glass formation.

(a) Goldschmidt's radius ratio criterion

Goldschmidt's **[11]** pointed out that a relationship exists between a simple oxide's capacity to make glass and the size differences between the oxygen ion and cation in the general formula A_mO_n. Glass forming oxides are those have four anions around each cation and a ratio of cation radius between 0.2 and 0.4, with the anions being stimulated at the corners of a tetrahedron. Based on these findings, Goldschmidt's asserts that the creation of glass requires a tetrahedral arrangement of the oxygen ions around the cation A. Zachariasen **[12].** When it was later noted that not all oxides with a radius ratio in the stated range are glass formers, the Goldschmidt criterion was found to be unsatisfactory even as an empirical rule. BeO being one such case ($RBe\ /\ Ro\ = 0.221$).

(b) The Zachariasen's random network model

Zachariasen's **[12]** pointed out that as both forms share similar mechanical and density characteristics, interatomic forces in an oxide glass must be comparable to those in the equivalent crystal. The atoms in the glasses must form extended three-dimensional networks similar to those in crystals but these networks are not symmetrical or periodic since the x-ray diffraction pattern exhibits diffuse rings. Additionally, he noted that due to the random network of glass has a slightly higher internal energy than the corresponding crystal, which implies that polyhedral of the same kind as in the crystal must be joined together similarly in the glass. For instance, SiO_4 tetrahedral linked at their corners are present in the crystalline form of silica. The main distinction between crystalline and glassy forms of silica is that in the crystal, the orientation of adjacent tetrahedral is always the same throughout the structure as opposed to being varied in vitreous silica. Zachariasen's presented the following set of topological principles known as Zachariasen's rules based on the for mentioned theory.

Any glass forming oxide A_nO_m satisfies the fallowing

1. There is no more than two atoms of a connected to an oxygen atom.
2. The atom must be surrounded by a minimal number of oxygen atoms, either 3 or 4.
3. Instead of faces or edges, the oxygen polyhedral only share their corners.

If the network is to be three dimensional, at least three of the polyhedrons corners must be shared.

Oxides of the type A_2O (Na_2O- K_2O- etc.,) and AO (BaO, MgO, MnO) which cannot satisfy these rules do not form glasses. Glass forming oxides such as B_2O_3, SiO_2, GeO_2 etc. all satisfy these rules and good glass formers. With a few additional modifications, Zachariasen extended these rules to multicomponent glasses as well. These modifications are (i) the sample contains a high percentage of cations that are surrounded by oxygen tetrahedra or triangles, (ii) these tetrahedra or triangles share only corners with one another (iii) some oxygen atoms are linked to only two such a cation and do not form further bonds with any other cations. According to the Zachariasen model, an oxide that is "networking forming" is one that is a component of the vitreous framework whereas an oxide that is "network modifying" is one that is not.

(c) Other hypothesis of glass forming

When compared to the criterion for glass formation based on crystallization laws, Zachariasen's rule is quite effective at predicting the glass formation. Viscous flow is relatively challenging since it necessitates the breakdown of main chemical bonds, which is necessary for the oxide to form a three-dimensional network. According to Sun **[13],** an oxide's propensity to form glass is directly correlated with how tightly its oxygen and metal ions are bound. Oxygen-metal bond strengths are below this threshold for modifying ions that are not a component of the oxide network and are higher than this threshold for glass formers. As already mentioned, the necessity of the glass and crystal's energies be close to one another suggests that the heat of fusion for a glass former is lower than that for other chemically comparable materials. For similar materials lower rate of fusion will result in a lower rate of nucleation and crystallization, this factor may have some bearing on forecasting the propensity for glass formation. The following requirements for glass production have been proposed by Stanworth **[14].**

1. The cation must be three or more.
2. The tendency of glass formation increases with decreasing cation size.
3. The electronegativity of the cation should be between 1.5 and 2.1 on Pauling' scale.

Sun's criterion of bond strength and oxides' propensity to form glass has been amended by Rawson **[15]** to compare the ratios of bond strength to melting temperature. According to Rawson, this ratio takes into account both the bonds' strengths and the heat energy that is available to break them.

According to Dietzel [16], the field strength, (z/a2), where z is the charge on the cation in electron units and cation ionic radius is another important factor in determining the production of glass. Dietzel asserts that cations with a field strength larger than 1.3 are effective network formers, whereas cations with a field strength less than 0.5 are network modifiers.

(d) Kinetic approach

The rate of nucleation and crystal development on the one hand and the rate at which thermal energy can be removed from the cooling liquid on the other determine whether or not a given liquid will crystallize during cooling before Tg (the glass transition temperature) is achieved. Additionally, it has been shown that whereas some materials readily form glasses, others require rapid cooling or quenching in order to do so. This insight serves as the cornerstone of Turnbull's kinetic methodology**. [16].** He emphasized that almost all materials can be formed as amorphous solids "if cooled fast and far enough." When a liquid is supercooled, crystallization can occur between Tg and $Tm*$ (where $Tm*$ is the liquid's temperature). It must be chilled 'far enough' below Tg during this time to avoid crystallization. Consequently, it is appropriate to inquire as to the circumstances in which a glass may form. Turnbull has examined numerous factors that govern a liquid's rate of crystallization in order to explain why crystallization must be avoided in order for glass to develop The rate of nucleation, growth, or the advancement of the crystal-liquid interface determines the crystallization rate of a supercooled liquid. $Trg = Tg/Tm$, the decrease transition temperature, greatly influences both of these factors. The capacity to create glass should eventually improve as Tg/Tm

rises. based on the straightforward nucleation hypothesis [**17**]. The melts with $Trg > 2/3$ should form glasses readily.

The time-temperature transition (TTT) diagram was used by Uhlmann [18] to predict the cooling rate necessary for a material to make glass, further developing the kinetic techniques of Turnbull. The minimum amount of time needed for a particular percentage to crystallize is represented by the extremum of each TTT diagram, which depicts the struggle between the driving force (crystallization) and mobility of the molecules, atoms, or ions. The relation can be used to roughly predict the cooling rate Tc needed to prevent crystallization of a given percentage.

$$Tc = (\Delta\, {}^{TN}/_{tN})$$

Where $\Delta\ T_N = (T_E - T_N)$ T_E is the liquid temperature T_N and t_N are the temperature and time respectively of the nose of TTT curve

1.2 THE GLASS TRANSITIONS

When a melt is cooled, one of two things can happen: either the liquid crystallizes below the melting point (Tm) or it becomes "super cooled" below Tm, where it becomes more viscous with falling temperature and eventually solidifies into glass. Figure 1.1, which depicts the volume temperature relationship which can help explain this process. While glass formation is characterized by a progressive change in slope, the crystallization process is exhibited by an abrupt shift in volume at the melting temperature (Tm). The glass transition temperature is the area where there is a change in slope (T_g). Sensitive DTA or DSC can be used to measure T_g and crystallization temperature, and other thermodynamic parameters like heat capacity, entropy, and enthalpy also exhibit comparable behavior. It is frequently convenient to also utilise a fictive temperature Tf **[19]** because the transition to the glassy state is continuous and the glass transition is not clearly defined. This is referred to as the precise temperature where the extrapolated liquid and glass curves meet. If the glass is brought to Tf instantly, it will be in the metastable equilibrium. Although it may appear that Tf defined in this manner is a precise temperature, this is not the case since it depends on the rate of cooling of the supercooled liquid; the slower the rate of cooling, the larger the region for which the liquid may be supercooled, and consequently, the lower the fictive or glass transition temperature of a particular material; this temperature is not an intrinsic property. The temperature Tg and the cooling rate g are related by the equation.

$$q = q_0 \, exp \left[\frac{1}{c(\frac{1}{Tg} - \frac{1}{Tm})} \right]$$

where q_0 and c are constant for a given material

It should be noted that glasses prepared in different ways. With different cooling rates do not exhibit the glass transition at the same temperature. a number of models were proposed and reviewed by Rao **[20]** and Elliot **[6]** to explain the phenomenon of glass transition. We now summarize some of the important models.

Free volume theory

This concept was initially created for fluids in hard, dense spheres. According to Veronoi polyhedra, it is hypothesized that the particles oscillate within their own cages **[20].** The cell encircling a given site that contains all the points closer to it is referred to as a veronoi polyhedron. The idea is more suited for basic metals and rare gas solids than for materials where covalent bonding is the dominant kind of bonding. The oscillatory motion of particles becomes diffusive as a result of rising temperature, which also causes an increase in volume. The free volume is the excess cage volume that allows for diffusive motion. The occurrence of transport is caused by the whole free volume motion. The model predicts that as the free volume declines, the viscosity grows exponentially, causing the free volume to drop up to a point at which the distribution of free volume does not permit voids with volumes higher than or equal to the free volume. The consequence is a frozen phase known as glass as molecular transport stops. This too simplistic model is primarily used for investigations on viscosity and transport. The failure of this model to take into consideration crystals that melt with a negative volume change as well as the pressure dependency of Tg. In addition, because it ignores the prevalence of directed covalent bonds in well-known covalently bonded inorganic glass-forming liquids like SiO_2, B_2O_3, and P_2O_5, the hard sphere model of liquid proposed by the free volume approach may not be relevant to them.

Entropy model

According to the entropy model, transport is the locally cooperative re-arranging of particles into various configurations, which adds to the entropy of the configuration **[21].** A greater number of particles in the system are involved in collaboratively attaining configurationally changes as the melt's temperature is dropped, which results in a decrease in configurationally entropy. A second order phase transition that is characteristic of a perfect glass occurs at sufficiently low temperatures when the configurationally entropy reaches zero.

The viscosity of some glasses, such SiO_2, BeF_2, and GeO_2, whose configurationally entropy is temperature dependent is not taken into account by the entropy model, which only takes into account the pressure dependence of Tg and the non-linear viscosity seen in a number of glass-forming oxides. Based on how their glass transition temperature varied depending on temperature, Rao and Angell **[22]** divided these (glass forming liquids) into three categories: strong, intermediate, and fragile.

Bond lattice

Given that glasses have been found to be solids, it is interesting to consider glass transition as a characteristic of the amorphous solid state. The authors of this paradigm are Angell and Rao **[23].** According to this theory, a glass is a lattice of bonds with an irregular structure. These bonds may be disrupted when the glass is heated. The well-known transport would emerge from a suitable concentration of bonds surrounding the atom (or any final species). When the temperature approaches Tg, the model explains why heat capacity increases quickly. However, it is impossible to anticipate a heat capacity discontinuity.

Cluster model

The existence of intermediary short-range order is not taken into account by the model given so far. The glass is believed to be uniform in phase and utterly random in its structural arrangement. This might be a contributing factor in the aforementioned models' failure. The cluster model of glass established by Rao and Rao [**24**] takes into account the existence of intermediate-range organisation in the glass. This supposition is supported by numerous experimental experiments **[25, 27].** This model states that a glass is made up of organized regions or clusters that are contained within connective "tissue-like material" that is lower density. The majority of ionic glasses are probably going to share this cluster tissues texture. The compositional changes and relatively large-scale density of the supercooled liquid, which form organized clusters at low temperatures, are its distinguishing features. However, the cluster size is limited by itself to between 50 and 100 A^0.

A glass transition happens when a significant portion of the melt transforms into clusters that interfere with one another; the remaining tissue material simply freezes. This model takes into account a number of well-known characteristics of the glass transition, including pressure-related variations in Tg.

Computer simulation model

Studies using computer simulations have produced some extremely intriguing and significant findings both kinds of inquiries. The Monte-Carlo **[28]** casino. Additionally, simulations of molecular dynamics **[29, 30]** have been run on a model system of particles interacting with different kinds of model potential. The quenching rate is one of these methods' drawbacks. System cooling is necessary for the simulation procedure, and the rate is 10^{10} k/sec. The quickest quenching rate attainable in a laboratory is around six orders of magnitude slower than this rate.

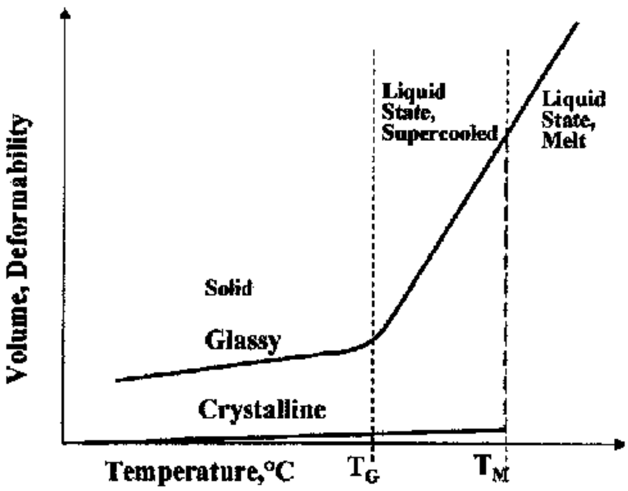

Fig 1: The change in the volume with temperature in a supercooled liquid through the glass transition T_g

1.3 CLASSIFICATION OF OXIDE GLASSES

The oxide glasses are widely studied are phosphate, tellurite, silicate, vanadate, borate glasses etc. these glasses have application in domestic, scientific, technological and commercial fronts.

1.3.1 Phosphate glasses

P_2O_5 is the one of the Zachariasen glass forming oxides. Studies on P_2O_5 glasses are limited because of how easily they volatilize due to their strong reactions with oxygen and water. Oxide-modified phosphate glasses, however, are comparatively stable. Phosphate glasses are used to create solid state battery reference electrodes and as host materials for lasers. Additionally, they are employed to store nuclear waste. P_2O_5 exists in three different crystal forms: tetragonal (T), orthorhombic (O), and hexagonal (H) all three types are built around the PO_4 Tetrahedron. The P_4O_{10} discrete molecules in the "H" state are a vapour connected by weak van der wall forces. The "O" forms are a three-dimensional network made up of rings made of six PO_4 tetrahedra. The "T" form is a multi-component glass that relies on covalent bonds between PO_4 tetrahedra that are connected to one another in chains or rings by oxygen bridges. The metal cation and the two non-bridging oxygen atoms of each PO_4 tetrahedron form cross bonds that keep adjacent phosphate chains together. P-O-P bonds between PO_4 tetrahedra in chains are significantly more powerful than cross bonds formed by metal cations. **[31].**

1.3.2 Tellurite glasses

The electrical conductivity of tellurite, a p-type semiconductor, is higher in some directions. Due to the photoelectric effect, Te's conductivity marginally increases when it is exposed to light. Tellurium dioxide is a well-known conditional glass maker, meaning that it produces glass in response to the addition of modest amounts of a different compound, such as an oxide or halide. One of Zachariasen's geometrical criteria, which states that only oxygen triangles may form a glass with energy comparable to that of the crystalline form, is in conflict with the presence of TeO_2 glass. Numerous investigations have shown that if a compound's coordination complex has more than four atoms, the resulting edge-sharing of the polyhedron's face will fix the symmetry in a number of directions. A shared face increases the lattice's stiffness, but a shared edge just leaves the angles at the edge open and a shared corner allows for unlimited angle variation at the polyhedron's common corner. Tellurite glasses have a high refractive index and transmit electromagnetic radiation into the mid-infrared region. The glasses can be utilised for active devices like laser fiber amplifiers and non-linear components, although they are primarily investigated for applications as passive devices (lenses, windows, fibers, etc.). Tellurite glasses are also employed as solar cell substrates, solid state batteries, optical switches, pressure sensors, laser hosts, fiber and amplifier glass substrates. **[32,33]**

1.3.3 Silicate glasses

The majority of commercially used glasses are a silicate because they are resistant to air moisture, acids, etc. The SiO_4 tetrahedron is the fundamental unit of construction for these glasses, according to XRD research. By means of silicon-oxygen connections at their corners, four additional tetrahedron are randomly joined to one another. Si-O-Si bonds are broken when any modifying oxides are added, resulting in the creation of non-bridging oxygen. The network's interstitial still has the modifiers' cation. Glasses commonly used for soda or soft glasses are manufactured by burning lime stone, sodium carbonate, and silica together. These materials comprise sodium and calcium silicates. Glassware that can endure high temperatures is made from hard glass. Flint glass is made of potash and lead, whereas potassium carbonate is utilized in hard glasses in place of sodium carbonate. When the calcium is replaced with lead, sodium, and partially potassium, higher refractive indices (RI) can be obtained. These high RI glasses are used to create ornamental glass, prisms, mirrors, and lenses, as well as optical components for electrical bulbs. Glass made of borosilicate and aluminum borosilicate's is known as Pyrex. This is comprised of boron trioxide and silicon dioxide. It has a small coefficient of thermal expansion. Low temperature cryostats are made using this. **[34].**

1.3.4 Vanadate glasses

Chemically, V_2O_5 glasses are comparable to P_2O_5. V_2O_5, however, is a poor network former, much like P_2O_5. However, using unique quick quenching techniques like splat cooling and thermal decomposition, it can be transformed into an amorphous state. The structure of vanadate glasses has a significant impact on their physical characteristics. These glasses have characteristics of a semiconductor. It is interesting to research vanadate glasses because they can be used to create threshold devices, which could have uses in electronics. Each vanadium ion in these glasses is surrounded by five oxygen atoms in the corners of a trigonal bi-pyramid (V_2O_5) group. These groups are connected to one another partially by edges and partially by corners to create layers. **[35].**

1.3.5 Borate glasses

Because of its unusual characteristic known as "The Boron Anomaly," boronate glasses attracted a large number of workers and earned special significance. Additionally, these glasses are quickly damaged by moisture, therefore there are not many technological uses for them. However, some borates have unique uses, such as rare-earth borates with high refractive indices, lead-borate glasses for plasma soldering, and sodium resistant alumino-borate glasses for sodium discharge lamps. Academically these glasses gained importance because of two main reasons – (i) the marked difference in the properties of vitreous B_2O_3 and SiO_2 which cannot be easily explained in terms of what is known about their structures (ii) the ability of the boron atoms in borate glasses to be coordinated with either three or four oxygen atoms.

The majority of investigations on the structural properties of borate-glass have attempted to provide an explanation for the observed maxima, minima, or inflection in the physical property v/s composition curves. The "boron anomaly" was used to explain a variety of rapid property changes in binary borate glasses with compositions near 15 mol% modifier oxide **[3,4,36].** These maxima minima were not seen in glasses made without boron.

Planar BO_3 units make up pure B_2O_3, which is made up of three-dimensional networks of randomly connected BO_3 units that share all three of their neighboring oxygen atoms. The third orbital is empty and extends in directions that are perpendicular to the planar BO_3 units, which are likely engaged in Sp^2 hybridization. A partial double bond is created when the oxygen atoms' unoccupied orbital takes an electron.

When network-modifying oxides are added, the following network modifications may occur: I B-O-B bonds may be broken by oxygen anions to form a non-bridging oxygen atom, similar to what happens when a silica network breaks down; (ii) a filled oxygen anion orbital may overlap with an empty P-orbital of a boron atom, forming a Sp^3 tetrahedron arrangement that results in a BO_4 tetra and (iii) Two BO_3 units may receive an electron pair from an oxygen atom, changing the coordination of the two borons from Sp^2 and Sp^3 hybridization and without the presence of non-bridging oxygen.

On the basis of a variety of creative structural models, earlier experimental findings **[36]** were attempted. All of these theories are based on boron's extremely unique capacity to exist in two different coordination states. However, the NMR studies **[37,38]** showed that four – coordinated boron BO_4 varies smoothly as $x/(1-x)$ where x is varied from 0 to 30 mol% modifier oxide without any unusual behavior in the critical range 15-20 mol% of modifier oxide

The earliest results on borate glasses exhibiting anomalous trends, such as thermal expansion, showed a clear minimum of roughly 10 mol% of Na_2O concentration. Biscoe and Warren **[39]** explained these findings. Assuming that an addition will cause some boron to transition to tetrahedral coordination is fallacious.

The structure is connected in three dimensions as opposed to two because the BO_4 groups are attached to the other components in four different orientations. This will result in a noticeable improvement in the structure's strength and tightness, which is due to the quick reduction in thermal expansion's coefficient of motion when Na_2O concentrations rises from 0 to 16 mol% Na_2O. Many workers excepted the conclusion that the fraction of four coordinated boron in glasses of composition x Me_2O – (1-x) B_2O_3 fallowed the relation,

$$N_{BO_4} = x / (1-x)$$

At least up to the "anomalous" range near 16 mol% (x = 0.16) of Me_2O. at higher concentrations, a number of hypothesis involving numerical rules were put forward but the NMR studies show that they were not correct and the above equation holds true even up to x = 0.3 therefore the boron oxide anomaly cannot be explained in terms of change of boron coordination alone.

Crystalline and glassy borate Krough moe have been the subject of in-depth research [30]. A new model for the structure of borosilicate glass was proposed and is now widely used. Borate glasses, in his opinion, are not just a random arrangement of BO_3 triangles and BO_4 tetrahedra joined at the corners, but rather, they also contain segments of a disordered framework that are well defined and stable groups of borates. These borate groups should be the same as the groupings found in crystalline borates. The result of thermodynamic **[40]** and infrared **[41]** studies lead to the classification into four different kinds of structural groupings viz, the boroxol, pentaborate, triborate groups **(fig. 1.2)** further pentaborate and triborate groups **(fig. 1.2)** always occur in pairs and these pairs are referred to as "tetraborate groups" .

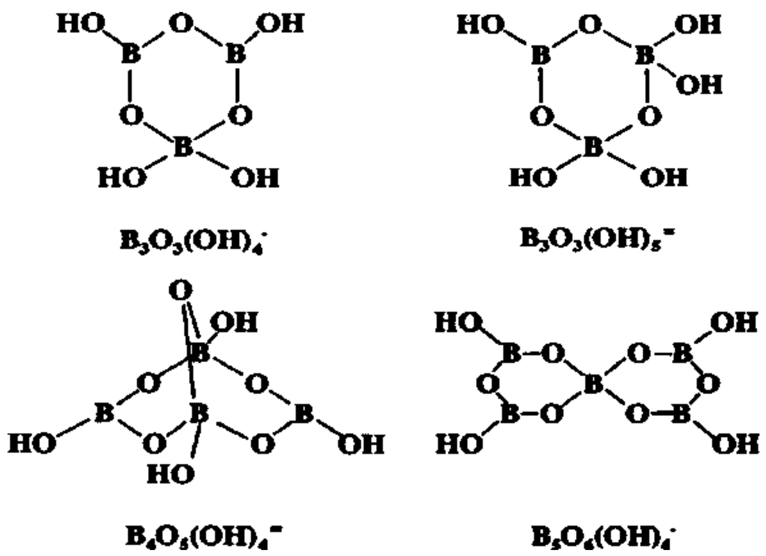

Fig 1.2 : Boron- oxygen structural groupings.

1.4 LANTHANIDES

The group of atomic number (Z) having 57 to 71 are usually classified as lanthanides and very often referred as rare-earths (RE’s). they are situated at the bottom of the periodic table, one row above the actinides as group III A elements in table **1.2** the lanthanides are arranged in ascending order of Z along with its atomic weight, abundance in nature and color.

In addition to the lanthanides, the phrase "rare earth" also refers to the elements yttrium (Z=39) and scandium (Z=21). Although earlier scientists used the term "earth" to denote the element, in a strict sense it refers to the oxide. The term "rare earth" is accurate but also deceptive because these substances are not actually rare (table 1.2) are instead of metals rather than earths. People who work in the field frequently refer to the "lighter lanthanides" of the "yttrium group" of elements. Z = 64 to 71 elements are considered heavy lanthanides by this arbitrary classification. Numerous more subgroups exist, such as the terbium group, which consists of the elements gadolinium, terbium, and dysprosium. One stable form of only one lanthanide, promethium, does not exist in nature. Promethium was created artificially in 1941 by bombarding praseodymium and neodymium with neutrons, deuterons, and alpha particles, making radioactive isotopes the only known forms of the element. **[42].**

Table 1.2 : The rare-earth element and their features

Atomic No. (Z)	Element	Symbol	Atomic weight (amu)	Abundance (ppm)	Physical appearance
57	Lanthanum	La	138.92	18	-
58	Cerium	Ce	140.13	46	Colorless
59	Praseodymium	Pr	140.92	5.5	yellow green
60	Neodymium	Nd	144.27	24	Red violet
61	Promethium	Pm	[147]	-	Unknown
62	Samarium	Sm	150.35	6.5	Yellow
63	Europium	Eu	152.00	0.5	Essentially colorless
64	Gadolinium	Gd	157.26	6.4	Colorless
65	Terbium	Tb	158.93	0.9	Essentially colorless
66	Dysprosium	Dy	162.51	5.0	Light yellow green
67	Holmium	Ho	164.94	1.2	Brownish yellow
68	Erbium	Er	167.27	4.0	Pink
69	Thulium	Th	168.94	0.4	Light green
70	Ytterbium	Yt	173.04	2.7	Colorless
71	Lutetium	Lu	174.99	0.8	-

The lanthanides are abundant in the crust of the earth. Yttrium is the strictest definition of the word "rare," even though the term "rare earths" is still used to refer to the scandium and lanthanide elements. They are more common than many of our everyday materials. When the relative abundance of lanthanides and other elements in the earth's crust are compared, many people are surprised. It was discovered that the total concentration of lanthanides is comparable to that of chromium (130 ppm) and zinc (320 ppm), and is roughly half that of carbon (320 ppm) (200 ppm) Even rarer than lanthanide are silver (0.1 ppm), gold (0.005 ppm), and platinum (0.005 ppm). In the earth's crust, cerium is more prevalent than tin (40 ppm).) **[43].**

1.5 RARE EARTH ION DOPED GLASSES

Glass is a superb optical material that is highly transparent over a broad spectral range and optically homogeneous, allowing for the production of bulk glasses, fibres, and waveguides of high optical quality. Glass has a random network of octahedral or tetrahedral polyhedra that contains a large number of special sites for foreign atoms. When modifiers are added, the packing ratio of a glass decreases as a result of the development of non-bridging oxygen atoms, increasing the size of interstitial positions and allowing for the easy accommodation of larger size ions. Since the arrangements of an ion around the rare-earth ions vary from site to site, the spectral lines' inhomogeneous broadening results. Additionally, the glasses can be cast in a variety of sizes according to the need.

$Nd^{3+,}$ $Dy^{3+,}$ and Sm^{3+} doped glasses are effective luminescence emitters that can be used as laser active materials or optical fibre amplifiers because they contain rare earth ions. One of the most important factors for obtaining high stimulated emission is the host material's refractive index (n), which depends on its composition. Most glasses have refractive indices between 1.4 and 2.5, making them more desirable to use as hosts for luminescent ions in cross-section. By modifying the composition or type of modifier compounds, it is possible to tailor the glass's refractive index and phonon energy **[44].**

1.6 JUDD-OFLET THEORY

Typically, we calculate certain parameters using the theoretical Judd and Oflet model and contrast them with the experimental results we have acquired. For different concentrations of rare earth ions in any host, we can estimate the transitions assignments and determine the oscillatory strength using both experimental, calculated root mean square value, and bonding parameters. Similar to the previously published work, these calculations were completed. The JO intensity parameters Ω_λ (2,6 and 4) for all concentrations are further determined using JO theory, which applies the least square fit approach method. Furthermore, the JO theory's ability to predict spectral intensities was validated by the low root mean square value. **[45,46]**

The optical absorption spectra were used to determine the band gap energy of the material. The optical absorption coefficient, (αλ) was determined using the fallowing equation.

$$\alpha\,(\lambda) \;=\; 2.303\;\frac{A}{d} \qquad 1$$

where, d is the thickness of the glass sample and A is the absorbance. The band gap energy was calculated using the Tauc's equation;

$$\alpha h\upsilon \;=\; B\,(h\upsilon\;-Eg)\,n \qquad 2$$

where, B is a constant, hυ is the photon energy 'E_g' is the optical energy band gap 'n' is a number which characterizes the transition process. The exponent 'n' takes the values; 1/2, 2, 3, and 3/2 for indirect allowed, indirect forbidden, direct allowed and direct forbidden transitions, respectively. Experimental data was well fitted for both $n = ½$ (direct allowed) and $n = 2$ (indirect allowed) using the above equation **(2)**

The Nephelauxetic ratio (β) and bonding parameter (δ) are estimated using the fallowing relation;

$$\beta = \frac{Va}{Vc} \qquad 3$$

and

$$\delta = \left(1 - \frac{\beta}{\beta}\right) \times 100 \qquad 4$$

where, Va and Vc are the number of the corresponding transitions in the complex ion in present glass and free ion respectively. Here the values of **β** are determined for all the transitions and the average value (**β)** is further used to calculate the bonding parameter δ.

The experimental oscillator strength (f_{exp}) for the glass is estimated from the area of absorption band using the fallowing equation

$$f_{exp} = 4.318\int\alpha\,(v)\,dv \qquad 5$$

Where α (v) is the molar absorptivity of a band at wave number (v) in cm^{-1}. The theoretical oscillator strength for the present glass system is estimated from the JO theory using the fallowing equation;

$$f_{cal}\ \ (\psi J \rightarrow \psi\text{'}J\text{'}) = \frac{8\pi mcv\,(n^2+2)^2}{3h(2J+1)9n}\ \ \sum\lambda = 2{,}4{,}6\ \Omega\lambda\ \ (\psi J\|U\lambda\|\,\psi\text{'}J\text{'})^2 \qquad 6$$

Where, m is the mass of an electron, c is the velocity of the light in vacuum, h is the plank's constant, n is the refractive index. In the above equation the term $(n^2+2)^2/9n$

is the Lorentz local field correction for the absorption band. The spontaneous emission probability (A) of transition is estimated using the fallowing equation;

$$A\,(\psi' J;\, \psi J\,) \;=\; \frac{64\pi^4}{3h(2J+1)\lambda^3} \;\left[\frac{n}{9}\,(n^2\,+2)2\;S_{ed}\;+\;n^3\,S_{md}\right] \qquad 7$$

Where, the factor $\frac{n}{9}\,(n^2\,+2)^2$ is the local field correction to the $Nd3^+$ for the initial manifold, S_{ed} and S_{md} represent the line strength for the induced electric and magnetic – dipole transitions respectively, which can be evaluated by using fallowing equations.

$$S_{ed} \;=\; e^2 \textstyle\sum\lambda \;=\; 2{,}4{,}6\;\Omega_\lambda\;\;(\psi J\|U\lambda\,\|\psi\,'J')^2 \qquad 8$$

$$S_{md} \;=\; \left(\frac{e^2\;h^2}{16\pi^2}\right)\,(\psi J\|L+2S\|\psi\,'J')^2 \qquad 9$$

The total radiative transition probability (A_T) and the radiative life time (τ_{rad}) are calculated using the fallowing equation;

$$A_{T} = \textstyle\sum A\,(\psi^{|}\,J;\,\psi'\,J'\,) \qquad 10$$

$$\tau_{rad} = 1/\,A_T(\psi'\,J;\,\psi'\,J'\,) \qquad 11$$

The branching ratio (β_R) corresponds to the emission from ψ' J' excited level to ψJ lower level can be calculated from transition probabilities using the equation**,**

$$\beta_R\;\;(\psi' J;\;\psi J'\,)\;=\;A\,(\psi' J;\;\psi J)\,/\,AT(\psi' J;\;\psi J) \qquad 12$$

from the luminescence spectra the peak stimulated emission cross-section ($\sigma_e\,(\lambda p)$) is determined using the fallowing equations;

$$\sigma_e\;\;(\lambda_p)\;=\;\left[\frac{\lambda^4}{8\pi n^2\,\Delta\lambda_{eff}}\right]A\,(\psi' J;\psi J) \qquad 13$$

Where $\Delta\lambda_{eff}$ = ($\int I(\lambda)d\lambda/I_{max}$) is effective band width λ_p emission band peak wavelength.

The experimental life time for exponential decay curves can be estimated using the equation;

$\tau_{exp} = \int \frac{1\,(t)dt}{I_0}$ where I(t) and (I_0) are the emission intensities at time t = t and t = 0 respectively. The quantum efficiency (η) is determined using the fallowing equation;

$$\eta\,(\%) = \left(\frac{\tau_{exp}}{\tau_{rad}}\right) \times 100 \qquad 14$$

using the above equation, we have estimates certain optical parameters which is playing vital role in deciding various applications relative of the host and dopant.

1.7 RADIATIVE PROPERTIES

The J-O parameters along with refractive index (n) are used to predict the radiative properties of excited states of Ln^{3+} ion. The radiative transition probabilities (A) for a transition $\psi J \rightarrow \psi' J'$ can be calculated from the fallowing equation **[47].**

$$A\,(\psi J, \psi' J') = \frac{64\pi^4 v^3}{3h(2J+1)} \frac{n\left(n^2+2\right)^2}{9} S_{ed} + \frac{64\pi^4 v^3}{3h(2J+1)} n^3 S_{md} \qquad 15$$

The total radiative transition probabilities (A) for an excited state is the sum of the $A\,(\psi J, \psi' J')$ terms calculated over all the terminal states

$$A_r\,(\psi J) = \sum A(\psi J, \psi' J') \qquad 16$$

A_τ is related to the radiative life time (τ_{rad}) of an excited state by

$$\tau_{rad}(\psi J) = \frac{1}{A_\tau(\psi J)} \qquad 17$$

Strong emission probabilities and more transitions from level lead to faster decay and shorter lifetimes. The theoretical life time $\tau_{rad}(\psi J)$calculated from the JO intensity parameters $(\Omega\lambda)$, can be compared with measured life times $\tau_{exp}(\psi J)$. The discrepancy between predicted and experimental lifetimes can be attributed to non-radiative relaxation (multiphonon decay and/or energy transfer). The branching ratio (β_R) corresponding to the emission from an excited ψ'J' level to its lower level $\psi'J'$ is given by

$$\beta_R(\psi J, \psi'J') = \frac{A(\psi J,\psi'J')}{A_\tau(\psi J)} \qquad 18$$

The branching ratio can be used to predict the relative intensities of all emission lines originating from a given excited state. The experimental branching ratio can be found from the relative areas of the emission bands.

The peaks stimulated emission cross-section $\sigma(P)$ $(\psi J, \psi'J')$, between the states ψJ and $\psi'J'$ having a probability of A $(\psi J, \psi'J')$ can be expressed as

$$\sigma(P)(\psi J, \psi'J'), = \frac{\lambda_p^4}{8\pi c n^2 \Delta\lambda_{eff}} A\ (\psi J, \psi'J') \qquad 19$$

where λp is the transition peaks wavelength and $\Delta\lambda_{eff}$ its effective line, width found by dividing the area of the emission band by its average height. Good laser transitions are characterized by large cross-section for stimulated emission.

In terms of interaction parameters, the experimental data can therefore be combined with the theoretical models that are already in use to provide lanthanide-ligand-radiation, ion-ion, and ion-ligand pathways. Thus, an accurate evaluation of these interactions may enable the design, suggestion, or prediction of optical devices for specific applications.

1.8 CHROMATICITY COLOR COORDINATES

The International commission for Illumination (Commission International deI'Eclairage, CIE) has standardized the measurement of color by means of color matching functions and the chromaticity diagram. The color matching functions are obtained by adjusting the intensities of the red, green and blue light of a source under test with the standard monochromatic light source. The three-color matching functions can be obtained by performing a series of such matches using different monochromatic light sources represented as $\bar{x}(\lambda)$, $\bar{y}(\lambda)$ and $\bar{z}(\lambda)$

So, the color if any source can be described by using three variables referred to as trichromacy. The degree of stimulation required to match a color of special power density $p(\lambda)$ is given by tristimulus values X, Y and Z, that represents the three primary colors i.e., red, green, blue, respectively, and they can have evaluated using the fallowing equation **[48].**

$$X = \int_{\lambda} \bar{x}(\lambda) P(\lambda) d\lambda \quad 20$$

$$Y = \int_{\lambda} \bar{y}(\lambda) P(\lambda) d\lambda \quad 21$$

$$Z = \int_{\lambda} \bar{z}(\lambda) P(\lambda) d\lambda \quad 22$$

The chromaticity diagram in Figure 1.3 was developed by the Commission International de I'Eclairage (CIE) in 1931. The design's perimeter is formed by the envelope of all monochromatic color coordinates, and all chromatic wavelengths fall inside its region**.**

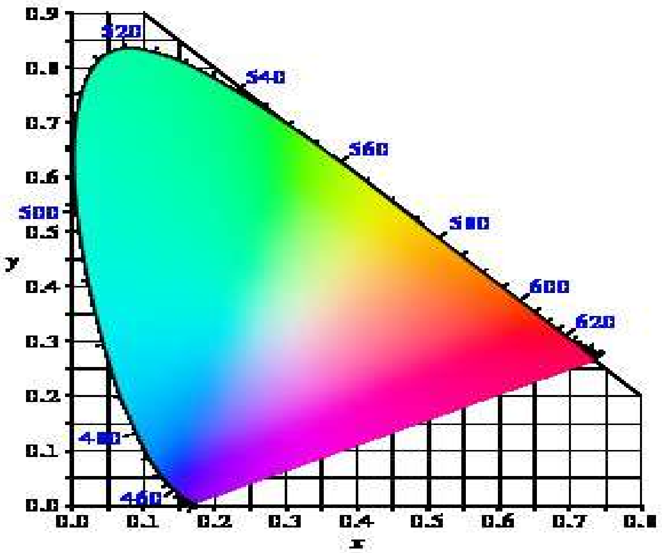

Figure 1.3 CIE 1931chromaticity diagram

The chromaticity coordinates x and y of a light source can be calculated from the tristimulus values according to the equations.

$$x = \frac{X}{X+Y+Z} \tag{23}$$

$$y = \frac{Y}{X+Y+Z} \tag{24}$$

The distance between the emission color coordinates and the coordinates of an equal energy point is used to determine the color purity or color saturation of a specific dominating color of a source. divided by the chromaticity diagram's distance from the equal energy point to the dominant wavelength point. Thus, the color purity can be expressed as

$$\text{Color purity} = \frac{\sqrt{(x_s-x_i)^2+(y_s-y_i)^2}}{\sqrt{(x_d-x_i)^2+(y_d-y_i)^2}} \tag{25}$$

Where the chromaticity coordinates of the emission light equal energy point and the dominating wavelength points, respectively, are (X, Y) and (Xd, Yd).The dominant wavelength is defined as the wavelength located on the perimeter of the chromaticity diagram that appears to be closest to the color of the test light source.

1.9 LITERATURE REVIEW

P. Manasa *et. al.* 2019 **[49]** has been investigated "spectroscopic properties of Nd^{3+} ions in Niobium phosphate glasses for laser applications". in their study they have evaluated Judd- ofelt intensity parameters for 1 mol% Nd^{3+} absorption spectrum they have observed strong NIR emission for $^4F_{3/2}$ to $^4I_{11/2}$ transitions at 1.056 µm by the λex of 808 nm laser and their result shows that 1 mol% Nd^{3+} glasses might be use for laser gain media at 1.056 µm region.

D. UmaMaheshwar *et al.,* 2011 **[50]** have been studied "investigations on 1.07 µm laser emission in Nd^{3+} doped sodium fluoroborate glasses. They have analyzed energy level using free ion Hamiltonian model. In their study they evaluated J-O parameters and radiative properties. The fluorescence spectra for different concentrations of Nd^{3+} ions were recorded by exciting samples at 514nm for Art ion laser

Y. H. Elbashar *et al.,* 2016 **[51]** have been studied Judd-Ofelt study of absorption spectrum Neodymium doped borate glasses. They have reported the spectroscopic analysis based on J-O theory using that they have found oscillating strength and intensity parameters from their result the glasses have good optical properties and applicable for photonic like lasing medium

Jihong. Zhang *et al.,* 2014 **[52]** have investigated direct observation on Nd^{3+} and Tm^{3+} ion distribution in oxyfluoride glass ceramics congaing PbF_2 Nano crystal. they have reported the stark splitting in the absorption peak enhanced photoluminescence and prolonged life time that β- PbF_2 Nano crystal formation increased the luminescence of rare earth ion such as Nd^{3+} and Tm^{3+} ion where incorporated in to Nano crystal.

V. Mehta *et al.,* 1995 **[53]** have been studied optical properties and spectroscopic parameters of Nd^{3+} doped phosphate and Borate glasses. In their study it was reported that using J-O theory they have evaluated value of absorption line, strengths, spontaneous emission probabilities from $^4F_{3/2}$ level and stimulated emission cross-section of the $^4F_{3/2}$ to $^4I_{11/2}$ transitions. For Nd^{3+} they result show that the values of emission cross-section are comparable with those glasses used solid state laser applications.

J. Pisarska *et al.,* 2008 **[54]** have been investigated Nd doped oxyfluoro phosphate glasses and glass ceramics for NIR laser application. They have reported that Nd doped ox fluoroborate glasses have been investigated as function of PbF_2 concentrations and thermal treatment it was observed from their result the florescence decays from $^4F_{3/2}$ excited state of Nd^{3+} ions are independent on PbF_2 concentrations.

M. dajmal *et al*., 2020 **[55]** have been studied spectroscopic properties of Nd^{3+} ion doped Zn-Al-Ba-Borate glasses for NIR emitting device applications. They have carried out FTIR studies, UV-absorption studies and J-O theory it was absorber that that the J-O theory was used to analyzed the radiative properties of Nd_2O_3 doped glasses. To derive the parameter like J-O parameters, oscillators strength, radiative transition probability, and branching ratio. Their result show that optimum concentrations of Nd_2O_3 in their studied glass found to be 1.0 mol% based luminescence intensity from their glasses are used for lasing potentiality.

Shweta. Mohan *et al*., 2017 **[56]** have been studied optical and spectroscopic properties of Neodymium doped Cadmium- Sodium- Borate glasses. they have reported physical properties, Uv absorption studies and photoluminescence studies. The effect of compositional changes on the spectroscopic characteristics of Nd^{3+} ion have been studied and reported the values of J-O intensity parameters ($\Omega_{2)}$ decrease with the decrease in the sodium content and increases from their its cadmium content increases from their it was observed higher values of branching ratio and stimulated emission cross-section for the prepared glass pointed towards laser host materials.

Optical properties of Nd^{3+} ions doped in oxyfloroborate glasses. Studied by Akshaya Kumar *et al.,* **[57]** in their report J-O analysis has been accomplished on the basis of UV-VIS-NIR absorption spectrum they have calculated various radiative parameters such as electronic dipole lines strength, transitions probabilities, branching ratio and life time of various energy levels.

Spectroscopic and glass transitions investigation on Nd^{3+} doped NaF- Na_2O-B_2O_3 glasses. Studied by B. Karthikeyan *et al.,* **[58]** in their report spectroscopic and glass transition property were analyzed the absorption studies were carried out the using J-O theory.The experimental and theoretical oscillator strength were calculated. The spectral study was done for the 1 mol% Nd doped glasses and the spontaneous emission, probability, life time analysis was investigated.

Sushila K Lenkennavar *et al.,* 2018 **[59]** have been studied physical and structural properties of Dy^{3+} and Nd^{3+} ion doped oxyfluoride glasses. They have prepared glass containing Potassium-zinc -Boro oxyfluoride were doped with Nd^{3+} and Dy^{3+} ion. They have analyzed physical properties and structural studied. From their results refractive index 1.62 is obtained for all glasses that results in optical behavior of nature of glass and single doped co-doped system presents not many changes structural modes.

K. Mari Selvam e*t al*., 2017 **[60]** have been investigated optical properties of Nd^{3+} doped barium lithium fluoroborate glasses for NIR emission. They have been reported optical emission, and absorption spectra the optical band gap and urbac energy were calculated using absorption spectra. The J-O intensity parameters were determined from the analysis of absorption spectrum of neodymium doped in the prepared glass in their result the emission intensity of the $^4F_{3/2}$ to $^4I_{11/2}$ transitions Increases with the increase in Nd concentrations up to 0.5 wt. % and the concentration quenching mechanism was observed for 1 and 2 wt.% concentration. The life time of the $^4F_{3/2}$ level was found to decreases with increasing Nd^{3+} ion concentration for their result it was observed that the nature energy transfer process was a single exponential curve which was studied for all the glasses and analyzed.

Stimulated and upconverted emission of Nd^{3+} in a transparent oxyfluoride glass ceramics studied by Victor Uvin *et al.,* 2004 **[61]** they have studied ultraviolet and visible emission generated by up conversion process inside the laser cavity under lasing and num lasing conditions and they have estimated the expected losses produced by these processes.

Spectroscopic investigations of Nd^{3+} doped gadolinium-calcium -silica-borate glasses for the NIR emission at 1.059nm. were studied by C. R. Keshavalu *et al.,* 2018 **[62]** they have characterized structural, thermal, absorption, emission and decay time measurements based on the J-O intensity parameters and radiative properties were calculated absorption spectrum they have evaluated emission cross-section, effective band width, from their study the emission spectra for, BSGDCANd glasses gives the emission transitions (903nm, 1059nm, and 1344nm). their result show that the high emission cross-section, branching ratio, and long-life time indicating that the glass system BSGDCANd 0.5 % system could be consider as a good candidate for strong NIR laser 1059nm.

Nisha Deopa *et al.,* 2018 **[63]** have been carried out spectroscopic investigation of Nd^{3+} doped lithium-lead-alumina-borate glasses. For 1.06μm laser application. They have measured oscillator strengths from the absorption spectra were used to estimate the J-O intensity parameters. The emission spectra recorder for the prepared glass under investigation exhibit to emission transition $^4F_{3/2}$ to $^4I_{11/2}$ (1063) nm and $^4F_{3/2}$ to $^4I_{9/2}$ (1050) for which radiative parameters have been evaluated their results show that the relatively higher values of emission cross - section, branching ratio and quantum efficiency values obtained for 1.0 mol% of Nd^{3+} ions in their glass suggest that it is suitable for generating lasing action at 1063 nm in NIR region.

Comparative impact on Nd^{3+} doping concentration on near infrared laser emission in lead borate glassy material were studied by K. Venkat Rao *et al.,* 2019 **[64]** in their studied based on the calculations of J-O theory derived from the optical absorption spectra. J-O parameters have been obtained luminescence spectra were measured for all the prepared samples it has been observed that luminescent intensity gradually increased up to 0.8 mol% of Nd^{3+} and further increased in concentration causes the luminescent intensity falls due to concentration quenching of Nd^{3+} ions. Their glass system with 0.8 mol% is found to be most intensive in emission at 1.06 μm related to $^4F_{3/2}$ to $^4I_{9/2}$ in NIR excitation.

1.06 μm emission of Nd^{3+} doped Al-Ba-Lithium phosphate glasses for NIR laser medium material. has been studied by P. Thongyoyi *et al.,* 2022 **[65]** they have investigated the effect of Nd^{3+} on prepared phosphate glass the wavelength at 1066 nm was observed is the highest emission intensity they have calculated J-O parameters and radiative properties using absorption spectra their result showed that Nd^{3+} doped Al-Ba-Lithium phosphate glass with a 1066nm emission might be used as a NIR laser medium materials.

Luminescence characteristics of Nd^{3+} doped bismuth borate glasses for photonic applications. Were studied by B. Munisudhakar *et al.,* 2019 **[66]** in their studied it is observed that Ω_λ =(λ=2,4,6) and radiative parameters analyzed from the J-O analysis. The emission spectra are observed that the laser transition $^4F_{3/2}$ to $^4I_{11/2}$ at 1059nm is more intense transitions and the decay curves for their prepared glasses excited single exponential decay the result suggest Nd^{3+} doped BBZPA glasses could be suggest for photonic applications.

K. Vijaykumar *et al.,* 2012 **[67]** have been studied spectroscopic properties of Nd^{3+} doped borate glasses. In their work Racah, spin orbital and configuration interaction parameters have been evaluated from the spectral data. J-O parameters were calculated from the intensity of the absorption spectra and also radiative properties such as transition probabilities, lifetime, branching ratio, absorption cross-section have been computed their result show that the stimulated emission cross section for the potential lasing transition for all the glasses under their study.

Juniastel. Rajagukguk *et al.,* 2019 **[68]** have been investigated structural, spectroscopic and optical gain of Nd^{3+} doped fluorophosphate glasses for solid state laser applications. In their study the spectroscopic analysis has been carried out using J-O parameters and oscillator strength to determined radiative properties such as radiative transitions probabilities, branching ratio, life time, and quantum efficiency their result show that the addition of Nd^{3+} ion in to phosphate glasses could enhance the spectroscopic properties which could play as a potential candidate solid state device application.

T. G. V.M. Rao *et al*., 2013 **[69]** has been studied optical and structural investigation of Sm^{3+} -Nd^{3+} codoped in magnesium led borosilicate glasses. The glasses are examined by optical absorption luminescence and Raman spectral studies. J- O intensities parameters are calculated for observed bands of Sm^{3+} ions their result suggested that prepared glasses are responsible for orange luminescence and might be used in the development of materials for LED's and another optical device in the visible region.

I. Kashif *et al.,* 2020 **[70]** have been investigated spectroscopic properties of lithium borate glasses containing Sm^{3+} -Nd^{3+} ions. they have investigated luminescence spectra of their glass sample excited at 400nm arounded and observed these luminescence band in visible region which may due to spectra material (Sm^{3+}, Nd^{3+}) the result show that their glass sample responsible orange emission and used in the important of materials for LED and optical devices.

Concentrations dependent of spectroscopic properties and energy transfer analysis of the fluorophosphate glasses with small phosphate content doped with Nd^{3+} ions· were studied by E. Kolobkova *et al.,* 2019 **[71]** in their study they have calculated radiative parameter based on J- O intensity parameter with different Nd^{3+} concentrations. They have observed the high emission cross- section and large quantum efficiency suggest that the glass is potential for compact 1.06 µm laser applications. The analysis luminescence kinetics as shown the formation of Nd ion cluster beginning from Nd concentration of 1.006×10^{-20} cm^3.

Judd-Oflet analysis of emission spectrum for Neodymium doped borate glasses Material used for laser medium applications. They have been studied by B. M. A Makram *et al.,* 2021 **[72]** in their study it is observed that the variation between the borate oxide and sodium oxide causes a change of the oscillator strength which gives us a good optimization for choosing the best chemical composition. They have also analyzed spectroscopic properties based on J-O theory and calculate radiative parameters.

Synthesis and luminescence properties of lithium-aluminum phosphate glass doped with Nd^{3+} ion for laser medium were studied by N. Sangwaranatee *et al.,* 2020 **[73]** the optical and luminescence properties were studied by investigating absorption and NIR emission spectra of the prepared samples. From their studies the photoluminescence properties the sample showed the strongest emission at the 1063 nm when it was excited by the 581nm which gives to the energy transition of the Nd^{3+} the J-O and radiative parameters were calculated the result show that there is a possibility using their glass as a laser material.

Investigation on spectroscopic properties of Nd^{3+} doped alkali bismuth phosphate glasses for 1.053 μm laser applications were done by S. Damodaraiha *et al.,* 2019 **[74]** the spectroscopic parameter has been determined from absorption and emission spectra together with J-O analysis. Addition of bismuth oxide to the phosphate matrix significantly increased radiative parameters such as transition probabilities, quantum efficiency, and major life time and stimulated emission cross-section their result show that the quite larger value for laser parameters like gain band width optical gains and saturation intensity have been obtained for $^4F_{3/2}$ to $^4I_{11/2}$ transition of Nd^{3+} ions in alkali bismuth phosphate glass which promising materials for NIR laser applications at 1.053μm.

Neodymium doped multicomponent borate/phosphate glasses for NIR solid-state material applications were studied by J. Kaewkhao *et al.,* 2021 **[75]** in their study the absorption spectra are used to investigate the optical band gap value and structural disorder observed in the synthesis glasses. The hypersensitive transitions were positioned around 581nm in the Uv-visible absorption spectra electronic polarizability of the oxide ion and optical basicity of the synthesized glasses were calculated were using optical band gap and they have analyzed photoluminescence spectra.

Optical straights of Neodymium doped new types of borate glasses: J-O analysis were studied by A. U. Ahmed *et al.,* 2019 **[76]** in their study they have evaluated J-O intensity parameters of Nd^{3+} doped glasses. FTIR-spectra of glasses reveals the bond stretching and vibration of different borate functional groups from the uv- visible absorption spectra they have observed twelve absorption bonds. Accompanied by hypersensitive transition at 581 nm which were used to calculate the oscillate strength. Their result show that proposed glass material was found to be effective for the enhancement spectroscopic quality factor of Nd^{3+} (1.2603) suggesting this usefulness in photonic device.

Nd^{3+} doped B_2O_3+Li_2O+CaO+CaF_2 glass system: structural and optical properties were studied by A. R. Venugopal *et al.,* 2022 **[77]** in their study Uv-visible NIR spectrum of the glass revile the prepared glass have strong absorption at 584nm in the visible region and 805 nm in the NIR region for the transitions $^4F_{9/2}$

to $^4G_{5/2}$ and $^4F_{9/2}$ to $^4F_{5/2}$ these are due to excitation of electron by induced absorption they have also evaluated J-O parameters radiative parameters by absorption spectra this result show that the Nd doped borate glasses exhibit a high peak power due to its emission at 1.049nm wavelength and has its application as lasing materials.

Structural luminescence and NMR studies of Nd^{3+} doped sodium-calcium-borate glasses for laser applications. Were carried out by Jamson. T. James *et al.,* 2020 **[78]** they have studied optical properties, Raman spectra, NMR, and luminescence for the possible applications as laser gain medium from UV-visible spectra they have evaluated J-O parameters and further used for calculating the various radiative parameter from the emission spectra. The effect of Nd^{3+} concentrations on the life time of the $^4F_{3/2}$ luminescent was analyzed from the decay curve the investigated results suggest that prepared glasses can be utilized as gain medium to generate laser at around 1.05μm.

Absorption and emission spectral studies of Sm^{3+} and Dy^{3+} ions in PbO-PbF_2 glasses were carried out by P. Nachimuthu 1997 **[79]** they have studied J-O parameter and emission spectral properties the stimulated emission cross-section indicative of potential for lasers have been obtained the fluorescent decay process for both ions fallow single exponential at lower concentration their studies show that for some oxyfluoride glasses can be better suitable for fluoride glasses.

Garima *et al.*, 2022 **[80]** have been studied optical properties of Sm^{3+} doped in CaO- Al_2O_3- Na_2O-BaO-B_2O_3 glasses for under-sea optical device applications. In their study they have evaluated J-O parameters and shows $\Omega_2 > \Omega_4 > \Omega >_6$ trends the photoluminescence spectra reviled three emission peaks originating from 565, 602, 649nm corresponds to $^4G_{5/2}$ to $^6H_{5/2,}$ $^6H_{7/2}$ to $^6H_{9/2}$ respectively. The radiative properties were calculated and shows higher values for 0.3 mol% Sm_2O_3 sample. Their result show that observed radiative for the prepared glass system show that their efficient for developing under-sea-optical device applications in the reddish orange spectral region.

Luminescent characteristics of Dy^{3+} doped Gd_2O_3-CaO-SiO_2-B_2O_3 scintillation glasses. Were studied by J. Kaewkhao *et al.,* 2016 **[81]** in the luminescence spectra they have observed absorption bands the emission spectra of prepared glass showed two strong peak 577nm and 482 nm the highest emission intensity was observed from the prepared glass at 0.4 mol% of Dy_2O_3 as the efficient energy transfer takes place Gd^{3+} to Dy^{3+} their result show that the integral scintillation efficiency of the prepared glass was determined by 27% that of the commercially available BGO Crystal.

R. Rajaramkrishna *et al*., 2019 **[82]** were carried out structural analysis and luminescence studies of Ce^{3+} : Dy^{3+} calcium -zinc-gadolinium-borate glasses using EXAFS. In their studied they have evaluated J-O intensity parameters and round that the trend faces **Ω_2>Ω_4>Ω>$_6$** they have also investigated radiative properties using J-O parameters. The photoluminescence and radioluminescence spectra exhibit two prominent emission peaks at 482nm (blue) 575nm(yellow) that corresponds to the $^4F_{9/2}$ to $^6H_{15/2}$ and $^4F_{9/2}$ to $^6H_{13/2}$ respectively. The result obtained in their work demonstrate that the prepared glass could be potential candidate for used in WLED’s solid state device applications.

Physical thermal, structural and optical properties of Dy^{3+} doped lithium alumina borate glasses for bright WLED’s. were studied by P. P. pawar *et al.,* 2017 **[83]** in their work it was observed that thermal properties of glasses and photoluminescence excitations and emission spectra were measured at room temperature they have found the emission spectra shows two intense emission bands at around 482nm (blue) and 575nm (yellow) correspondence to the $^4F_{9/2}$ to $^6H_{15/2}$ and $^4F_{9/2}$ to $^6H_{13/2}$ transitions respectively their result show that prepared glasses having emission in the white region and thus can be used for bright WLED.

Influence of PbF_2 concentration on spectroscopic properties of Eu^{3+} and Dy^{3+} ions in lead borate glasses were investigated by Lidia- Jur *et al.,* 2013 **[84]** in their study effects of PbF_2 on spectroscopic properties of Eu^{3+} and Dy^{3+} ions in lead borate glasses have been studied they have analyzed luminescence spectra and their decays in details they have also found luminescence intensity ratio R (Eu^{3+}) and Y (Dy^{3+}) as well as luminescence life time in the excited states of rare earth ion.

Luminescence studies of Dy^{3+} doped bismuth-zinc-borate glasses were carried out by B. Shanmugawelu *et al.,* 2014 **[85]** in their work optical absorption spectra have been analyzed using J-O theory they have calculated asymmetric ratio the intensity ratio of yellow to blue transitions from the emission spectra to understand the symmetry around the Dy^{3+} ions in the glass matrix from the CIE diagram and decay curve measurements exhibit single exponential behavior.

Judd -Ofelt analysis and spectral properties of Dy^{3+} ion doped niobium containing calcium-zinc borate glass were studied by O. Ravi *et al.,* 2014 **[86]** in their study they have calculated J-O intensity parameters from UV-spectra and also calculated radiative properties it was found that Dy^{3+} ion the transition $^4F_{9/2}$ to $^6H_{13/2}$ shows highest emission cross – section at 1.0 mol% in the glass matrix. The intensity ratio and chromaticity color coordinates are also estimated their results show that the prepared glasses exhibit good luminescence properties are suitable for generation of white light.

Dysprosium doped niobium zinc-fluorosilicate glass: intensity materials for white light emitting devices were studied by J. Prabhakar 2018 **[87]** in their work they have carried out structural, photoluminescence and decay properties were studied it was observed that the emission spectra of prepared glass exhibit two intense band at 480 nm and 570 nm beside a weak red emission at 650nm. The decay profile of Dy^{3+} ion for the $^4F_{9/2}$ level exhibit a non-exponential behavior for the all the glasses. The color coordination has been evaluated from the emission spectra of the glasses. The co-related color temperatures match well to the summer sunlight region this result indicates that glasses could be a potential candidate for white light emitting device.

Luminescence properties of the Dy^{3+} doped different fluorophosphate glasses for solid state lighting applications were investigated by S. Babu *et al.,* 2015 **[88]** in their work they have studied and evaluated J-O intensity parameter are used to calculate various radiative property for different Dy^{3+} transitions. The photoluminescence spectra exhibit band in the blue, yellow, red regions and from the decay curve analysis the life times of the excited states $^4F_{9/2}$ have been measured the CIE diagram for Dy^{3+} doped different fluorophosphate glasses are discussed.

1.10 OBJECTIVES OF THESIS

- To study X – Ray Diffractometer for conforming glassy state.
- To study Density can be measured by using Archimedes principle to calculate the molar refraction and molar volume etc.
- To understood UV-Vis-IR spectrophotometer for absorption, transmission, reflection studies and finding parameters like Optical band gap, absorption coefficient, theoretical refractive index and phonon energy.
- To study IR spectrometer for structural studies.
- To understood time resolved spectrofluorometer for photoluminescence studies and radiative life time measurements.

REFERENCES

[1] Morey G. W., "The properties of glasses", 2nd edition. (Reinhold, N. y, 1954).

[2] Weyl W.A.and Marboe E C. "The constitution of glasses", vol. I and II (Wiley, N. Y, 1962)

[3] Rawson H., "In organic glass forming system". (Academic press, N. Y, 1967).

[4] Pye L.D., "Introduction to glass science", Eds., Pye L. D., Stevans H. I. and Lacourse j. (Plenum Press, N. Y, 1973).

[5] Doremus R. H., "Introduction of glass sciences", (Academic press N. Y, 1973).

[6] Elliot S. R., "Physics of Amorphous materials", (Longmann, London 1982).

[7] Warren B. E., Z. Krist., 86,349, (1932).

[8] Stanworth J. E. J. Soc. Glass Technol., 30, 56 (1946).

[9] Secrist D. R. and Mackenzie J. D., "Modern aspects the vitreous state", Vol. 3, (Butterworths, London, 1960).

[10] Uhlmann D. R., J. Non-cryst. Solids. 14, 42 (1974).

[11] Goldschmidt V. M. Trans. Faraday Soc., 25, 253 (1929).

[12] Zachariasen W. H., J. Am. Chem. Soc., 54, 3841 (1932).

[13] Sun K. H., J. Am. Ceram, Soc., 30, 277 (1947).

[14] Stanworth J. E., Physical properties of glasses (CP).

[15] Rawson H., "proceedings IV international Congress Glass", Imprimeric Chaix, Paris, P. 62-69 (1956).

[16] Dietzel A., Glastechn. Ber., 22, 41 (1948).

[17] Turnbull D., Contemp. Phys. 10, 473 (1969).

[18] Uhlmann D. R., J. Non-cryst. Solids. 7, 337 (1972).

[19] Jones G. O., Glass (Methuen) 1956.

[20] Rao K. J., Bull. Mater. Sci., 1, 181 (1979).

[21] Adam G. and Gibbs J. H., J. Chem. Phys. 43, 139 (1965).

[22] Rao K. J., and Angell C. A. in relaxation in complex systems, Eds. Nazi k. and Wrigent G. B. (National Tech. Infor. Ser., U. S. Dept. of commerce Spring Field, VA22161).

[23] Angell C. A. Rao K. J., J. Chem. Phys. 57, 470 (1972).

[24] Rao K. J., and Rao, C. N. R. Mater. Res. Bull., 17, 1337, (1982).

[25] Bursill L.A Thomas J.M. and Rao K. J. Nature, 289, 157 (1981).

[26] Hemalatha s., Parathasarathy, G., Lakshmikumar S. T., and Rao K. J., Phil. Mag., B47, 291 (1983)

[27] Phillips J. c., Solid state phys., 37, 93 (1983).

[28] Lee J. K., Barker A. J. and Abraham F., J. Chem. Phys. 48, 3166 (1973).

[29] Woodcock L. V., J. Chem. Soc., Faraday Trans. II, 74, 11, (1978).

[30] Woodcock L. V., Ann. N. Y. Acad. Sci., 371, 274 (1981).

[31] P. Abdul Azeem, Ph.D. thesis, Sreekrishnadevaraya. University (2002).

[32] K. W. Bagnall, The Chemistry of Selenium, Tellurium and Polonium, Elsevier, London (1996).

[33] R. El-Mallavny, Tellurite glasses handbook, CRC press (2002).

[34] T. Sujatha, Ph.D. thesis, Gulbarga University (2016).

[35] Devidas G B. Ph.D. thesis, Gulbarga University (2008).

[36] Pye L. D., Frechette V. D. and Kredi N. J., “Borate Glass”, (Plenum Press, 1977).

[37] Savnson S. E., Forslind E. and Krogh Moe J., J. Phys. Chem., 66, 174 (1962).

[38] Bray P.J. and O' Keefe J. G., Phys. Chem. Glasses, 4, 37 (1963).

[39] Biscoe J. and Warran B. E., J. Am. Ceram. Soc., 21, 287 (1938).

[40] Krogh Moe., J., Phys. Chem. Glasses, 3, 101 (1962).

[41] Krogh Moe., J., Phys. Chem. Glasses, 6, 46 (1965).

[42] D. R. Lide Handbook of chemistry and Physics, 74th edition (CRC press, Boca Raton, 1994

[43] R. Praveena Ph.D. thesis, Sri Venkateshwara University Tirupati (2008).

[44] G. Venkaiah Ph.D. thesis, Sri Venkateshwara University Tirupati (2016).

[45] B. R. Judd. Phys. Rev., 127 (1962) 750.

[46] G. S. Ofelt. J. Chem. Phys., 37 (1962) 511.

[47] W. T. Carnall, Hand book on the physics and chemistry of rare –earths, E d. k. A Gschnei Jr. and L. Eyring, north Holland, Amsterdam, 1979, vol3, p.171

[48] E. Fred Schubert, Light emitting diodes, 2nd edition, Cambridge University press, New York, USA, 2006

[49] Manasa, P., Srihari, T., Basavapoornima, C., Joshi, A. S., & Jayasankar, C. K. (2019). Spectroscopic investigations of Nd3+ ions in niobium phosphate glasses for laser applications. *Journal of Luminescence*, *211*, 233-242.

[50] Umamaheswari, D., Jamalaiah, B. C., Sasikala, T., Reddy, G. L., & Moorthy, L. R. (2012). Investigation on 1.07 μm laser emission in Nd3+-doped sodium fluoroborate glasses. *Journal of Rare Earths*, *30*(5), 413-417.

[51] Elbashar, Y. H., & Rayan, D. A. (2016). Judd Ofelt study of absorption spectrum for neodymium doped borate glass. *Int. J. Appl. Chem*, *12*(1), 57-63.

[52] Zhang, J., Zhao, Z., Liu, C., Zhang, G., Zhao, X., Heo, J., & Jiang, Y. (2014). Direct observation of Nd3+ and Tm3+ ion distributions in oxy-fluoride glass

ceramics containing PbF2 nanocrystals. *Materials characterization*, *98*, 228-232.

[53] Mehta, V., Aka, G., Dawar, A. L., & Mansingh, A. (1999). Optical properties and spectroscopic parameters of Nd3+-doped phosphate and borate glasses. *Optical materials*, *12*(1), 53-63.

[54] Pisarska, J., Ryba-Romanowski, W., Dominiak-Dzik, G., Goryczka, T., & Pisarski, W. A. (2008). Nd-doped oxyfluoroborate glasses and glass-ceramics for NIR laser applications. *Journal of Alloys and Compounds*, *451*(1-2), 223-225.

[55] Djamal, M., Yuliantini, L., Hidayat, R., Rauf, N., Horprathum, M., Rajaramakrishna, R., ... & Kothan, S. (2020). Spectroscopic study of Nd3+ ion-doped Zn-Al-Ba borate glasses for NIR emitting device applications. *Optical Materials*, *107*, 110018.

[56] Mohan, S., & Thind, K. S. (2017). Optical and spectroscopic properties of neodymium doped cadmium-sodium borate glasses. *Optics & Laser Technology*, *95*, 36-41.

[57] Akshaya Kumar, D. K. Rai, S. B. Rai (2002) Optical properties of Nd^{3+} ions doped in oxyfloroborate glasses. Spectrochimica acta part A 58, 1379-1387.

[58] Karthikeyan, B., & Mohan, S. (2004). Spectroscopic and glass transition investigations on Nd3+-doped NaF–Na2O–B2O3 glasses. *Materials Research Bulletin*, *39*(10), 1507-1515.

[59] Lenkennavar, S. K., & Kokila, M. K. (2019, July). Physical and structural properties of Dy3+ and Nd3+-ions doped oxy-fluoride glasses. In *AIP Conference Proceedings* (Vol. 2115, No. 1, p. 030240). AIP Publishing LLC.

[60] Mariselvam, K., Kumar, R. A., & Suresh, K. (2018). Optical properties of Nd3+ doped barium lithium fluoroborate glasses for near-infrared (NIR) emission. *Physica B: Condensed Matter*, *534*, 68-75.

[61] Lavın, V., Iparraguirre, I., Azkargorta, J., Mendioroz, A., González-Platas, J., Balda, R., & Fernández, J. (2004). Stimulated and upconverted emissions of Nd3+ in a transparent oxyfluoride glass-ceramic. *Optical Materials*, *25*(2), 201-208.

[62] Kesavulu, C. R., Kim, H. J., Lee, S. W., Kaewkhao, J., Wantana, N., Kaewnuam, E., ... & Kaewjaeng, S. (2017). Spectroscopic investigations of Nd3+ doped gadolinium calcium silica borate glasses for the NIR emission at 1059 nm. *Journal of Alloys and Compounds*, *695*, 590-598.

[63] Deopa, N., Rao, A. S., Gupta, M., & Prakash, G. V. (2018). Spectroscopic investigations of Nd3+ doped lithium lead alumino borate glasses for 1.06 µm laser applications. *Optical Materials*, *75*, 127-134.

[64] Rao, K. V., Babu, S., Balanarayana, C., & Ratnakaram, Y. C. (2020). Comparative impact of Nd3+ ion doping concentration on near-infrared laser emission in lead borate glassy materials. *Optik*, *202*, 163562.

[65] Thongyoy, P., Kedkaew, C., Meejitpaisan, P., Minh, P. H., Keawmon, T., Rajaramakrishna, R., & Kaewkhao, J. (2022). 1.06 µm emission of Nd3+-doped aluminium barium lithium phosphate glasses for near IR laser medium material. *Optik*, *269*, 169852.

[66] Munisudhakar, B., Raju, C. N., Babu, M. R., Reddy, N. M., & Moorthy, L. R. (2020). Luminescence characteristics of Nd3+ doped bismuth borate glasses for photonic applications. *Materials Today: Proceedings*, *26*, 5-10.

[67] Kumar, K. V., & Kumar, A. S. (2012). Spectroscopic properties of Nd3+ doped borate glasses. *Optical Materials*, *35*(1), 12-17.

[68] Rajagukguk, J., Situmorang, R., Djamal, M., Rajaramakrishna, R., Kaewkhao, J., & Minh, P. H. (2019). Structural, spectroscopic and optical gain of Nd3+ doped fluorophosphate glasses for solid state laser application. *Journal of Luminescence*, *216*, 116738.

[69] Rao, T. G. V. M., Kumar, A. R., Veeraiah, N., & Reddy, M. R. (2013). Optical and structural investigation of Sm3+–Nd3+ co-doped in magnesium lead

borosilicate glasses. *Journal of Physics and Chemistry of Solids*, *74*(3), 410-417.

[70] Kashif, I., Ratep, A., & Ahmed, S. (2020). Spectroscopic properties of lithium borate glass containing Sm3+ and Nd3+ ions. *IJAAS*, *9*(3), 211.

[71] Kolobkova, E., Yasukevich, A., Kuleshov, N., Nikonorov, N., & Babkina, A. (2019). Concentration dependence of spectroscopic properties and energy transfer analysis of the fluorophosphate glasses with small phosphates content doped with Nd3+ ions. *Journal of Non-Crystalline Solids*, *526*, 119703.

[72] Makram, B. M. A., Khaliel, J., Rayan, D. A., Ayoub, H., & Elbashar, Y. H. (2021). Judd–Ofelt analysis of emission spectrum for neodymium ion doped borate glass matrix used for laser medium applications. *Journal of Optics*, 1-6.

[73] Sangwaranatee, N., Chanthima, N., Kaewkhao, J., & Tariwong, Y. (2020). Synthesis and luminescence properties of lithium aluminium phosphate glasses doped with Nd3+ ion for laser medium. In *Journal of physics: conference series* (Vol. 1428, No. 1, p. 012032). IOP Publishing.

[74] Damodaraiah, S., Prasad, V. R., & Ratnakaram, Y. C. (2019). Investigations on spectroscopic properties of Nd3+ doped alkali bismuth phosphate glasses for 1.053 μm laser applications. *Optics & Laser Technology*, *113*, 322-329.

[75] Kaewkhao, J., Tamilselvan, B., Pavan, H. L., Biju, A. K., Meghana, E. P., Tomy, A., & Rajaramakrishna, R. (2022). Neodymium-Doped Multi-Component Borate/Phosphate Glasses for NIR Solid-State Material Applications. *Integrated Ferroelectrics*, *224*(1), 13-32.

[76] Ahmad, A. U., Hashim, S., & Goshal, S. K. (2019). Optical traits of neodymium-doped new types of borate glasses: Judd-Ofelt analysis. *Optik*, *199*, 163515.

[77] Venugopal, A. R., Rajaramakrishna, R., Rajashekara, K. M., Pattar, V., Wongdamnern, N., Kothan, S., & Kaewkhao, J. (2022). Nd3+ doped B2O3+ Li2O+ CaO+ CaF2 glass systems: Structural and optical properties. *Optical Materials*, *133*, 112979.

[78] James, J. T., Jose, J. K., Manjunatha, M., Suresh, K., & Madhu, A. (2020). Structural, luminescence and NMR studies on Nd3+-doped sodium–calcium-borate glasses for lasing applications. *Ceramics International*, *46*(17), 27099-27109.

[79] Nachimuthu, P., Jagannathan, R., Kumar, V. N., & Rao, D. N. (1997). Absorption and emission spectral studies of Sm3+ and Dy3+ ions in PbO□ PbF2 glasses. *Journal of non-crystalline solids*, *217*(2-3), 215-223.

[80] Hebbar, D., Gurav, B., Kaewkhao, J., Intachai, N., Kothan, S., & Rajaramakrishna, R. (2022). Optical properties of Sm3+ doped in CaO-Al2O3-Na2O-BaO-B2O3 glasses for under-sea optical device applications. *Optik*, *262*, 169366.

[81] Kaewkhao, J., Wantana, N., Kaewjaeng, S., Kothan, S., & Kim, H. J. (2016). Luminescence characteristics of Dy3+ doped Gd2O3-CaO-SiO2-B2O3 scintillating glasses. *Journal of rare earths*, *34*(6), 583-589.

[82] Rajaramakrishna, R., Ruangtaweep, Y., Sattayaporn, S., Kidkhunthod, P., Kothan, S., & Kaewkhao, J. (2020). Structural analysis and luminescence studies of Ce3+: Dy3+ co-doped calcium zinc gadolinium borate glasses using EXAFS. *Radiation Physics and Chemistry*, *171*, 108695.

[83] Pawar, P. P., Munishwar, S. R., Gautam, S., & Gedam, R. S. (2017). Physical, thermal, structural and optical properties of Dy3+ doped lithium alumino-borate glasses for bright W-LED. *Journal of Luminescence*, *183*, 79-88.

[84] Żur, L., Pisarska, J., & Pisarski, W. A. (2013). Influence of PbF2 concentration on spectroscopic properties of Eu3+ and Dy3+ ions in lead borate glasses. *Journal of non-crystalline solids*, *377*, 114-118.

[85] Shanmugavelu, B., & Kumar, V. R. K. (2014). Luminescence studies of Dy3+ doped bismuth zinc borate glasses. *Journal of luminescence*, *146*, 358-363.

[86] Ravi, O., Reddy, C. M., Reddy, B. S., & Raju, B. D. P. (2014). Judd–Ofelt analysis and spectral properties of Dy3+ ions doped niobium containing tellurium calcium zinc borate glasses. *Optics Communications*, *312*, 263-268.

[87] Prabhakar, J., Kummara, V. K., Linganna, K., Babu, P., Jayasankar, C. K., Kim, J., & Venkatramu, V. (2019). Dysprosium doped niobium zinc fluorosilicate glasses: interesting materials for white light emitting devices. *Optik*, *176*, 457-463.

[88] Babu, S., Prasad, V. R., Rajesh, D., & Ratnakaram, Y. C. (2015). Luminescence properties of Dy3+ doped different fluoro-phosphate glasses for solid state lighting applications. *Journal of Molecular Structure*, *1080*, 153-161.

2.1 INTRODUCTION

The performance of an optical device application depends on its chemical composition, structure, optical quality, transparency region, thermal stability interactions between dopant ions and the host network. The phonon energy of the host, defect centers, and various forms of interactions among RE^{3+} dopants These affects in the likelihood of emissions in the UV-visible, and infrared regions as well as the quantum efficiency phenomena of rare-earth ions.

In the present course work various process and measurements were carried out to theprepare the synthesis and characterization of certain Oxide and Oxyfluoride glasses doped with rare earth ion. The optical properties of these glasses were influenced by the glass composition, Glass structure, optical quality and stability process of the glasses. The present thesis deals with the concentration dependent optical properties of $Nd^{3+,}$ $Dy^{3+,}$ ions in oxide and oxyfluoride glasses. Different analytical spectroscopic technique used an overview of the instruments and their specifications along with the characteristic's properties of the host glass.

2.2 GLASS PREPARATION

The fallowing methods are generally used for the preparation of non-crystalline solids which are reviewed by Zarzyki **[1]**

- Melt quenching
- Sputtering
- Chemical vapour deposition
- Electrolytic deposition

- Reaction amorphization
- Shock-wave transformation
- Thermal evaporation
- Glow-discharge decomposition
- Chemical reaction
- Irradiation
- Shear amorphization

Among all the techniques, the well-established and versatile technique for the production of an amorphous solid is the melt quenching method because of the following reasons:

- ✓ Preparation and handling of glass is very easy.
- ✓ Consume less time and can be possible to prepare with different composition.
- ✓ Mass productions of bulk glasses.

In the present days 21st century, the melt quenching method was the straightforward approach by which glasses in an appropriate size for practical application could be manufactured. Additionally, more than 99% of practical glasses are currently produced using this process. The melt quenching process, which involves fusing crystalline raw material into the molten viscous liquid and abruptly quenching to a glass, differs from other methods of glass manufacturing in a number of aspects, including the available system. The disordered state of the liquid is kept in the solid state, regardless of the product's size, shape, number of components, etc. When the pace of temperature decline is adequate to avoid crystallization.

In compared to poly crystalline materials, the melt quenching method's extra properties provide a high degree of flexibility for a glass's geometry and an advantage for producing large-scale materials. The gain pulse laser is a nice illustration of a product based on these properties. The other benefit of using the melt quenching technique over sol-gel or chemical vapour deposition is the composition's high degree of compositional flexibility. These allows for the use of various constituent types in a range of ratios from a few to several tens of percent. Faraday rotator whose overall performance is dependent on the size of materials. It is also made reasonably simple to dope or co-dope active ions, such as transition metals or Lanthanide$^{3+,}$ with a tiny quantity of percent or less, which is realistically significant for the creation of glasses with specific required qualities.

The key point about the melt quenching technique is that the majority of the information above is accurate not only for the well-known systems of phosphate (P_2O_5), silicate (SiO_2), and borate (B_2O_3), but also for the numerous exotic glasses of the oxide system as well as the non-oxide glasses like fluoride and metal alloy systems. The rare-earth ion doped glass samples that are the subject of this thesis were made using melt quenching methods. In respect to table 2.1 molar composition (in mol%) and their labels are shown.

Table 2.1. Glass composition (in mol%) and their labels of Nd^{3+}, Dy^{3+}, doped borate glasses.

Glass compositions	Labels
Nd_2O_3 oxide glasses	
23CaO-10Al_2O_3-50.9B_2O_3-6BaO-10Na_2O-0.1Nd_2O_3	CaAlBBaNaNd0.1
23CaO-10Al_2O_3-50.7B_2O_3-6BaO-10Na_2O-0.3Nd_2O_3	CaAlBBaNaNd0.3
23CaO-10Al_2O_3-50.5B_2O_3-6BaO-10Na_2O-0.3Nd_2O_3	CaAlBBaNaNd0.5
Nd_2O_3 oxyfluoride glasses	
23CaO-10Al_2O_3-50.5B_2O_3-6BaF_2-10Na_2O-0.5Nd_2O_3	CaAlBBaFNaNd0.5
23CaO-10Al_2O_3-50. B_2O_3-6BaF_2-10NaFO-1.0Nd_2O_3	CaAlBBaFNaFNd1.0
23CaO-10Al_2O_3-50.5B_2O_3-6BaF-10NaF-0.5Nd_2O_3	CaAlBBaFNaFNd0.5
23CaO-10Al_2O_3-50. B_2O_3-6BaO-10NaF-1.0Nd_2O_3	CaAlBBaNaFNd1.0
Dy_2O_3 oxide glasses	
23CaO-10Al_2O_3-50.9B_2O_3-6BaO-10Na_2O-0.1Dy_2O_3	CaAlBBaNaDy0.1
23CaO-10Al_2O_3-50.7B_2O_3-6BaO-10Na_2O-0.3Dy_2O_3	CaAlBBaNaDy0.3
23CaO-10Al_2O_3-50.5B_2O_3-6BaO-10Na_2O-0.3Dy_2O_3	CaAlBBaNaDy0.5
23CaO-10Al_2O_3-50. B_2O_3-6BaO-10Na_2O-0.3Dy_2O_3	CaAlBBaNaDy1.0
Dy_2O_3 Oxyfluoride glasses	
23CaO-10Al_2O_3-50.5B_2O_3-6Bao-10NaF- 0.5Dy_2O_3	CaAlBBaNaFDy (0.5)
23CaO-10 Al_2O_3-50 B_2O_3-6Bao-10NaF- 1.0 Dy_2O_3	CaAlBBaNaFDy (1.0)
23CaO-10 Al_2O_3-50.5 B_2O_3-6BaF-10NaF- 0.5 Dy_2O_3	CaAlBBaFNaFDy (0.5)
23CaO-10 Al_2O_3-50 B_2O_3-6BaF-10NaF- 1.0 Dy_2O_3	CaAlBBaFNaFDy (1.0)

2.2.1 Glass melt quenching technique

Glass preparation involves the preparation of the appropriate mixture of raw materials, a melting and an annealing process. The appropriate raw material required for each glass sample were calculated according to the mol% of each component of the glass and weighed to produce reaction mixture.

The high purity of chemical H_3BO_3, $CaCO_3$,Al_2O_3, Ba_2CO_3, Na_2CO_3, and Dy_2O_3, Nd_2O_3 Approximately 15gm of raw material where mixed in pestle mortar were grinded to the fine powder to total amount of each batch of glass formula was thoroughly mixed in an as it for homogeneous and weighed to 15 gram per melt and placed all composition in high temperature electrical muffle furnace using high force line crucible. The prepared mixture was then heated at 1150^0 c for 3 hours in electrical furnace the melt was then quickly poured in to a free heated brass plate and quenched the melt to prepare glass which were the annealed at 650^0 for overnight to reduce thermal stress and were left to cool down slowly at room temperature. The obtained glass samples were cut and polished in to a proper shape for characterization.[2]

Weighing balance

Glass melting

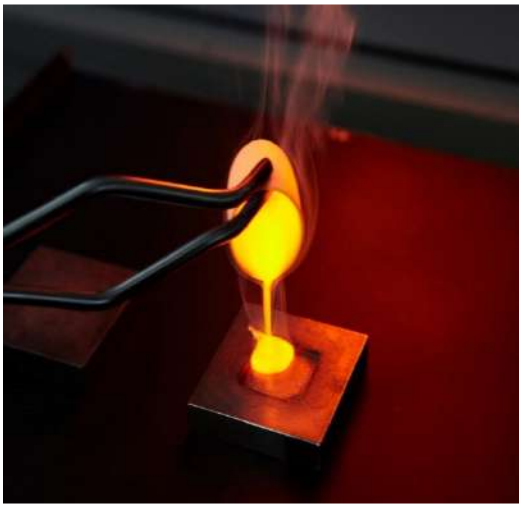

Glass casting

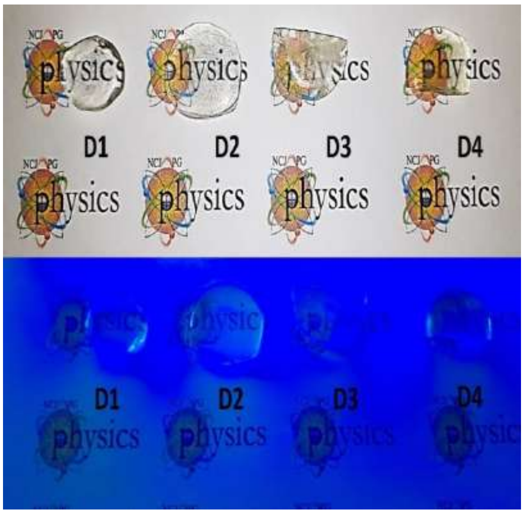

Some of Ln^{3+} doped glass samples

Fig 2.1: Different stages involved in the glass preparations

2.2.2 Annealing process

The stresses in the prepared glasses may be caused by the rapid cooling of the glasses through the glass transition region (by the glass Tg), leaving insufficient time for the constituent atoms to occupy the lowest energy sites. The prepared glasses were heated at room temperature near their Tg for an over night and then slowly cooled at room temperature. As a result, the majority of the properties of glass, including Tg, the thermal expansion coefficient, and dn/dT, rely on both time and temperature (thermal history). This means that altering the rate of heating and cooling can cause changes in the characteristics of glass. A glass can shrink to a metastable equilibrium volume and become dense when it is cooled more slowly. On the other hand, if the glass is cooled quickly, there isn't enough time for contraction, therefore the glass structure that freezers has a shrink volume. The structural components of the glass are rearranged into denser, lower energy sites during heating at the glass transition area, which results in a reduction in the volume of the glass. These structural alterations may have an impact on the glass property measurements.

2.2.3 Glass polishing

It is necessary to polish the glass before going to the characterization their optical properties. This was because the melted glasses can have rough and uneven surface using a polishing paper sheet numbers 200,400,600,800,1000, and 1200, was used to produced glass with smooth, flat and optical transparent surface for the optical measurements carried out the within this work. Samples flatness was not a critical aspects and above polishing produces described were sufficient in producing transparent and optically polished glass surface for characterization.

In this present thesis Oxide and Oxyfluoride glasses doped with different rare earth ions (RE^{3+}) concentrations have been prepared polished to characterization their optical measurements.

2.3 Characterization of the host.

In this chapter gives a brief description of the techniques used to prepare different glasses of investigations will be discussed. to determined physical properties, structural properties, optical properties of the prepared glass samples. Measurements techniques and different characterization used in present work includes molar volume and density measurements, Ultra -violet/visible/Near infrared (UV-VIS-NIR) spectroscopy, X-ray diffraction (XRD), Fourier Transform Infra-red (FTIR) spectroscopy, Photoluminescence spectroscopy (PL), Judd-ofelt (J-O), radiative property of prepared glass materials is discussed briefly.

2.3.1 Physical properties

The density (D) of the glass samples were determined by Archimedes principle using toluene as an immersion liquid at room temperature using the fallowing formula

$$D = \frac{w}{w-w1} \qquad 2.1$$

where w = the weight of the glass sample in air,

w_1 = the weight of the glass sample in water,

The concentration of (C) of the Lanthanide (Ln) ion in the glass (mol/lit) was found from the expression

$$C = \frac{2\times y\ d}{MW\ x} \times 1000\ (mol/lit) \qquad 2.2$$

Where y = Ln salt mass, x = total mass of chemical composition, D = density of the glass and M_w = molecular weight of Ln salt. The concentration in mol/lit can be converted in to ion/cm^3 (N) by multiplying it with a factor of $N_A/1000$, where N_A is the Avogadro's number as [2].

$$N = \frac{C \times NA}{1000} \quad (ions/cm^3) \qquad 2.3$$

2.3.2 Molar volume

Molar volume (V_M) can be calculated by the expression [2].

$$V_M\,(cm^3/\,mol) = \frac{M}{d} \qquad 2.4$$

Where M is the average molecular weight of the glass.

Where d is the density of glass sample.

2.3.3 Dielectric constant

Dielectric constant (ϵ) is given by [2].

$$\epsilon = n^2 \qquad 2.5$$

Where n is refractive index of the sample.

2.3.4 Inter-ionic distance

Inter-ionic distance (r_i) can be calculated by using the expression [2].

$$ri\,(A) = \left(\frac{1}{N}\right)^{1/3} \qquad 2.6$$

2.3.5 Polaron radius

Polaron radius radius (r_p) is given by terms of Ln^{3+} ion concentration is calculated by using the formula

$$r_p\ (\dot{A})\ ½ \left(\frac{\pi}{6N}\right)^{1/3} \qquad 2.7$$

2.3.6 Field strength

Field strength (F) is determined by the equation [2].

$$F\ (cm^{-2})\ = \frac{z}{rp^2} \qquad 2.8$$

2.3.7 Electronic polarizability

Electronic polarizability (α), is given by Lorentz-Lorentz equation [2], as

$$\alpha\ (cm^{-3}) = \left(\frac{3}{4\pi NA}\right) \times R_M \qquad 2.9$$

2.3.8 Metallization Criteria (M)

Metallization Criteria (M), can be used for predicting metallic or insulating behavior in the solid-state material is given by

$$M = 1 - (\ Rm/Vm) \qquad 2.10$$

2.3.9 X- ray diffraction

One of the most important tools for learning about the chemical makeup of powders and crystals as well as their structure is X-ray diffraction. Determine the molecular structures of crystals and powders with this technique, which is used for materials characterization and quality control.

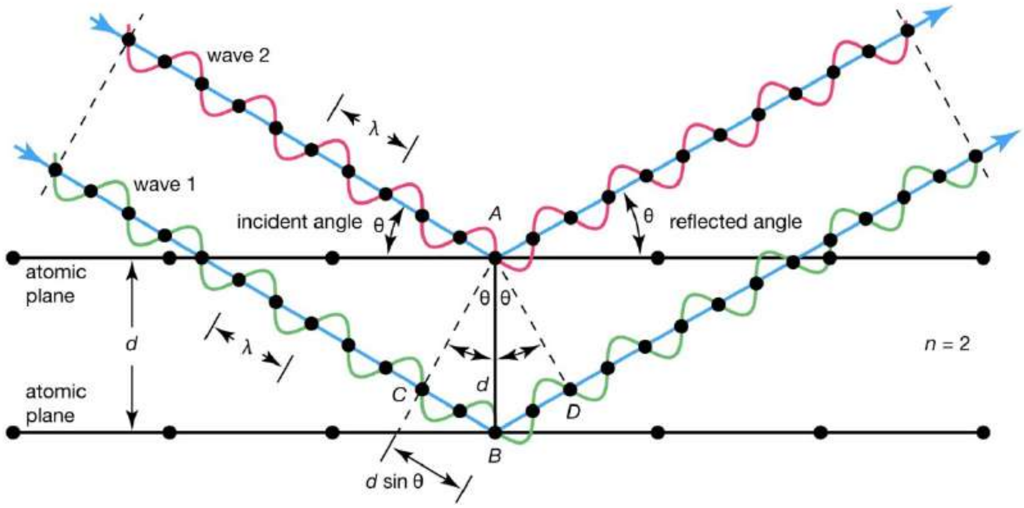

Fig 2.2: Braggs XRD pattern

X-rays are electromagnetic radiation with wavelengths between 10 and 80 cm that are identical to light in nature. The wavelength of the X Rays utilised for diffraction ranges from 0.5 to 2.5 AO. We are aware that the atomic configuration of a material affects its physical properties, including its optical, electrical, magnetic, ferroelectric, etc.

Therefore, X-ray powder diffraction is a quick analytical method for determining a crystalline material's phase and can give details on a unit cell dimension. In 1912, Max van Lace made the discovery that the distance between the planes in a crystal lattice acts as a 3-dimensional diffraction grating for x-ray wavelength. Therefore, the characterization of materials using fingerprints and material determination were used. When the conditions satisfy Bragg's law given below, XRD is based on constructive interference of the monochromatic X-ray & crystalline sample.

$$n\lambda=2d \sin \Theta$$

Where, d= spacing between atomic planes

λ= X ray wavelength

Θ = angle of diffraction n = 1, 2, 3,

The sample is then scanned through a range of 20 angles in order to identify, process, and count the diffracted x-rays. Due to the powder crystal's random orientation, this should capture all potential lattice diffraction directions. One of the most vital tools used in material science and solid-state chemistry/physics is the conversion of diffraction peak to d-spacing, which enables identification of a mineral because each mineral has a unique set of d-spacing xrd.[3]

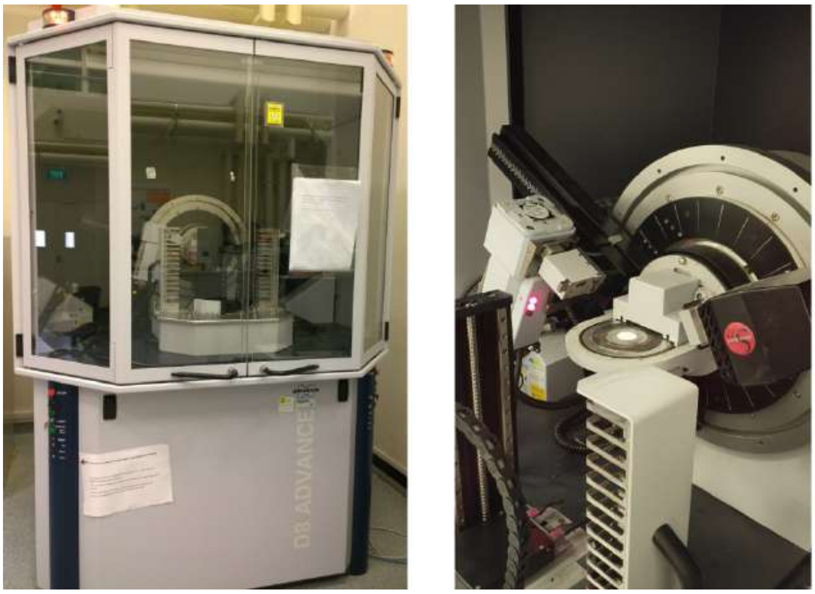

Fig.2.3XRD Bruker D8 Advance

The present glasses were subjected to X-RD. studies at National aerospace laboratory (NAL) Bangalore. Powder x-ray diffractometer D8 advanced (manufactured by Bruker) D8 goniometer is maintenance free with vertical theta/2 geometry. and this has source Cu K-α with radiation $1.5406A^{0.}$

2.3.10 Fourier Transform infra-red (FTIR)spectroscopy

Infrared spectroscopy is one of the most important techniques for the determinations of functional groups in this spectroscopy. IR radiation is passed through the sample some of the IR radiation is absorbed by the samples and some of it is transmitted from the samples.as a result spectrum from the it represents the molecular absorbance and transmittance. in IR spectral region there are molecular vibrations for the electromagnetic waves the FTIR spectroscopy is based on an instrument called Michelson's interferometer which is used to produced and interferogram and is related to IR spectrum by mathematical operations the spectrum of a compound is the super position of absorption band of specific functional groups band intensities in IR spectrum may be expressed as transmittance (T) or absorbance (A). the powder samples were thoroughly mixed with dry KBr (potassium bromide powder) and the pellets were formed under a pressure 10-12 terms.[4]

Fig. 2.4 Fourier Transform infra-red (FTIR)spectroscopy

Infrared transmittance spectra were recovered at room temperature using Perkin Elmer lambda frontier (MIV-FIR) spectrometer over the range 400-4000 for the oxide glasses for our samples. Fourier transform infrared spectroscopy (FTIR) characterization was carried out at National Aerospace Laboratory (NAL) Bangalore.

2.3.11 UV-Vis-NIR spectroscopy

The absorption and emission of electromagnetic radiation by atoms or molecules are measured using UV-visible spectroscopy.UV absorption spectroscopy is primarily based on measurements of light attenuation after a beam of light has passed through sample. The reflected from a sample surface. The oxide glasses have a broad absorption edge and are extremely transparent in both the visible and ultraviolet regions. The electrical transitions between the excitation levels or between the valence and conduction bands are linked to the first type of oxide glasses, which also interact with the vibration of molecules. The position and shape of the absorption edge relies on the material composition as well as the type of network formation. It is generally accepted that the uv-visible absorption in newly found materials like oxide and oxyfluoride glass involves the excitation of electronic nature. Perkin Elmer lambda uv -visible spectrometer of double beam and direct measuring system. In this spectrometer provides the analysing of films powder and liquids.[5,6]

Optical Absorption

A useful method for analysing the electrical structures of amorphous semiconductors is an optical absorption investigation. All of the borate glasses' absorption spectra have been gathered. Optical absorption coefficient (α) is estimated using the following expression,

$$\alpha = 2.303\,(A/t) \qquad (1)$$

where, t is glass thickness and A is absorbance.

In present study, two kinds of optical transitions were analysed i.e direct and indirect transitions. This analysis is based on Tauc's equation given below.

$$(\alpha h\nu)^n = B(h\nu - E_{opt}) \qquad (2)$$

Where, $h\nu$ is energy of incident photon, E_{opt} is optical band gap, B is band tailoring parameter, and n is the index which represent type of transition, n = 1/2 for indirect and n = 2 for direct transition.

Fig.2.5 Perkin Elmer Lambda-950 UV -Visible Spectrometer

Perkin Elmer lambda is equipped with integrating sphere was used for reflectance and transmittance measurement of opac or translucent over a wide wavelength range from 190-3300 nm. In our sample optical absorption spectra of polished glass samples in the wavelength range 250-2500 nm using UV-Vis-NIR double beam spectrophotometer. This characterization facility was used from National Aerospace laboratory (NAL) Bangalore.

2.3.12 Luminescence studies

There are several energy conversion processes that can occur when a solid absorbs photons or charged particles, including electron emission and chemical or structural change, as well as photon emission (luminescence).

The definition of luminescence is the absorption of photons by a substance followed by an excessive photon emission caused by thermal agitation and which is highly reliant on the nature of the emitting substance.

In fields like material science, physics, chemistry, biology, medicine, and pharmaceutical research, luminescence has numerous uses.

Photoluminescence studies

When radiation is incident on a substance, some of its energy is absorbed and reemitted as alight of longer wavelengths which is known as luminescence. The uv-visible spectrum includes of two comparable processes, florescence and phosphorescence. The wavelength of the light released to determines a substance's luminescence. The light emitted may be visible light, ultraviolet light, or infrared light. Cold emission is the type of emission that does not involve black body emission.

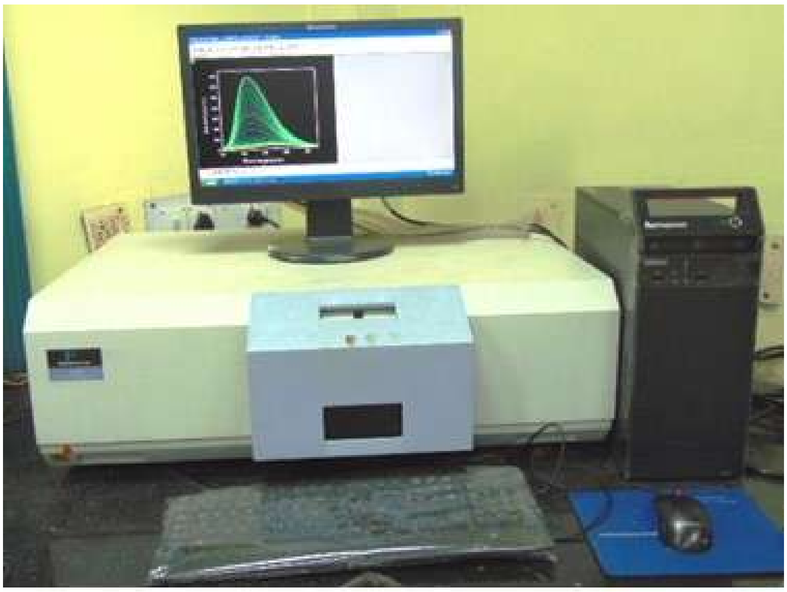

Fig 2.6 Luminescence Spectrometer

The present glasses were subjected to photoluminescence studied (JNCSAR) at Bangalore

REFERENCES

[1] J. Zarzycki,glasses and the vitreous state, Cambridge University Press, Cambridge, 1991

[2] S. R. lliot, Physics of Amorphous materials; Longnan Scintific and Technical London(1990)

[3] B. D Cullity, elements of X-ray diffraction, 2nd edition ., addirtion-wesly publishing Co., London UK, 1997

[4] A. Aronne V. N. Sigaev, B Champagnon, E. Fanelli, V. Califano, L. Z. Usmanova and P. Pernice, J. non –cryst. Solids 351(2005) 3610.

[5] Manual of perkin elmer lamda 950 Uv-vis-nir spectrophotometer, perkin elmer company, USA.

[6] http:www. Perkin elmer. CO.UK/catlog/product/ Id/L950

CHAPTER-3

RARE-EARTH ION EFFECT BORATE GLASS FOR NIR EMITTING SOLID STATE DEVICE APPLICATIONS

The present chapter reports the systematic analysis of the effects of B_2O_3 replaced by Nd_2O_3 studies on the spectroscopic characteristics of trivalent neodymium (Nd^{3+})-doped glasses were investigated using XRD, FTIR, absorption, and emission spectroscopy. The glasses were synthesized using the conventional melt quenching technique at 1150^0 C. The amorphous nature of the samples was confirmed by x-ray diffraction studies. The addition of Nd_2O_3 concentration affects the absorption and emission properties of the Nd^{3+} ion measured in the near-infrared luminescence range from 0.9µm, 1.06 µm, and 1.36µm associated with the $^4F_{3/2}\rightarrow{}^4I_J$ (J = 9/2, 11/2, 13/2) transitions. The novelty of the present work is to fully understand and characterize the luminescence of Nd^{3+} doped borate bulk glasses with different doping concentrations. So as to gain an insight of 1.06 µm corresponding to $^4F_{3/2}\rightarrow{}^4F_{11/2}$ transition, these glasses are highly potential one which is an applicable to NIR emitting solid state device.

3.1 INTRODUCTION

Glasses are the most advanced material in terms of technology and utilized in a wide range of applications. They are notable for being optically transparent and brittle. Due to their wide range of prospective uses and applications in the design and development of photonic devices, the rare-earth (RE) doped glass materials have attracted a lot of attention **[1-2]**. Due to their high transparency, low melting point, great thermal stability, and potent solubilities in rare earth ions, borate-based glass hosts have been demonstrated to be capable of lasing in the NIR range. A particularly good optical medium are borate glasses **[3].** The addition of alkaline element improves the chemical stability by modifying the glass network due to their charge transfer with the neighbor host element **[4].** Optical material activated by Nd3+ ions are very interesting for emitting devices. Especially Nd^{3+} ions are very attractive active media for powerful solid-state laser working in the NIR spectral region [5]. Dinesh Kumar *et al.,* (2019) had studied Nd^{3+} doped sodium strontium borate glasses their results shows that their prepared glasses are suitable for thermoluminescence device materials **[6].** Photoluminescence properties have not been investigated. Kashif. *et al.,* (2020) had studied Nd^{3+} ion doped lithium borate glasses their result show their prepared glasses are the potential for application of "photovoltaics" **[7].** they have not studied NIR emitting solid state device applications. Y. S. Ramah *et al.,* (2022) had studied cadmium lead-borate glasses doped with Nd^{3+} ions and their investigations show that the materials are applicable for optoelectronics and photo electric devices [8]. NIR emitting device applications have not been studied.

In present work we focus on the optical properties of Nd^{3+} ions doped in Calcium -Aluminum-Borate-Barium-Sodium glass matrix. The direct and indirect band gaps Nd^{3+} concentration dependent was evaluated. The optical properties of CaO-Al_2O_3-BaO-B_2O_3-Na-Nd_2O_3(where x=0.1,0.3, and 0.5 mol%) host glass were optimized for Nd^{3+} concentration and understand the feasibility of using it for NIR emitting solid state device applications.

3.1.1 Methodology

The glass system of 23CaO-10Al_2O_3-(51-X) B_2O_3-6BaO-10Na_2O-XNd_2O_3 where X=0.1,0.3, and 0.5, (coded as CaAlBBaNaNd0.1,CaAlBBa NaNd0.3, CaAlB BaNaNd0.5 mol%) where prepared by conventional melt quenching technique. The high purity chemicals $CaCO_3$, Al_2O_3, H_3BO_3, $BaCO_3$, Na_2CO_3, and Nd_2O_3 were mixed and grinded by using agate, mortar to make fine powder and the total amount of each batch of glass formula was thoroughly mixed till it obtained a homogeneous mixture and weighed to 15 gm. The prepared mixture was then heated at 11500 C for 3hours, the homogeneous oxides melt remained and then swiftly dispensed on the brass plate that had been pre - heated, and it was quenched to create uniform thick glass samples. To reduce thermal stress, the glass underwent an entire day of annealing at 550^0C before being allowed to cool gradually to ambient temperature. The powdered approach was utilized to capture the X-ray diffraction pattern of glass samples. Cu K-α with a wavelength of 1.54 nm, was employed as a source in the Diffractometer. The FTIR spectra were recorded at room temperature using Perkin Elmer Lambda PRONTIER(MIV-FTIR) The acquired glass sample were shaped for characterization. Using Perkin Elmer lambda 950 UV/VIS/NIR spectrophotometer, the optical absorption spectra of present glass were measured in UV/VIS/NIR region of 250-2500nm. The photoluminescence spectra were recorded using near-infrared spectrophotometers (Quanta Master (QM)-300, PTI-Horiba) using Xenon as a source.

3.2 Results and Discussion

3.2.1. Physical properties

Table 1. Glass samples with different compositions

Samples	**Glass composition (mol%)**
$CaAlBBaNaNd_{0.1}$ (N1)	$23CaO-10Al_2O_3-50.9B_2O_3.6BaO-10Na_2O--0.1Nd_2O_3$
$CaAlBBaNaNd_{0.3}$ (N2)	$23CaO-10Al_2O_3-50.7B_2O_3.6BaO-10Na_2O--0.3Nd_2O_3$
$CaAlBBaNaNd_{0.5}$ (N3)	$23CaO-10Al_2O_3-50.5B_2O_3.6BaO-10Na_2O--0.5Nd_2O_3$

Table 2. Physical properties of Nd_2O_3 concentration doped in oxide borate glasses.

Physical properties	**N1**	**N2**	**N3**
Density(g/cm^3)	2.55	1.92	2.57
Molar volume(cm^3/mol)	29.54	38.96	29.34
Refractive index (n)	1.57	1.57	1.57
Dielectric constant(Ɛ)	2.46	2.46	2.46
Nd^{3+}ionconcentration ($x10^{21}$ions/cm^3)	20.45	15.39	20.63
Polaron radius (A°)	5.57	4.25	3.26
Interionic distance r_i(A°)	7.61	5.81	4.46
Field Strength ($Fx10^{20}$)cm^{-2}	9.64	1.65	2.80
Average boron-boron separation (d_{B-B})(A°)	2.25	2.48	2.25
Molar refraction (R)(cm^3/mol)	9.55	12.78	9.62
Molar cation polarizability (α_{cat})	3.79	5.07	3.82
No. of oxides in chemical formula (N_{O2}^-)	2.22	2.22	2.22
Electronic oxide polarizability (α_{o2}-n)	1.60	2.17	1.61
Optical basicity(Λ)	0.62	0.90	0.63
Metallization Criteria(M)	0.86	0.86	0.86
Theoretical Basicity(Λ_{theo})	0.69	0.69	0.69

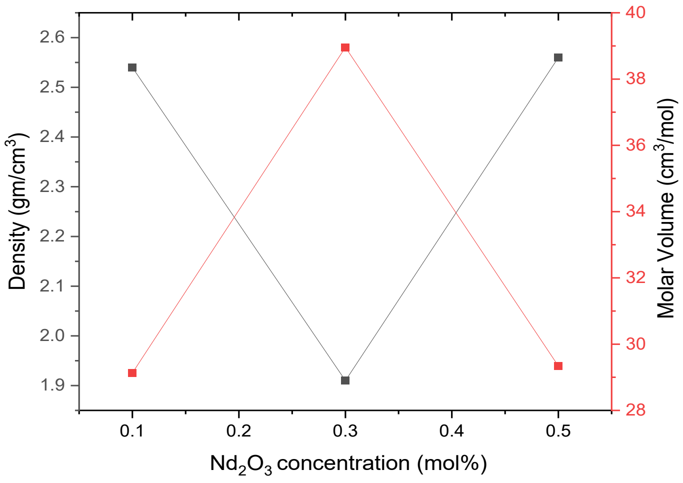

Fig 3.1. Density, Molar volume Vs concentration of Nd_2O_3

3.2.2. Density, molar volume and dielectric constant:

With the addition of Nd_2O_3, the samples' average molecular weight rises. Since (Nd_2O_3), which has a greater molecular weight (336.4782), substitutes (B_2O_3), which has a lower molecular weight (69.6202), this is evident. In relation to the geometrical configuration, cross-link density, interstitial space sizes, coordination number, and refractive index, changes in the density of the glass can have an impact on the optical band gaps of the glass system. The density values in the current glass are 2.55, 1.92, and 2.57; following the first value, the second value decreased to 1.92; the first value increases as a result of the substitution of Nd_2O_3 with B_2O_3, which has a greater molecular weight. While the creation of non-bridging oxygen (NBO) atoms in the glass matrix may be responsible for the drop-in density in the second sample. The nature of the glass density and the modifying impact of neodymium ions by producing interstitial gaps with NBO in the glass matrix are credited with the trend of the molar volume of its values. Due to the excessive dopant concentration in the glass, the polaron radius and interionic distance shrank as the concentration of neodymium ions rose. The other physical parameters like field strength, average boron-boron separation, molar cation polarizability, electronic optical polarizability, optical basicity, metallization criteria were calculated using the relations given in literatures **[9-10].**

3.2.3.X-Ray Diffraction Studies:

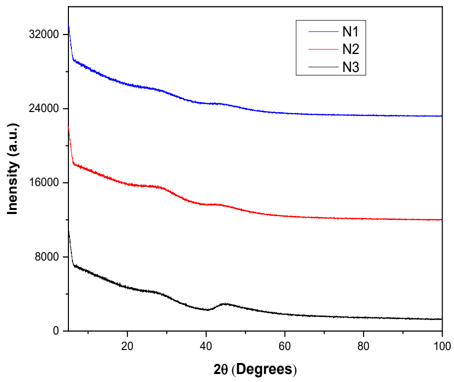

Fig.3.2. X-Ray diffraction patterns of CaAlBBaNaNd glasses.

The Figure shows the X-ray diffraction profiles of all the glass samples doped with Nd^{3+} ions. For all of the samples, the diffracted intensity was measured for the angular distribution of scattered x-ray energy between 0^0 and 100^0. No sharp peaks were observed in XRD spectra indicating that all of the synthesized CaAlBBaNaNd glass samples are amorphous in nature. **[11].**

3.2.4.IR Studies:

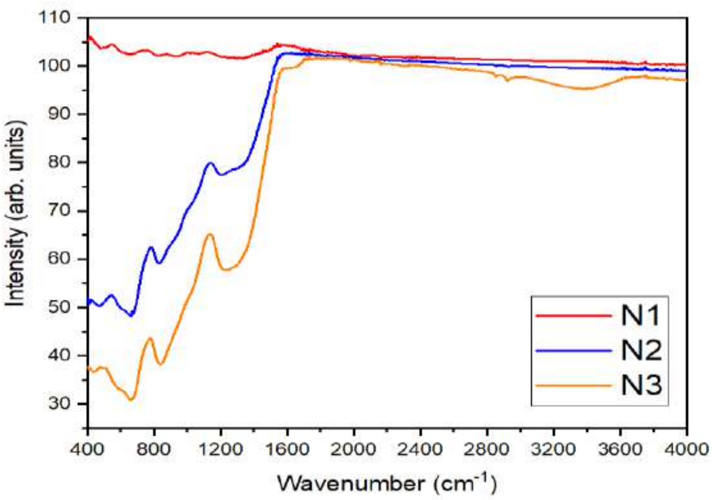

Fig.3.3. FTIR of CaAlBBaNaNd glasses.

The analysis of IR spectra can reveal information on the rotation and vibration of different molecules within a glass matrix. The features of a molecule's vibrations are related to frequency; these vibrations are distinct from those of other groups of molecules in the matrix and each has a unique characteristic of vibrational frequency. The above figure show the CaAlBBaNaNd glasses' recorded Fourier transform infrared spectra at room temperature. The spectrum shows eight conventional bands coming from different elements in the current glasses doped with Nd^{3+}ions and it reflects the functional groups significant changes in the band positions are observed from fig.

In the prepared glass samples the peaks were located at 411cm^{-1},544cm^{-1},672cm^{-1} ,826cm^{-1}, 1227cm^{-1},1659cm^{-1}, 2974cm^{-1} ,3389cm^{-1}. The intensities of these bands differ from one composition to another. The band observed at 400-500cm is due to Ca^{2+} cation vibrations. The second band observed at 769-1200 cm^{-1} due to presence of B-O bond stretching in BO_{4-} structural unit from a diborate group. The band observed at 1200-1569 due to the stretching vibrations of NBOs of trigonal units of BO_3. The existence of symmetric hydrogen bond (OH) group vibrations in the referred glasses is what causes the final strong broad band at 3389 cm^{-1}. Alkali and alkali earth elements which have functional fundamental properties vibrational wave number for the pertinent element groups present in the glass network during the formation which results in the bands seen in the spectrum **[12]**.

3.2.5. Optical Absorption studies:

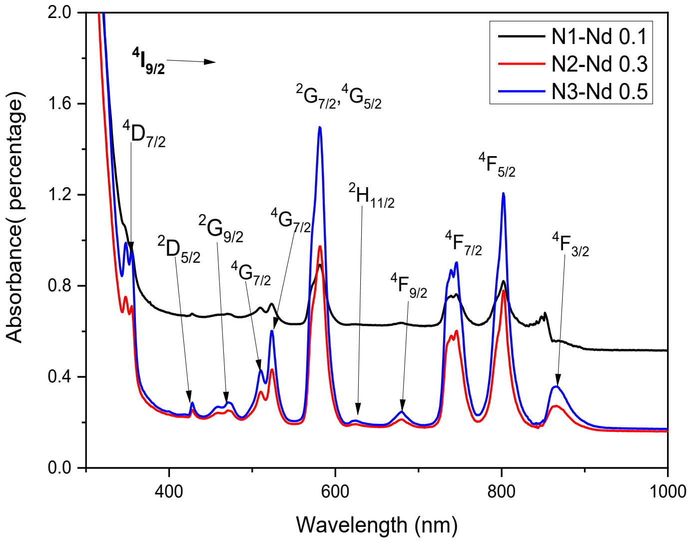

Fig.3.4. UV–Vis–NIR absorbance of CaAlBBaNaNd glasses

The optical absorption spectra of the studied glass the optical absorption of spectra consists of ten transitions that are originated from $^4I_{9/2}$, level various excited level including $^4D7_{/2,}{}^2D_{5/2,}{}^{2G}9_{/2,}{}^4G_{7/2,}{}^4G_{7/2+}{}^4G_{5/2,}{}^2H_{11/2}$, $^4F_{9/2}$, $^4F_{7/2,}{}^4F_{5/2}$ and $^4F_{3/2}$ States which are peaked at 348,427, 470, 509, 523, 580, 622, 678, 745, 802, and 866nm respectively. The spectral shapes and positions of these transitions are similar to reported ones. As can be seen from fig the strongest transitions called hyper-sensitive transitions centered at 580 nm due to transition from $^4I_{9/2}$ level $^2G_{7/2+}{}^4G_{5/2,}$ level the hyper sensitive fallows the quadrupole selection rules $\Delta J \leq 2$; $\Delta L \leq 2$; $\Delta S \leq$ O.

The optical band gap energy as illustrated in Figures 5 (direct band gap) and 6 (indirect band gap) extrapolates the absorption edge of the graph. As indicated in the table, the addition of Nd_2O_3 concentration causes both the direct and indirect band gap energy of the glasses to grow. The direct and indirect band gap energy of the glasses is determined to be in the range of 3.54 to 3.65 eV and 3.24 to 3.41 eV, respectively. The optical band gap of the glass system is impacted by such structural modifications brought about by the insertion of Nd^{3+} ions. When Nd^{3+} ions are added to glasses, the glass's structure changes, and this has an impact on the optical band gap's values. **[13,14].**

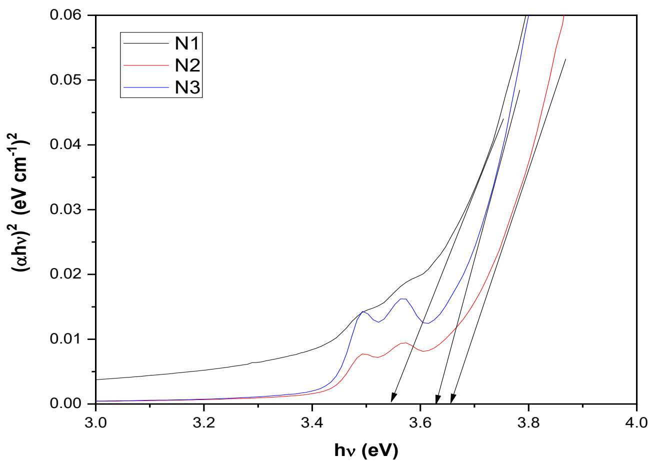

Fig.3.5. Direct energy band gap of CaAlBBaNaNd glasses

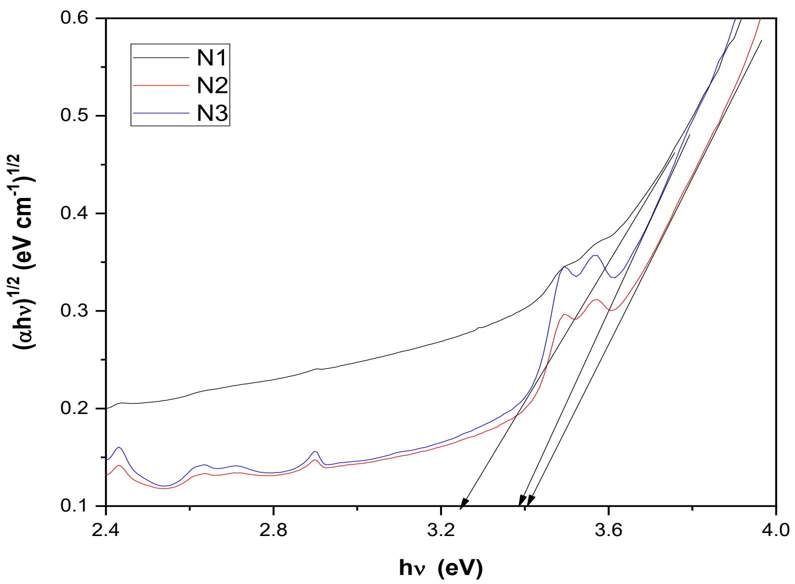

Fig.3.6.Indirect energy Band Gap of CaAlBBaNaNd glasses

Table. 3. Direct /Indirect energy band gap of the prepared Nd^{3+} glasses.

Sl.No.	Glasses	Direct band gap (eV)	Indirect band gap (eV)	References
01	(N1) CaAlBBaNaNd 0.1	3.54	3.24	Present work
02	(N2) CaAlBBaNaNd0.3	3.65	3.41	Present work
03	(N3) CaAlBBaNaNd0.5	3.62	3.38	Present work
04	M1 (borate :ca+al+na)	3.835	3.363	**[15]**
05	Nd 0.5	3.51	3.14	**[16]**
06	BBaAzNd	3.40	3.15	**[17]**

3.2.6. Luminescence studies:

3.2.6.1.NIR-Emission spectra:

The NIR emission spectra of $Nd3^{+}$ ions doped CaAlBBaNaNd glasses under 582 nm excitation wavelength were recorded and shown in the fig 7- It was focused 3 emission bands at 903, 1074, and 1345nm, these peaks were assigned as $^4F_{3/2\rightarrow}$ to $^4I_{9/2,}$ $^4F_{3/2}$ to and $^4F_{3/2}$ to $^4I_{13/2}$ respectively $^4I_{11/2}$ the emission spectra here assigned by comparing the band positions in the emission spectra with these reported in the literature. Among them the emission band at 1074nm corresponding to $^4F_{3/2}$ to $^4I_{11/2}$ transitions is the most intense and sharp. It can be seen from the emission spectra that by varying the doping concentration in the glass system, the emission intensity increases up to 0.3 mol% of neodymium before decreasing. It can be observed that during increasing concentration from 0.1 mol% to 0.5mol% of Neodymium, emission intensity is enhanced two-fold times and then decreases. The concentration quenching effect can also be seen when added in higher concentration of Nd_2O_3 content **[18-19]**. The intensity of the emission increases with increasing Nd_2O_3 content, and the transition $^4F_{3/2}$ to $^4I_{11/2}$ corresponding to 1074 nm whereas the reported literature **[20]** show at 1049 nm and literature **[21]** show at 1066.

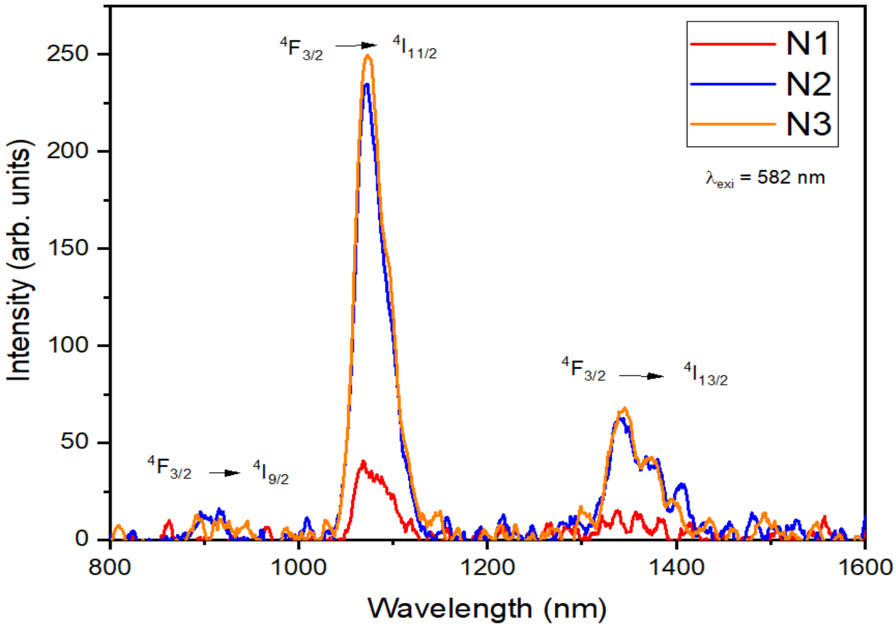

Fig.3.7. Photo luminescence Spectra of CaAlBBaNaNd glasses monitored at 582nm.

3.3 Conclusion:

The glasses were prepared using melt quenching technique. With the addition of Nd_2O_3, the samples' show average molecular weight increases. The absorbance studies of 23CaO–10Al_2O_3–(51-x) B_2O_3-6BaO-10Na_2O glass doped with various concentrations of Nd_2O_3 are evaluated using UV–VIS-NIR**.** Amorphous nature of the glass was confirmed by X-ray diffraction study. Signature bands of borate network was observed especially BO_3 and BO_4 vibrational units were observed using Fourier transform infra-red spectra. Excitation of 582 nm was used as source to excite the Nd^{3+} ions in CaAlBBaNaNd glass from $^4I_{9/2}$ ground state to $^4F_{3/2}$ excited state the peaks corresponding to $^4F_{3/2}$ to $^4I_{9/2}$ and $^4F_{3/2}$ to $^4F_{13/2}$ are absorbed at 1074 and 1341nm respectively among two bands a transitions corresponds to $^4F_{3/2}\rightarrow{}^4I_{11/2}$ (1074nm) is a potential laser transition having high intensity than the remaining transitions for all the as prepared glasses. These glasses are potential for NIR emitting solid state device applications.

References

[1] Rajagukguk J, Situmorang R, Nasution B, Rajagukguk DH, Susilorini RM, Sarumaha CS, Kaewkhao J. Synthesis and Structural Properties of Sm3+ doped Sodium Lithium zinc Lead Borate Glasses. InJournal of Physics: Conference Series 2021 Mar 1 (Vol. 1811, No. 1, p. 012112). IOP Publishing. https://doi.org/10.1088/1742-6596/1811/1/012112

[2] James JT, Jose JK, Manjunatha M, Suresh K, Madhu A. Structural, luminescence and NMR studies on Nd3+-doped sodium–calcium-borate glasses for lasing applications. Ceramics International. 2020 Dec 1;46(17):27099-109.https://doi.org/10.1016/j.ceramint.2020.07.187

[3] Shaalan M, El-Damrawi G, Hassan A, Misbah MH. Structural role of Nd2O3 as a dopant material in modified borate glasses and glass ceramics. Journal of Materials Science: Materials in Electronics. 2021 May;32(9):12348-57. https://doi.org/10.1007/s10854-021-05866-x

[4] Hemalatha S, Nagaraja M, Madhu A, Suresh K, Srinatha N. The role of Sm2O3 on the structural, optical and spectroscopic properties of multi-component ternary borate glasses for orange-red emission applications. Journal of Non-Crystalline Solids. 2021 Feb 15;554:120602. https://doi.org/10.1016/j.jnoncrysol.2020.120602

[5] Kindrat II, Padlyak BV, Lisiecki R, Adamiv VT. Spectroscopic and luminescent properties of the lithium tetraborate glass co-doped with Nd and Ag. Journal of Alloys and Compounds. 2021 Feb 5; 853:157321. https://doi.org/10.1016/j.jallcom.2020.157321

[6] Kumar D, Bhatia V, Rao SM, Chen CL, Kaur N, Singh SP. Synthesis of NaSrB: Nd3+ glass system for the analysis of structural, optical and thermoluminescence properties. Materials Chemistry and Physics. 2020 Mar 1; 243:122546. https://doi.org/10.1016/j.matchemphys.2019.122546

[7] Kashif I, Ratep A, Ahmed S. Spectroscopic properties of lithium borate glass containing Sm3+ and Nd3+ ions. IJAAS. 2020 Sep;9(3):211.https://DOI.org/10.11591/ijaas.v9.i3.pp211-219

[8] Rammah YS, Zakaly HM, Issa SA, Tekin HO, Hessien MM, Saudi HA, Henaish AM. Fabrication, physical, structural, and optical investigation of cadmium lead-borate glasses doped with Nd3+ ions: An experimental study. Journal of Materials Science: Materials in Electronics. 2022 Feb;33(4):1877-87https://doi.org/10.1007/s10854-021-07387-z

[9] Kaewjaeng S, Kothan S, Chaiphaksa W, Chanthima N, Rajaramakrishna R, Kim HJ, Kaewkhao J. High transparency La2O3-CaO-B2O3-SiO2 glass for diagnosis x-rays shielding material application. Radiation Physics and Chemistry. 2019 Jul 1;160:41-7.

https://doi.org/10.1016/j.radphyschem.2019.03.018

[10] Shaaban MH, Rammah YS, Ahmed EM, Ali AA. Fabrication, physical, thermal and optical properties of oxyfluoride glasses doped with rare earth oxides. Journal of Materials Science: Materials in Electronics. 2021 Jul;32(14):18951-67.https://doi.org/10.1007/s10854-021-06410-7

[11] Rao KV, Babu S, Balanarayana C, Ratnakaram YC. Comparative impact of Nd3+ ion doping concentration on near-infrared laser emission in lead borate glassy materials. Optik. 2020 Feb 1;202:163562.https://doi.org/10.1016/j.ijleo.2019.163562

[12] Colak SC, Kilic G. Structural, physical, and optical characterization of (Nd3+/Eu3+)-doped zinc-rich silica–borate glasses. Journal of Materials Science: Materials in Electronics. 2022 Sep;33(27):21852-63.https://doi.org/10.1007/s10854-022-08972-6

[13] Ahmad AU, Hashim S, Goshal SK. Optical traits of neodymium-doped new types of borate glasses: Judd-Ofelt analysis. Optik. 2019 Dec 1;199:163515. https://doi.org/10.1016/j.ijleo.2019.163515

[14] Munisudhakar B, Raju CN, Babu MR, Reddy NM, Moorthy LR. Luminescence characteristics of Nd3+ doped bismuth borate glasses for photonic applications. Materials Today: Proceedings. 2020 Jan 1;26:5-10.https://doi.org/10.1016/j.matpr.2019.05.349

[15] Kaewkhao J, Tamilselvan B, Pavan HL, Biju AK, Meghana EP, Tomy A, Rajaramakrishna R. Neodymium-Doped Multi-Component Borate/Phosphate Glasses for NIR Solid-State Material Applications. Integrated Ferroelectrics. 2022 Mar 28;224(1):13-32. https://doi.org/10.1080/10584587.2022.2035592

[16] Damodaraiah S, Prasad VR, Ratnakaram YC. Investigations on spectroscopic properties of Nd3+ doped alkali bismuth phosphate glasses for 1.053 μm laser applications. Optics & Laser Technology. 2019 May 1;113:322-9.https://doi.org/10.1016/j.optlastec.2019.01.010

[17] Djamal M, Yuliantini L, Hidayat R, Rauf N, Horprathum M, Rajaramakrishna R, Boonin K, Yasaka P, Kaewkhao J, Venkatramu V, Kothan S. Spectroscopic study of Nd3+ ion-doped Zn-Al-Ba borate glasses for NIR emitting device applications. Optical Materials. 2020 Sep 1;107:110018.https://doi.org/10.1016/j.optmat.2020.110018

[18] Sangwaranatee N, Chanthima N, Kaewkhao J, Tariwong Y. Synthesis and luminescence properties of lithium aluminium phosphate glasses doped with Nd3+ ion for laser medium. In Journal of physics: conference series 2020 (Vol. 1428, No. 1, p. 012032). IOP Publishing. https://DOI.org/10.1088/1742-6596/1428/1/012032

[19] Manasa P, Srihari T, Basavapoornima C, Joshi AS, Jayasankar CK. Spectroscopic investigations of Nd3+ ions in niobium phosphate glasses for laser applications. Journal of Luminescence. 2019 Jul 1;211:233-42.https://doi.org/10.1016/j.jlumin.2019.03.023

[20] Venugopal A. R, Rajaramkrishna. R, Rajashekar K, m, Wongdammem n, Kothan s *et al.*, Nd^{3+} doped B_2O_3+Li_2O+CaO+CaF_2 glass system : structural and optical properties 2022 133-133. DOI:10.1016/j.optmat.2022.112979

[21] Rajaramakrishna, R., Tariwong, Y., Srisittipokakun, N., Kothan, S., & Kaewkhao, J. (2023). 1.06 µm emission of neodymium doped P2O5+ Al2O3+ Li2O+ BaO+ Gd2O3/GdF3 glasses for solid-state NIR applications. Journal of Luminescence, 257, 119650. https://doi.org/10.1016/j.jlumin.2022.119650

CHAPTER-4

PHOTOLUMINESCENCE INTERACTION OF ALKALI FLUORIDE OVER ALKALI OXIDE IN ND^{3+} DOPED GLASSES FOR NIR APPLICATIONS

The present chapter reports the systematic analysis of borate glasses doped with Nd^{3+} ions with compositions $23CaO+10Al_2O_3+(51\text{-}x)\ B_2O_3+6BaF_2+10Na_2O+xNd_2O_3$ glasses were designed for understanding the optical properties of the emission, such as absorption, lifetime, and quantum efficiencies (QEs) of the glasses. The glasses were synthesized using the conventional melt-quenching technique at 1150^0C. The amorphous nature of the samples was confirmed by x-ray diffraction studies. The radiative QE (η) obtained from the radiative lifetime by Judd-Ofelt analysis, as well as directly measured lifetime using a 582 nm were measured and compared with other reported literature. The present work focuses on the replacement of fluorine ions to their alkali content and studied their stimulated emission cross section. The stimulated emission cross-section shows $\sigma_{emi}=25.3x10^{-21}cm^2$ and $\sigma_{emi}=18.5x10^{-21}cm^2$ for oxide (R1) and oxy-fluoride glasses (F2) with 0.5mol% Nd_20_3 content respectively. The stimulated emission cross section $\sigma_{emi}=29.9x10^{-21}cm^2$ and $\sigma_{emi}=32.5x10^{-21}cm^2$ for oxide (F1) and oxy-fluoride (A3) glasses with 1.0mol% Nd_20_3 content respectively. The data clearly suggests that addition of higher fluorine content in the glasses are suitable for NIR solid state device applications.

4.1 Introduction.

The use of Nd^{3+} glasses in the realm of technology has increased especially for applications involving photonic and solid-state devices like lasers, amplifiers, etc., rare-earth ions-doped glass is more appropriate among all the rare-earth ions, Nd^{3+} finds in the field of infrared optical communication and laser due to their efficient infrared $^4I_{9/2,11/2,13/2}$ with the emission at wavelengths around 946, 1064 and 1315 nm. The oxyfluoride glasses are found to have advantages of both oxide and fluoride glasses **[1,2].** In general, oxide glasses have good chemical resistance and stability, while fluoride glasses have very low phonon energies. However, when fluoride is replaced with oxygen, the structure and connectivity of the glass are affected. They are better suited to working in the ultraviolet spectrum and as laser materials **[3].** Among all glasses, borate glasses are being studied because of their very intriguing properties that change with variations in the cation modifier content and its size with these variations being well related to glass structure modification. These glasses also have good solubility and high transparency, act as a dopant host and are responsible for the intrinsic emission, and can be used in a variety of applications, including lasers and solid-state lighting, etc **[4,5].** M. Djmal et.at (2020), have investigated Nd^{3+} ion doped Zn-Al-Ba borate oxide glasses and reported that their glasses are applicable for NIR emitting devices **[21].** In present work instead of oxide, the addition of fluoride which enhances luminescence properties.

Mauricio Rodriguez Chilanza, *et al.*, (2021), had investigated oxy-fluoroborate glasses doped with Nd3+ and their results shows their glasses are applicable for thermoluminescence **[4].** P. Rekha rani,et.al (2020), had investigated B_2O_3-BaF_2-PbF_2-Al_2O_3 glasses. They have shown quantum efficiency is 16% for

BaPbAlFBNd2.5 glass **[13]**. In our cases we investigated quantum efficiency observed 28 to 47%. its more supportive to NIR- solid state device applications at 1.06μm.

4.1.2. Methodology

The glass sample with composition of 23CaO; $10Al_2O_3$; (51-X) B_2O_3; 6BaF2; $10Na_2O$; XNd_2O_3 Where X=0.5, and 1.0, (coded as CaAlBBaFNaNd 0.5), (coded as CaAlBBaFNaNd1.0), 23CaO; $10Al_2O_3$; (51-X) B_2O_3; 6BaF; 10NaF; XNd_2O_3 where X=0.5, (coded as CaAlBBaFNaFNd0.5), 23CaO; $10Al_2O_3$; (51-X) B_2O_3; 6BaO; 10NaF; XNd_2O_3 where X=1.0 (coded as CaAlBBaNaFNd1.0) mol% concentrations prepared by conventional melt quenching technique. The oxide chemicals with the high purity of $CaCO_3$, Al_2O_3, H_3BO_3, $BaCO_3$, Na_2CO_3, BaF_2, NaF and Nd_2O_3 were well mixed on pestle mortar and grind to fine powder till, it obtained a homogeneous mixture and weighed to 15 grams,. The prepared mixture was then heated at 1150^0 C for 3hours, the homogeneous oxides melt remained and then swifty dispensed into brass plate that had been pre - heated, it was quenched to create uniform thick glass samples. To reduce thermal stress, the glass underwent an entire day of annealing at 550^0C before being allowed to cool gradually to ambient temperature. The powdered approach was utilized to capture the X-ray diffraction pattern of glass samples. Cu K-α with a wavelength of 1.54 nm, was employed as a source in the Diffractometer. The acquired glass sample was shaped for characterization. By being cut and polished. Using Perkin Elmer lambda 950 UV/VIS/NIR spectrophotometer, the optical absorption spectra of present glass were measured in UV/VIS/NIR region of 250-2500nm. The photoluminescence spectra were recorded using near-infrared spectrophotometers (Quanta Master (QM)-300, PTI-Horiba) used as Xenon as a source.

4.2 Results and Discussion

4.2.1 Physical properties

Table 1. Physical properties of Nd_2O_3 concentration doped in barium oxide and oxy-fluoride borate glasses.

Optical Properties	*One oxygen and one fluoride Glasses*			*Two fluoride Glasses*
	BCaAlNa*O* Ba*f*Nd$_{0.5}$ (F1)	BCaAlNa*f*Ba*O* Nd$_{1.0}$ (R1)	BCaAlNa*f*Ba*f*Nd$_{0.5}$ (A3)	BCaAlNa*f*Ba*f* Nd$_{1.0}$ (F2)
Density (g/cm^3)	2.8914	2.9019	2.7946	2.7484
Molar Volume	26.511	25.732	26.714	28.376
Refractive Index (n)	1.56	1.57	1.57	1.56
Dielectric constant(Ɛ)	2.4336	2.4336	2.4649	2.4649
Optical Thickness	0.400	0.412	0.423	0.377
Polaron radius R_p (Å)	3.915	3.104	3.959	3.161
Inter-ionic radii R_i (Å)	9.534	7.558	9.643	7.696
Field strength (×10^{20})	10.00	15.91	9.779	15.34

4.2.2 Analysis of physical properties (Density, Molar volume V_m and dielectric constant):

The density of glass samples has been listed in Table.1 along with the physic al properties of Neodymium doped Calcium Aluminum Barium Sodium Barium Fluoride Sodium Fluoride–Borate glasses. From the results it’s found that mass density and V_m rises from 2.25414(gm/kg^3) to 2.90193(gm/kg^3) and 25.7306 (Cm^3/mol) to 40.7787(gm/kg^3) in accordance with the increase in mol concentration of Nd_2O_3 compositions. In The glass sample Nd_2O_3 concentration rises at the expense of B_2O_3 concentration. The increase molar weight of Nd_2O_3(336.48g/mol) which is greater than the molecular weight of the constituents in the glass samples accounts for the rise in glass density as (molecular weight of CaO, Al_2O_3, B_2O_3, BaO, Na_2O, BaF_2 and NaF are 56.08, 101.96, 69.6203, 153.33, 61.9789, 175.34, 41.998 g/mol respectively). Therefore, the glass network turns denser when Nd^{3+}ions are exchange internally along by B_2O_3. Whereas F1 glass show lower density and higher volume compared with other glasses suggesting a greater number of nonbridging oxygen's in the glass. The creation of non-bridging oxygen (NBO) and the expansion of CaAlBaNaBaFNaF borate glass network may be the causes of the rise in molar volume in the glass sample. The dielectric constant is somewhat increased by increasing the Nd_2O_3 content in the glass samples **[6,7].**

4.2.3 X-Ray Diffraction Studies:

Fig.1 Represents the X-ray diffraction profiles of all the prepared glass samples doped with Nd^{3+} ions in present work. For all of the samples the diffracted intensity was measured for the angular distribution of scattered x-ray energy between 10^0 and 100^0. Broad humps in the recorded XRD pattern plainly indicate that all of the manufactured Nd^{3+} doped glass samples are amorphous in nature **[8].**

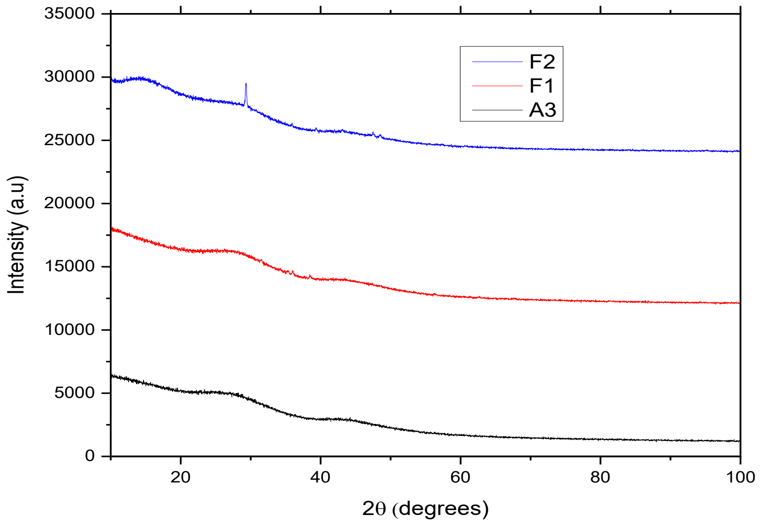

Figure 4.1 X-Ray diffraction pattern of prepared glasses

4.2.4 Optical Absorption studies:

The absorbance studies of 23CaO; $10Al_2O_3$; (51- X) B_2O_3; $6BaF_2$; $10Na_2O$; XNd_2O_3 where X=0.5, and 1.0, 23CaO; $10Al_2O_3$; (51-X) B_2O_3; 6BaF; 10NaF; $XNd_2O_3$where X=0.5, and 23CaO; $10Al_2O_3$; (51-X) B_2O_3; 6BaO; 10NaF; XNd_2O_3 1.0, glass doped with various concentrations of Nd_2O_3. The Uv- visible NIR absorption spectrum of prepared glasses. The wavelength range of 400-900 nm, recorded at room temperature, is displayed in **fig.2**. This absorption spectrum has 10 absorption bands and provides details on the non-crystalline material's band location, energy gap, and induced transitions. Centre around 430, 475, 511, 524, 583, 626, 681, 746, 803 and 875 nm which corresponding to electronic transitions state of ($^2P_{1/2}$+$^2D5_{/2}$), ($^2D_{3/2}$+$^{2G}9_{/2}$+$^2K_{15/2}$), $^4G_{9/2}$,$^4G_{7/2}$, ($^4G_{5/2}$+$^2G_{7/2}$),^{2} $H_{11/2}$,$^4F_{9/2}$ ($^4S_3/_2$+$^4F_{7/2}$) ($^4{}_{F5/2+}{}^2H_{9/2}$) and $^4F_{3/2}$ respectively of Nd^{3+} ions in the glass matrix. Electronic transition at $^4G_{5/2}$ + $^2G_{7/2}$ has highest intensity in the prepared glass samples at 626nm NIR region **[9].**

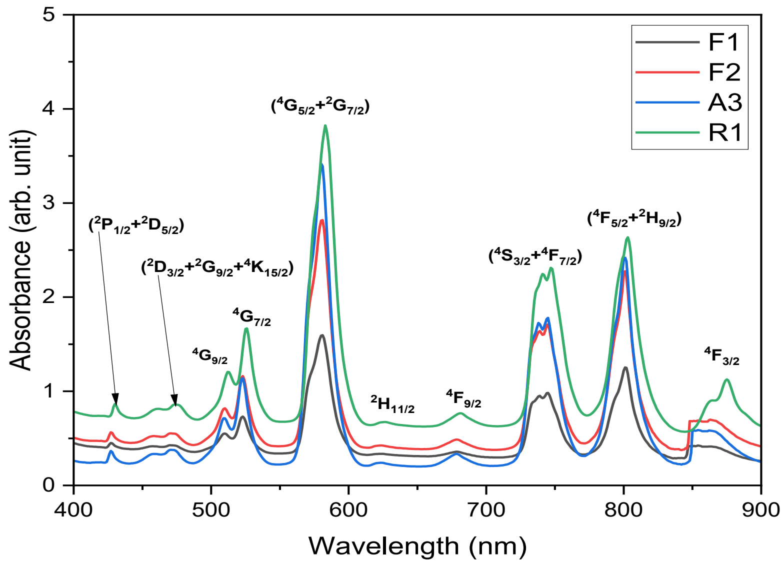

Figure 4.2. UV–Vis–NIR absorbance of BCaAlNaBaNd glasses

4.2.5 Photo-Emission spectra:

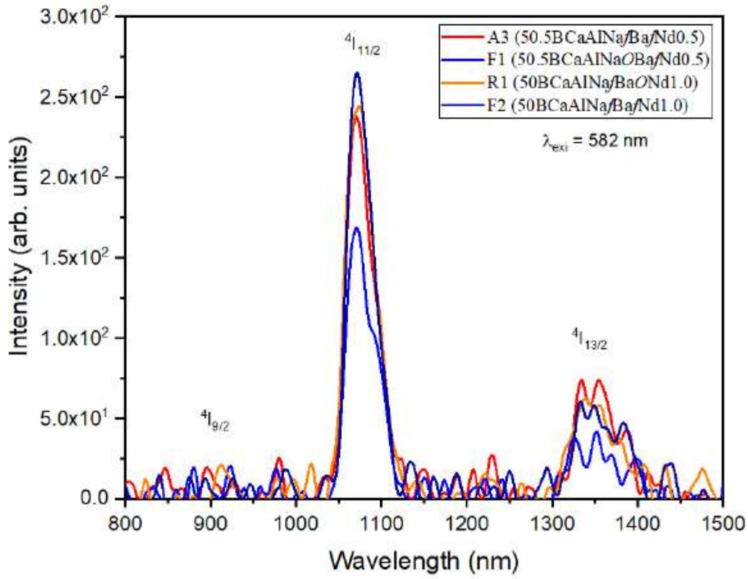

Figure 4.3 Photoluminescence Spectra of Emission of BCaAlNaBaNd glasses

The fig. 3.represents the NIR emission spectra of BCaAlNaBaNd glasses stimulated with a 582nm laser diode and doped with various Nd^{3+} ion concentrations within the spectral range of 800nm to 1500nm.The spectra reveal three intense emission bands centered at 891, 1070 and 1335nm corresponding to the $^4F_{3/2}\rightarrow{}^4I_{9/2}$ $^4F_{3/2}\rightarrow{}^4I_{11/2}$, $^4F_{3/2}\rightarrow{}^4I_{13/2}$, emission transitions respectively. There may be a transition with a higher intensity than the other two in the entire emission band at 1069nm that corresponds to the $^4F_{3/2}\rightarrow{}^4I_{11/2}$ transition. It has been noted that as the concentration of neodymium ions increases, the emission intensity of the $^4F_{3/2}\rightarrow{}^4I_{11/2}$ transition increases up to 0.5 mol% Nd_2O_3 and thereafter decreases. The concentration quenching effect may be to blame for this **[10, 11].** The emission intensity of oxyfluoride glasses is higher than that of oxide glasses. The lower phonon energy of oxyfluoride glasses is likely to be responsible for the observed discrepancy between emission intensity. Since oxyfluoride glasses have better radiative emission characteristics than oxide glasses because their phonon energy is higher **[12].**

4.2.6 Judd-Ofelt Analysis:

The J-O parameters clarify the glass network's structural characteristics, such as the type of bonding and rigidity. The table 2 displays the glass's BCaAlNaBaNd J-O measurements. As well as values for various other Nd^{3+} ion-doped CaAlBBaNaBaFNaF glasses that have been published in the literature. The J-O parameters are obtained for BCaAlNaBaNd glass are following the trends $\Omega_2>\Omega_6>\Omega_4$ and $\Omega_4>\Omega_6>\Omega_2$. Higher values of Ω_2 indicate non-symmetry in the crystal fields surrounding the location of Nd^{3+} ions as well as greater O-Nd covalency. table 3 reveals that the CaAlBBaNaBaFNaF (present) glass has greater Ω_2 values than some other host glasses. That shows more asymmetry of crystal field around Nd^{3+} ions in present glasses when compared with other glasses **[13,14,15].** Through absorption spectrum, experimental oscillator strengths (f_{exp}) of the f-f transitions of were found and are used in the work of J-O theory, in the current glasses the $\Omega_2$parameter has the greater value compare to Ω_2 and $\Omega_6$the emission intensity through the $^4F_{3/2}$ level of Nd^{3+}ions can be unique characterized, Ω_4 and $\Omega_6$intensity parameters are spectroscopic quality factors. The current oxyfluoride glasses have higher values of Ω_2 than most of the glasses in table 3 and exhibit higher covalency of Nd-O bonds and greater site asymmetry of structure around Nd^{3+} ions. In a similar manner, Ω_4, Ω_6 are related to the bulk properties of glasses **[12].**

Table 2. Assignment of absorption peaks of Nd^{3+} ions and their line strengths ($\times 10^{-6}$) and JO parameters (Ω_λ where λ=2,4,6) glasses.

Transition $^4I_{9/2}$	Level		A3		R1		F1		F2	
	(λ)	(cm^{-1})	f_{exp}	f_{cal}	f_{exp}	f_{cal}	f_{exp}	f_{cal}	f_{exp}	f_{cal}
$^4F_{3/2}$	854	11709	4.69	4.57	5.50	4.31	6.44	5.02	3.78	3.58
$^4F_{5/2}$, $^2H_{9/2}$	801	12484	10.3	9.80	7.20	2.28	8.89	9.33	6.14	6.52
$^4F_{7/2}$, $^4S_{3/2}$	745	13422	10.6	10.9	7.95	7.60	9.33	9.13	6.45	6.24
$^4F_{9/2}$	679	14727	0.31	0.87	0.41	0.64	052	0.77	0.29	0.53
$^2H_{11/2}$	624	16025	0.23	0.24	0.32	0.18	0.48	0.21	0.24	0.15
$^4G_{5/2,}$ $^2G_{7/2}$	581	17211	23.7	23.8	16.1	16.2	19.6	19.6	13.2	13.2
$^4G_{7/2,}$ $^4G_{9/2}$	523	19120	7.18	5.80	6.41	4.99	6.43	5.86	5.02	4.13
$^2G_{9/2,}$ $^2D_{3/2,}$ $^2K_{15/2}$	510	19607	0.53	0.73	0.52	0.45	0.79	0.55	0.40	0.37
	470	21276	1.57	1.75	1.73	1.56	2.54	1.83	1.51	1.29
$^2P_{1/2}$	429	23256	0.13	1.20	0.13	1.20	0.61	1.39	0.12	0.99
$^4D_{3/2,\ 5/2,}$ $^2I_{11/2,}$ $^2L_{15/2}$	353	28329	9.58	11.6	9.04	11.1	10.3	12.9	9.05	9.27
δ_{rms} (±)	11 transitions		0.866		0.945		0.996		0.420	
Ω_2 ($\times 10^{-20}$) cm^2			9.236		9.231		10.77		9.605	
Ω_4 ($\times 10^{-20}$) cm^2			2.944		0.190		5.661		7.733	
Ω_6 ($\times 10^{-20}$) cm^2			7.475		4.995		6.072		4.128	
JO Trend			$\Omega_2>\Omega_6>\Omega_4$		$\Omega_2>\Omega_6>\Omega_4$		$\Omega_4>\Omega_6>\Omega_2$		$\Omega_2>\Omega_4>\Omega_6$	

Table 3. Absorption peaks of Nd^{3+} ions and their line strengths ($\times 10^{-6}$) and JO parameters (Ω_λ where λ=2, 4, 6) glasses compared with other Nd^{3+} doped oxyfluoride glasses**.**

Sl.No.	Glass	$\Omega_2(\times 10^{20})$	$\Omega_4(\times 10^{20})$	$\Omega_6(\times 10^{20})$	J-O Trend	References
1	50.5BCaAlNa*f*Ba*f*Nd$_{0.5}$ (A3)	9.236	2.944	7.475	$\Omega_2>\Omega_6>\Omega_4$	Present Glass
2	50BCaAlNa*f*Ba*O*Nd$_{1.0}$ (R1)	9.231	0.190	4.995	$\Omega_2>\Omega_6>\Omega_4$	Present Glass
3	50.5BCaAlNa*O*Ba*f* Nd$_{0.5}$ (F1)	10.77	5.661	6.072	$\Omega_2>\Omega_6>\Omega_4$	Present Glass
4	50BCaAlNa*f*Ba*f*Nd$_{1.0}$ (F2)	9.605	7.733	4.128	$\Omega_2>\Omega_4>\Omega_6$	Present Glass
5	Oxyfluoride Glass	9.83	5.69	12.64	$\Omega_6>\Omega_2>\Omega_4$	**[12]**
6	BaPbAlFBNd1.0	5.77	3.68	4.01	$\Omega_2>\Omega_6>\Omega_4$	**[13]**
7	TBZBNd0.5	2.89	1.35	1.59	$\Omega_2>\Omega_6>\Omega_4$	**[14]**
8	Nd05Eu000	3.09	2.83	1.31	$\Omega_2>\Omega_4>\Omega_6$	**[15]**
9	OFBNd0.5	8.18	5.35	3.57	$\Omega_2>\Omega_4>\Omega_6$	**[16]**
10	1.0mol%	8.55	11.54	10.25	$\Omega_4>\Omega_6>\Omega_2$	**[17]**

4.2.7 Radiative properties:

Calculations based on the absorption spectra were used to calculate the produced glass samples' radiative characteristics such as their radiative transition probabilities (A_r), stimulated emission cross-sections (σ_e), branching ratios (β_{exp}, β_{cal}), radiative lifetime (τ_{rad}), and quantum efficiency (η) are tabulated in table.4. The computed radiative parameters all accord with the values found in the literature. The radiative emission spectra of all glasses are representing three emission bands correspondence to $^4F_{3/2} \rightarrow {}^4I_{9/2}, {}^4I_{11/2}$ and $^4I_{13/2}$ transitions are appearing around 900, 1066 and 1334 nm, respectively. Among these three bands $^4F_{3/2} \rightarrow {}^4I_{9/2}$ (900nm) is noticed that the most intense and $^4F_{3/2} \rightarrow {}^4I_{11/2}$ (1334) nm is noticed that weak intensity compared to other glasses using the J-O theory and are tabulated in the table 4. The findings of the $^4F_{3/2} \rightarrow {}^4I_{11/2}$ transitions show that the A_R is 2160 s^{-1} and 2398 s^{-1} for 0.5 and 0.5 mol% of Nd_2O_3 content in oxide (F1) and oxyfluoride (A3) glass respectively. The βCal and βExp are 0.44 and 0.43 respectively. The stimulated emission cross section σ_{emi}=29.9x$10^{-21}$$cm^2$ and σ_{emi}=32.5x$10^{-21}$$cm^2$ for oxide (F1) and oxy-fluoride (A3) glasses respectively. Similarly, for the $^4F_{3/2} \rightarrow {}^4I_{11/2}$ transitions show that A_R is 1842 s^{-1} and 1500 s^{-1} 1.0 and 1.0 mol% of Nd_2O_3 content in oxide (R1) oxyfluoride glasses (F2) respectively. The βCal are 0.43 and 0.43 respectively. The stimulated emission cross-section shows σ_{emi}=25.3x$10^{-21}$$cm^2$ and σ_{emi}=18.5x$10^{-21}$$cm^2$ for in oxide (R1) and oxy-fluoride glasses (F2) respectively. It is found that the oxy-fluoride glasses show higher stimulated emission cross section than compared to oxide glasses. When alkali ion oxygen is replaced by fluorine ion, they show more stimulated emission than compared to their oxygen counterpart. The quenching of emission intensity was not observed in the present case, the quenching can be observed due to energy transfer process through cross relaxation process **[18,19]**. Present samples retain their higher values of radiative properties for $^4F_{3/2} \rightarrow {}^4I_{11/2}$ transitions. One important factor that significantly influences lasing materials is the rate of energy extraction from a material, and the stimulated emission cross-section is a key measure for figuring out the rate of energy extraction. High optical gain materials require greater emission cross sections. Similar to this, the branching ratio is a crucial factor in determining if a certain transition has the potential for stimulated emission; it must be greater than 50% to be regarded suitable for laser applications. In our work the calculated values are more than 50% for $^4F_{3/2} \rightarrow {}^4I_{11/2}$ transition, hence the laser action is possible from $^4F_{3/2} \rightarrow {}^4I_{11/2}$ transition. table 5 show that oxyfluoride glasses exhibit greater values than oxide glasses at 1.6μm emission when compared among the samples and other reported literatures. As a result, the oxyfluoride glasses exhibit enhanced radiative characteristics and are therefore likely to be employed as a laser gain medium. **[13].**

Table 4. The emission band position (λp,nm), the stimulated emission cross-section (σ_{emi} $\times 10^{21}$ cm^2), the radiative transition probability (A_r, s^{-1}), the calculated and experimental branching ratio (β_{cal} and β_{exp}), radiative and experimental lifetime (τ in μs), and Quantum efficiency ($\eta=\tau_{exp}/\tau_{rad}$ (%)).

Transition	λp	σ_{emi}	A_r	β_{cal}	β_{exp}	τ_{rad}	τ_{exp}	η
50.5BCaAlNa*O*Ba*f*Nd$_{0.5}$	**F1**							
$^4F_{3/2} \rightarrow {}^4I_{9/2}$	900	3.92	2585	0.50	0.011			
$^4F_{3/2} \rightarrow {}^4I_{11/2}$	1066	29.9	2160	0.44	0.730	195	91.7	47.0
$^4F_{3/2} \rightarrow {}^4I_{13/2}$	1334	1.90	345.8	0.06	0.258			
50BCaAlNa*f*Ba*O*Nd$_{1.0}$	**R1**							
$^4F_{3/2} \rightarrow {}^4I_{9/2}$	900	6.34	2247	0.50	0.022			
$^4F_{3/2} \rightarrow {}^4I_{11/2}$	1066	25.3	1842	0.43	0.719	227	63.7	28.0
$^4F_{3/2} \rightarrow {}^4I_{13/2}$	1334	11.7	290.3	0.06	0.258			
50.5BCaAlNa*f*Ba*f*Nd$_{0.5}$	**A3**							
$^4F_{3/2} \rightarrow {}^4I_{9/2}$	900	3.28	2381	0.45	0.031			
$^4F_{3/2} \rightarrow {}^4I_{11/2}$	1066	32.5	2398	0.45	0.674	190	62.9	33.1
$^4F_{3/2} \rightarrow {}^4I_{13/2}$	1334	17.8	434.5	0.08	0.294			
50BCaAlNa*f*Ba*f*Nd$_{1.0}$	**F2**							
$^4F_{3/2} \rightarrow {}^4I_{9/2}$	900	2.78	1842	0.49	0.021			
$^4F_{3/2} \rightarrow {}^4I_{11/2}$	1066	18.5	1500	0.43	0.720	278	61.3	22.0
$^4F_{3/2} \rightarrow {}^4I_{13/2}$	1334	9.41	235.1	0.06	0.258			

Table 5. Radiative properties of current glasses and compared with other Nd^{3+}doped glasses.

Glass	σ(cm^2)	A_r	βCal	βExp	References
λ=900 nm					
50.5BCaAlNa*O*Ba*f*$Nd_{0.5}$ (F1)	3.92	2585	0.50	0.011	Present work
50BCaAlNa*f*Ba*O*$Nd_{1.0}$ (R1)	6.34	2247	0.50	0.022	Present work
50.5BCaAlNa*f*Ba*f*$Nd_{0.5}$ (A3)	3.28	2381	0.45	0.031	Present work
50BCaAlNa*f*Ba*f*$Nd_{1.0}$ (F2)	2.78	1842	0.49	0.021	Present work
SFB	0.91	1500	0.31	0.39	**[3]**
Oxyfluoride Glass	0.74	0933	0.2938	0.42	**[12]**
TBZBNd0.5	7.50	419.89	0.40	0.01	**[14]**
1.0mol%	6.06	2917	0.44	0.40	**[17]**
B70BI$Nd_{1.0}$	0.81	2511	0.42	0.35	**[18]**
PABLNd1.0	0.16	715.1	0.30	0.17	**[19]**
B35L$C_{of}$$Nd_{0.3}$	1.293	1412	0.471	0.425	**[20]**
BBaAZNd1.0	0.79	1419	0.39	0.37	**[21]**
λ=1066nm					
50.5BCaAlNa*O*Ba*f*$Nd_{0.5}$ (F1)	29.9	2160	0.44	0.730	Present work
50BCaAlNa*f*Ba*O*$Nd_{1.0}$ (R1)	25.3	1842	0.43	0.719	Present work
50.5BCaAlNa*f*Ba*f*$Nd_{0.5}$ (A3)	32.5	2398	0.45	0.674	Present work
50BCaAlNa*f*Ba*f*$Nd_{1.0}$ (F2)	18.5	1500	0.43	0.720	Present work
SFB	1.07	2666	0.55	0.50	**[3]**
Oxyfluoride Glass	5.65	2339	0.5686	0.51	**[12]**
TBZBNd0.5	9.07	516.3	0.5	0.72	**[14]**
1.0mol%	15.10	3091	0.47	0.54	**[17]**
B70BI$Nd_{1.0}$	3.15	2921	0.48	0.6	**[18]**
PABLNd1.0	8.53	1321.5	0.57	0.57	**[19]**
B35L$C_{of}$$Nd_{0.3}$	3.561	1585	0.528	0.478	**[20]**
BBaAZNd1.0	3.03	1842	0.51	0.54	**[21]**
λ=1334nm					
50.5BCaAlNa*O*Ba*f*$Nd_{0.5}$ (F1)	1.90	345.8	0.06	0.258	Present work
50BCaAlNa*f*Ba*O*$Nd_{1.0}$ (R1)	11.7	290.3	0.06	0.258	Present work
50.5BCaAlNa*f*Ba*f*$Nd_{0.5}$ (A3)	17.8	434.5	0.08	0.294	Present work
50BCaAlNa*f*Ba*f*$Nd_{1.0}$ (F2)	9.41	235.1	0.06	0.258	Present work
SFB	1.34	601	0.13	0.10	**[3]**
Oxyfluoride Glass	2.21	561	0.1311	0.07	**[12]**
TBZBNd0.5	3.46	102.91	0.10	0.27	**[14]**
1.0mol%	6.55	576	0.09	0.06	**[17]**
B70BI$Nd_{1.0}$	1.69	569	0.10	0.05	**[18]**
PABLNd1.0	3.29	301.1	0.13	0.26	**[19]**
B35L$C_{of}$$Nd_{0.3}$	1.003	304	0.101	0.091	**[20]**
BBaAZNd1.0	0.81	377	0.10	0.09	**[21]**

Table 6. Experimental lifetime (τ in μs), and Quantum efficiency ($\eta=\tau_{exp}/\ \tau_{rad}$ (%)) of current glasses and compared with other Nd^{3+}doped glasses.

Glass	τ_{rad}	τ_{exp}	η	**References**
50.5BCaAlNa*O*Ba*f*$Nd_{0.5}$ (F1)	195	91.7	47.0	Present work
50BCaAlNa*f*Ba*O*$Nd_{1.0}$ (R1)	227	63.7	28.0	Present work
50.5BCaAlNa*f*Ba*f*$Nd_{0.5}$ (A3)	190	62.9	33.1	Present work
50BCaAlNa*f*Ba*f*$Nd_{1.0}$ (F2)	278	61.3	22.0	Present work
GeO2:TiO2 5:1	359	151	42	**[2]**
Oxyfluoride Glass	254	227	89.30	**[12]**
BBaAZNd1.0	275	52	19	**[21]**
PANCaFN1(0.5Nd^{3+})	295	141.62	48.01	**[22]**

4.2.8 Life time analysis

Experimental life times (τ_{exp}) is found to be 47, 33, 28 and 22μs for CaAlBNa BaFNd0.5CaAlBNaBaFNd1.0, CaAlBNaFBaFNd0.5 CaAlBNaFBaNd1.0, respectively. As a result of cross relaxation from $^4F_{3/2}$+$^4I_{9/2}$ to $^4I_{15/2}$+$^4I_{15/2}$, which is what reduces the life periods of $^4F_{3/2}$ level Nd^{3+}ions in the present glasses, energy is transferred from excited Nd^{3+} ions to ground state Nd^{3+} ions. As a result, the experimental life times (τ_{exp}) are decreased with increasing Nd_2O_3 concentration due to host defects in the glass structure Because of the high phonon energy of borate glass, it is found that all present glasses have radiative life times (τ_{rad}) that are longer than experimental life times (τ_{exp}). The ratio of experimental life times to radiative life times (τ_{exp}/τ_{rad}) is used to determine the quantum efficiency of the current glasses. As stated in table 6, BCaAlNaBaNd glasses have a quantum efficiency between 22% and 47%. The low efficiency of BCaAlNaBaNd glasses suggests that the borate glasses have more non-radiative transitional processes **[22].**

4.3 Conclusions:

The glasses were synthesized with conventional melt quenching techniques by variation of oxygen and fluorine content in the stoichiometry ratio. The oxide content glasses show more density that compared to fluorine content glasses. Judd-Ofelt analysis were employed to evaluate the JO parameters and follows the trends $\Omega_2>\Omega_6>\Omega_4$ and $\Omega_4>\Omega_6>\Omega_2$. It was found that higher intensity peak 1.06μm for higher fluorine content than compared to oxygen content. It was also, noted that the oxy-fluoride glasses show higher stimulated emission cross section than compared to oxide glasses. The present glasses show quantum efficiency around 22 to 47%. The data clearly suggests that addition of higher fluorine content in the glasses are suitable for NIR solid state device applications.

References

[1] Lenkennavar SK, Eraiah B, Kokila MK. Rare earths doped oxy-fluoride glasses as candidates for generating tunable visible light. Materials Today: Proceedings. 2020 Jan 1;33:2550-4, https://doi.org/10.1016/j.matpr.2019.12.066

[2] Pisarski WA, Kowalska K, Kuwik M, Pisarska J, Dorosz J, Żmojda J, Kochanowicz M, Dorosz D. Nd^{3+} doped titanate-germanate glasses for near-IR laser applications. Optical Materials Express. 2022 Jul 1;12(7):2912-26.

https://doi.org/10.1364/OME.463478

[3] Lenkennavar SK. The synthesis and properties of oxyfluoride borate glasses incorporated with neodymium ion. Journal of Scientific Research. 2021;65(8).

DOI:10.1063/5.0002078

[4] Chialanza MR, Azcune G, Pereira HB, Gasparotto G, de Santana RC, Maia LJ, Carvalho JF. Continuous trap distribution and variation of optical properties with concentration in oxi-fluoroborate glass doped with $Nd^{3+.}$ Journal of Non-Crystalline Solids. 2021 May 1;559:120683.

https://doi.org/10.1016/j.jnoncrysol.2021.120683

[5] James JT, Jose JK, Manjunatha M, Suresh K, Madhu A. Structural, luminescence and NMR studies on Nd3+-doped sodium–calcium-borate glasses for lasing applications. Ceramics International. 2020 Dec 1;46(17):27099-109.

https://doi.org/10.1016/j.ceramint.2020.07.187

[6] Kaewjaeng S, Kothan S, Chaiphaksa W, Chanthima N, Rajaramakrishna R, Kim HJ, Kaewkhao J. High transparency La_2O_3-CaO-B_2O_3-SiO_2 glass for diagnosis x-rays shielding material application. Radiation Physics and Chemistry. 2019 Jul 1;160:41-7.

https://doi.org/10.1016/j.radphyschem.2019.03.018

[7] Shaaban MH, Rammah YS, Ahmed EM, Ali AA. Fabrication, physical, thermal and optical properties of oxyfluoride glasses doped with rare earth oxides. Journal of Materials Science: Materials in Electronics. 2021 Jul;32(14):18951-67. https://link.springer.com/content/pdf/10.1007/s10854-021-06410-7

[8] Kashif I, Ratep A. ICMMS-2: Influences the Addition of Neodymium Oxide on Structural and Optical Properties of Oxyfluoride Lead Borate Glass. Egyptian Journal of Chemistry. 2021 Mar 1;64(3):1141-7.

https://dx.doi.org/10.21608/ejchem.2021.55860.3183

[9] Rao KV, Babu S, Balanarayana C, Ratnakaram YC. Comparative impact of Nd^{3+} ion doping concentration on near-infrared laser emission in lead borate glassy materials. Optik. 2020 Feb 1;202:163562.

https://doi.org/10.1016/j.ijleo.2019.163562

[10] Sreedhar VB, Doddoji R, Kumar KK, Reddy VR. A study of NIR emission and associated spectroscopic properties of $Nd^{3+:}$ P_2O_5+ K_2O+ Al_2O_3+ ZnF_2 glasses for 1.06 μm laser applications. Journal of Non-Crystalline Solids. 2021 Feb 1;553:12052. https://doi.org/10.1016/j.jnoncrysol.2020.120521

[11] Kumar M, Ratnakaram YC. Role of TeO2 coordination with the BaF2 and Bi2O3 on structural and emission properties in Nd^{3+} doped fluoro phosphate glasses for NIR 1.058 μm laser emission. Optical Materials. 2021 Feb 1;112:110738. https://doi.org/10.1016/j.optmat.2020.110738

[12] Shoaib M, Rooh G, Chanthima N, Sareein T, Kim HJ, Kothan S, Kaewkhao J. Luminescence behavior of Nd^{3+} ions doped ZnO-BaO-(Gd_2O_3/GdF_3)-P2O5 glasses for laser material applications. Journal of Luminescence. 2021 Aug 1;236:118139. https://doi.org/10.1016/j.jlumin.2021.118139

[13] Rani PR, Venkateswarlu M, Swapna K, Mahamuda S, Talewar RA, Devi CB, Rao AS. NIR photoluminescence studies of Nd^{3+} doped B_2O_3–BaF_2–PbF_2–Al_2O_3 glasses for 1.063 μm laser applications. Journal of Luminescence. 2021 Jan 1;229:117701. https://doi.org/10.1016/j.jlumin.2020.117701

[14] Yuliantini L, Djamal M, Hidayat R, Boonin K, Kaewkhao J, Yasaka P. Luminescence and Judd-Ofelt analysis of Nd^{3+} ion doped oxyfluoride boro-tellurite glass for near-infrared laser application. Materials Today: Proceedings. 2021 Jan 1;43:2655-62. https://doi.org/10.1016/j.matpr.2020.04.631

[15] Umamaheswar G, Gelija D, Rajesh M, Sushma NJ, Gowthami T, Nagajyothi PC, Ramasamy V, Raju BD. Effect of Eu^{3+} ions on optical and fluorescence studies of Nd^{3+} ions doped zinc-lithium fluoroborate glasses. Journal of Luminescence. 2019 Mar 1;207:201-8.

https://doi.org/10.1016/j.jlumin.2018.11.015

[16] Venkateswarlu M, Swapna K, Mahamuda S, Rani PR, Kumar JS, Prasad MS, Rao AS. Concentration dependent neodymium doped oxy fluoroborate glasses for 1.08 μm laser applications. Solid State Sciences. 2021 Mar 1;113:106543

https://doi.org/10.1016/j.solidstatesciences.2021.106543

[17] Shoaib M, Rooh G, Chanthima N, Kim HJ, Kaewkhao J. Luminescence properties of Nd3+ ions doped P_2O_5-Li_2O_3-GdF3 glasses for laser applications. Optik. 2019 Dec 1;199:163218. https://doi.org/10.1016/j.ijleo.2019.163218

[18] Kumar KU, Babu P, Basavapoornima C, Praveena R, Rani DS, Jayasankar CK. Spectroscopic properties of Nd^{3+}-doped boro-bismuth glasses for laser applications. Physica B: Condensed Matter. 2022 Dec 1;646:414327.

https://doi.org/10.1016/j.physb.2022.414327

[19] Thongyoy P, Kedkaew C, Meejitpaisan P, Minh PH, Keawmon T, Rajaramakrishna R, Kaewkhao J. 1.06 μm emission of Nd^{3+}-doped aluminium barium lithium phosphate glasses for near IR laser medium material. Optik. 2022 Nov 1;269:169852. https://doi.org/10.1016/j.ijleo.2022.169852

[20] Venugopal AR, Rajaramakrishna R, Rajashekara KM, Pattar V, Wongdamnern N, Kothan S, Kaewkhao J. Nd^{3+} doped B_2O_3+ Li_2O+ CaO+ CaF_2 glass systems: Structural and optical properties. Optical Materials. 2022 Nov 1;133:112979

https://doi.org/10.1016/j.optmat.2022.112979

[21] Djamal M, Yuliantini L, Hidayat R, Rauf N, Horprathum M, Rajaramakrishna R, Boonin K, Yasaka P, Kaewkhao J, Venkatramu V, Kothan S. Spectroscopic study of Nd^{3+} ion-doped Zn-Al-Ba borate glasses for NIR emitting device applications. Optical Materials. 2020 Sep 1;107:110018.

https://doi.org/10.1016/j.optmat.2020.110018

[22] Rajagukguk J, Situmorang R, Djamal M, Rajaramakrishna R, Kaewkhao J, Minh PH. Structural, spectroscopic and optical gain of Nd^{3+} doped fluorophosphate glasses for solid state laser application. Journal of Luminescence. 2019 Dec 1;216:116738

https://doi.org/10.1016/j.jlumin.2019.116738

CHAPTER – 5A

RARE-EARTH ION EFFECT BORATE GLASS FOR THE WHITE LIGHT-EMITTING (WLED'S) DEVICE APPLICATIONS

The present chapter reports the systematic analysis of Dysprosium activated calcium aluminium barium sodium borate glasses. These were synthesized for analysis through physical, optical, structural, and Photo-luminescence properties for their use in solid state in white light emitting device applications. The Judd-Ofelt intensity parameters were evaluated to understand the oscillator strength of ligands in the said ready glasses. The possible radiative transition probabilities, branching ratio, and stimulated emission cross-section for 575nm emission showed higher values than compared to other glasses in study. The parity in the yellow to blue (Y/B) ratio of the prepared glass sample was evaluated. The study of emission spectra, evaluation of CCT and D_{UV} values for the prepared glasses displays emission in white light region of CIE diagram.

5A.1 INTRODUCTION

Recently, Solid-state device applications are bringing out the significance of energy transfer characteristics due to co-doping Rare–earth ions (REI's) contributing to optical solid-state lighting and optical fibre technology. The glass itself indicates the potential for optical device application for white light-emitting diodes (W–LED's). One of the crucial components for visible optical devices is dysprosium. Glasses offer number of benefits, including the ease with which they can be fabricated and formed into any shape. The low cost of manufacture the high degree of thermal stability and the adaptability with which they may be chemically modified to improve certain characteristics of the host glass. The Borate glass has a high hygroscopicity low chemical resistance and poor mechanical stability. In the present work Barium and sodium are chosen to improve the characteristics of borate glass. Because of its high fluorescence performance through the white light emission range, Dy^{3+} ion is one among the interesting rare earth ions (REI's) and used as an activator in glasses **[1].** Trivalent Dysprosium Dy^{3+} is a excited activated of the present trivalent lanthanide ions, and is a favourable component for the light emitted in white light region **[2].** The various glass intermediates like Al_2O_3 are interesting oxides and it has been found more effective in optical application with increase in fluorescence when doped in host materials **[3].** Borate as a glass former still requires incorporations with other oxide modifiers like alkaline oxide to improve network stability. Dy^{3+} doped glass is more fascinating to study due to its emission highly intense in the visible region 400 – 800 nm and also the effect of CaO component on luminescence properties was studied **[4,5].** The area of white light passes the line joining the blue and yellow area of the CIE 1931 Chromatic picture. Generation of white light from the materials has been made possible by varying the intensity ratio yellow to blue (Y/B) and the mole% of rare earth ions glass composition including excitation wavelengths **[6].** The reported glass works were prepared conventional melt quenching with 23CaO–10Al_2O3 – (51–x) B_2O_3 – 6BaO – 10Na_2O – xDy_2O_3 (where x = 0.1, 0.3, 0.5, and 1.0 mol%) are synthesized, characterized their optical properties, employed Judd-Ofelt analysis and compared with reported literature.

5A.1.1 Methodology

The glass samples with composition of 23CaO; 10Al_2O_3; (51-x) B_2O_3; 6BaO; 10Na_2O; xDy_2O_3 (where x = 0.1, 0.3, 0.5, 1.0, and coded CaAlBBaNaDy0.1, CaAlBBaNaDy0.3CaAlBBaNaDy0.5 and CaAlBBaNaDy1.0) mol% concentrations prepared by conventional melt quenching technique. The oxide chemicals with high purity of $CaCO_3$, Al_2O_3, H_3BO_3, $BaCO_2$, Na_2CO_3, and Dy_2O_3 were well mixed on pestle mortar and ground to fine powder till it obtained a homogeneous mixture and weighed to 15 gm. The prepared mixture was heated at 1150^{0}C for 3hours. The homogeneous oxides melt remained and then swiftly dispensed into a brass plate block that had been preheated, and it was quenched to create uniform thickness glass samples. The glass was annealed at 550^0 degree Celsius for an entire day to diminish thermal stress and it was allow to cool gradually to room temperature. The acquired glass samples were shaped properly for the characterization by being cut and polished. Using a PerkinElmer LAMBDA 950 UV/Vis/NIR spectrophotometer, the optical absorption spectra of present glass were measured in the UV-Vis-NIR region of 250-2500 nm.

5A.2 Result and Discussion

5A.2.1Physical properties

Table 1. Prepared Glass series of samples with varying compositions.

Samples	Glass composition (mol%)
(D1) CaAlBBaNaDy (0.1)	$23CaO-10Al_2O_3-50.9B_2O_3-6BaO-10Na_2O--0.1Dy_2O_3$
(D2) CaAlBBaNaDy (0.3)	$23CaO-10Al_2O_3-50.7B_2O_3-6BaO-10Na_2O--0.3Dy2O_3$
(D3) CaAlBBaNaDy (0.5)	$23CaO-10Al_2O_3-50.5B_2O_3-6BaO-10Na_2O--0.5Dy_2O_3$
(D4) CaAlBBaNaDy (1.0)	$23CaO-10Al_2O_3-50.0B_2O_3-6BaO-10Na_2O--1.0Dy_2O_3$

Table 2. Physical Properties of D series with different Dy_2O_3 Concentration.

Physical properties	**D1**	**D2**	**D3**	**D4**
Density (g/cm^3)	2.4738	2.1746	2.9603	2.8424
Molar volume (cm3/mol)	29.783	34.442	25.5086	27.219
Refractive index (n)	1.58	1.58	1.57	1.58
Dielectric constant (Ɛ)	2.496	2.496	2.496	2.496
Dy^{3+}ion concentration ($x10^{21}ions/cm^3$)	0.551	1.429	3.217	6.031
Poloran radius rp (A°)	5.018	3.653	2.789	2.262
Interionic distance ri (A°)	1.222	0.889	0.678	0.550
Field Strength ($F \times 10^{20}$) cm^{-2}	0.148	0.279	0.479	0.728
Average boron- boron separation (dB-B) (A°)	3.931	3.957	3.992	4.031
Molar refraction (R) (cm^3/mol)	9.9120	11.4624	8.3691	9.0586
Molar cation polarizability (αcat)	0.253	0.253	0.253	0.253
No. of oxides in chemical formula (NO2-)	2.22	2.22	2.22	2.22
Electronic oxide polarizability (αo2-n)	1.657	1.934	1.381	1.504
Optical basicity (Λ)	0.6035	0.5170	0.7241	0.6648
Metallization Criteria (M)	0.667	0.667	0.671	0.667
Theoretical Basicity (Λtheo)	0.691	0.690	0.689	0.687

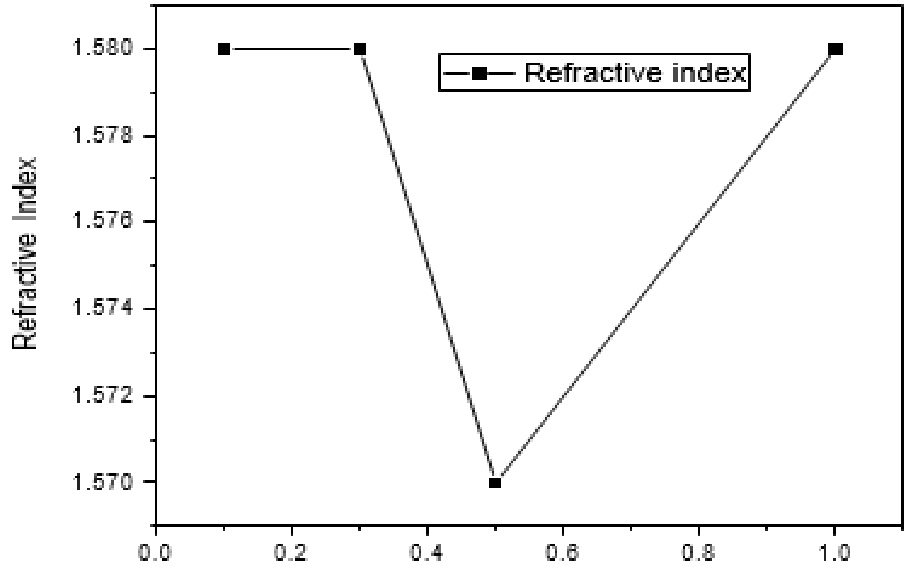

Fig. 5A.1. Refractive index Vs Concentration of Dy_2O_3 Content

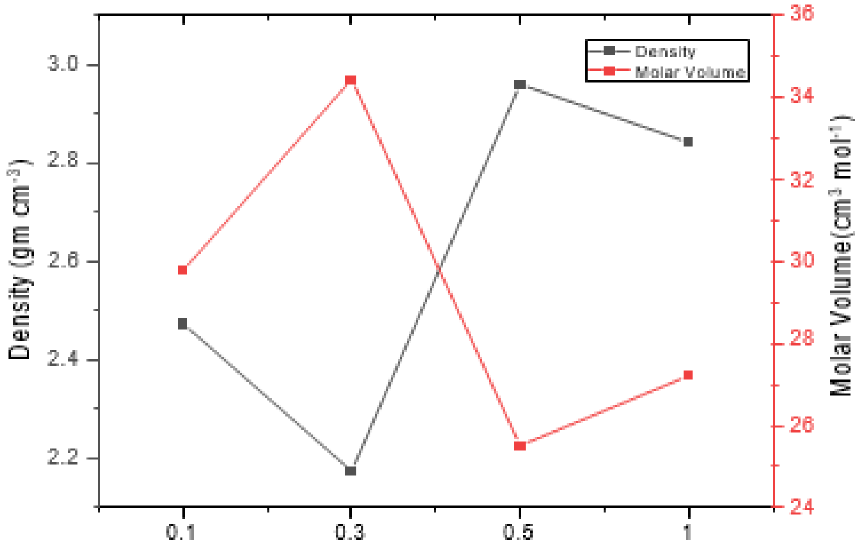

Fig. 5A.2. Density, Molar Volume Vs Concentration of Dy_2O_3 Content

5A.2.2 Analysis of physical properties (density, molar volume Vm and dielectric constant):

The density measurements were done in air and toluene by using a 3-digit sensitive microbalance (WENSAR Co Ltd) by using Archimede's principle, the density(ρ) of prepared glass measured applying ρ= {wa/(wa-wl)} where wa – the weight of glass sample in air, wl – the weight of glass sample in liquid and density of toluene (0.866 g/cm^3). The Vm calculations were done using the relation Vm = Mw/ ρg where Mw –weight mol% of glasses and ρg – mass density of glasses **[6].** The density of glass samples has been listed in Table 2 along with the physical properties of dysprosium doped Calcium Aluminium Barium Sodium –Borate glasses. From the results, it's found that density and Vm rises from 2.4738 (gm/kg^3) to 2.8424 (gm/kg^3) and 25.5086 (Cm^3/mol%) to 34.442 (gm/kg3) in accordance with the increase in mol% concentration of Dy_2O_3 composition. In the glass samples the Dy_2O_3 concentrations raises at the expense of B_2O_3 concentrations. The increase molecular weight of Dy_2O_3 (372.998 g/mol%) which is greater than the molecular weight of other constituents in the glass samples accounts for the rise in glass density. As (molecular weight of CaO, Al_2O_3, B_2O_3, BaO, Na_2O are 56.08, 101.96, 69.6203, 153.33 and 61.9789 g/mol% respectively). Therefore, the glass network turns denser when Dy^{3+}ions are exchanged internally along by B_2O_3. Whereas D2 glass show lower density and higher volume compared with other glasses suggesting more number of nonbridging oxygen's in the glass. The creation of non-bonding oxygen (NBO) and the expansion of the Calcium Aluminium Barium Sodium – Borate glass network may be increases in molar volume in the glass samples . The dielectric constant is somewhat increased by increasing the Dy_2O_3 content in the glass samples **[7].** And other physical parameters were calculated.

5A.3 IR Studies:

In IR spectra can be used to study information about the rotation and vibration of different molecules in glass matrix. Since each cluster of particles in the glass matrix has its own unique features of vibrational frequencies each group characteristic vibrations are related to frequencies. These pulsations are self-governing to that's of other groups particles existing in the matrix The below images shows the CaAlBBaNaDy glasses recorded FTIR at room temperature.

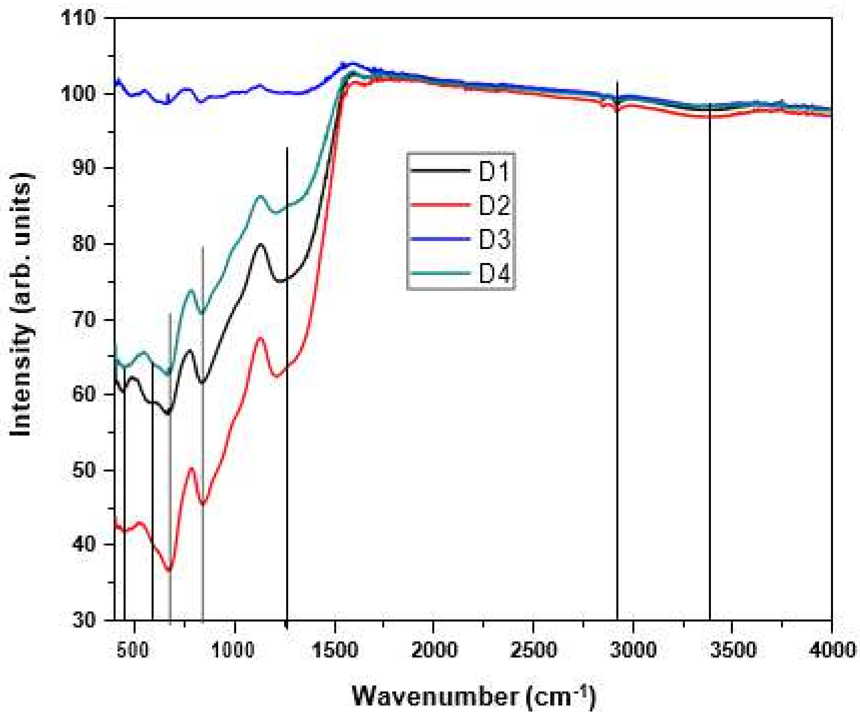

Fig.5A.3. FTIR of CaAlBBaNaDy glasses

The spectrum represents the glass matrix's functional groups which exhibits seven conventional bands originating for various elements in the present glasses doped with Dy^{3+} ions. Fig5A.3.shows the considerable shifts in band locations. The peaks where seen in the prepared glass samples at 440cm-1,583 cm-1, 669 cm-1,834 cm-1,1255 cm-1,2920 cm-1,3384cm-1. These band intensities vary from composition to composition. $Ca2^{+}$ cation vibrations are the caused the 400-500 cm-1 band that was detected **[8].** The second band observed at 769-1200 cm-1 owing to occurrence of B-O link broadening in BO4- structural unit from a di borate group. The band observed at 1200-1569 due to the stretching vibrations of NBO's of trigonal units of BO_3. The existence of synchronous of oscillation of hydrogen bond (OH) units in the named glasses is responsible for the last prominent wide band at 3384 cm-1**[9-10].**

5A.3.1 X- Ray Diffraction Studies:

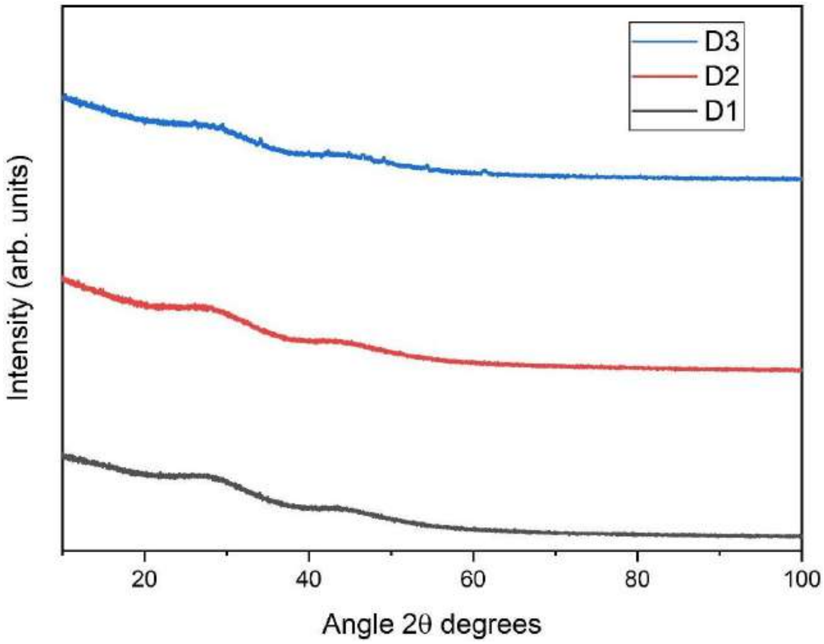

Fig.5A.4. X-Ray diffraction pattern of CaAlBBaNaDy glasses

The X –Ray diffraction characterstics of all the prepared samples activated with Dy^{3+} ions are depicted in the figure 5A.4. The intensity of the diffracted rays presented as the angular distribution of dispersed X ray energy was measured between 100 and 1000 for all samples. The XRD pattern shows large humps, it is clearly shows that all the prepared Dy^{3+} doped CaAlBBaNaDy glass samples are in amorphous nature **[11].**

5A.3.2Optical Absorption studies:

The absorbance studies of 23CaO – 10 Al_2O_3 – (51-x) B_2O_3 - 6 BaO - 10 Na_2O - x Dy_2O_3 glasses incorporated with different concentrations of Dy_2O_3 are characterized through in UV–VIS- NIR region are shown in the figure.5A.5. The absorption measurements consist of eleven interesting peaks positioned at 346, 362, 384, 423, 450, 745, 796, 889, 1077, 1255 and 1667 nm corresponding to electronic transitions of $^6P_{7/2}$, $^4P_{3/2}$, $^4F_{7/2}$, $^4G_{11/2}$, $^4I1_{5/2}$, $^6F_{3/2}$,, $^6F_{5/2}$,, $^6F_{7/2}$,, $^6F_{9/2}$, $^6H_{9/2}$, $^6H_{11/2}$ correspondingly. Electronic transition at $^6H_{9/2}$, has highest intensity in the prepared CaAlBBaNaDy glass samples at 1255 nm NIR region [11-12].

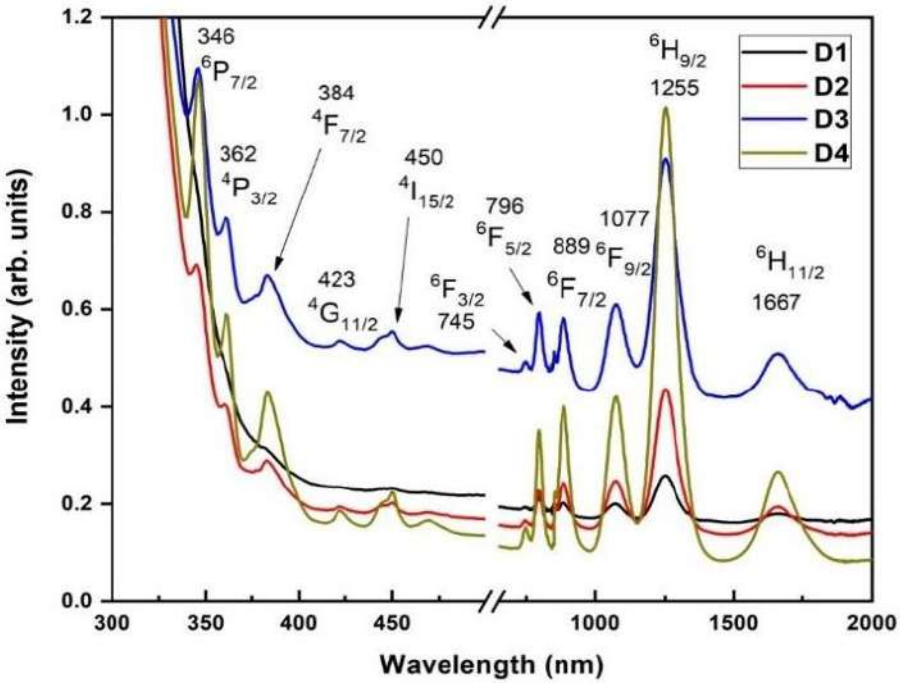

Fig.5A. 5. UV – Vis – NIR absorbance of CaAlBBaNaDy glasses

The equation can be used to express the optical absorption co-efficient (ν) that is called as optical absorption at functional edge and its frequency dependent.

$$\alpha(\nu) = [B/h\nu]\ [h\nu - Eg]n \quad (13)$$

Here, B is the optical band gap is 'Eg' and the transition type is defined by n, for direct and indirect band gaps n might be ½ and 2 respectively. When n = 2 by projecting the linear section of the contour in the light sensitive region yields the point of contact as direct band gap by plotting (hν)2 vs E graph as indicated in fig 5A.6. Eg direct = 3.76ev – 3.86 ev When n=1/2, extrapolating the linear component of the curve in the optical area and plotting (hυ) ½ vs E graph yields the values of interception as indirect band gap as indicated Eg indirect = 3.39eV-3.45 eV as shown in Fig. 5A.7. The disorderness in the glass structure can be evaluated using the Urbac energy plot ln(α) vs hν graph then taking the linear slope in the light sensitive region and reciprocating yields the value of Urbach energy EU = 0.50ev-0.58 ev. More disorderness was observed for D2 glass than compared to various Dy_2O_3 concentrations.

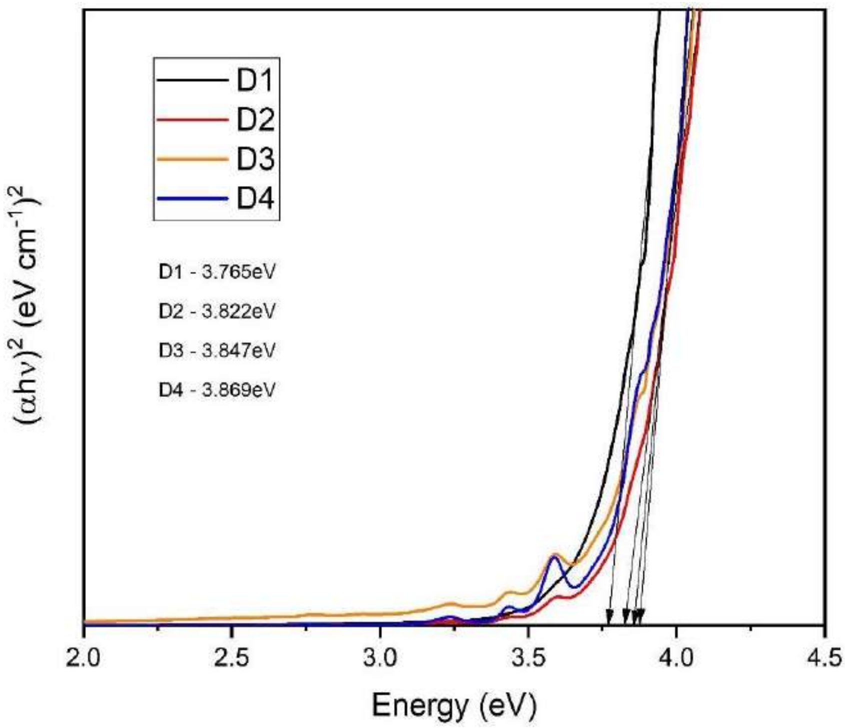

Fig.5A. 6. Direct EnergyBand Gap of CaAlBBaNaDy glasses

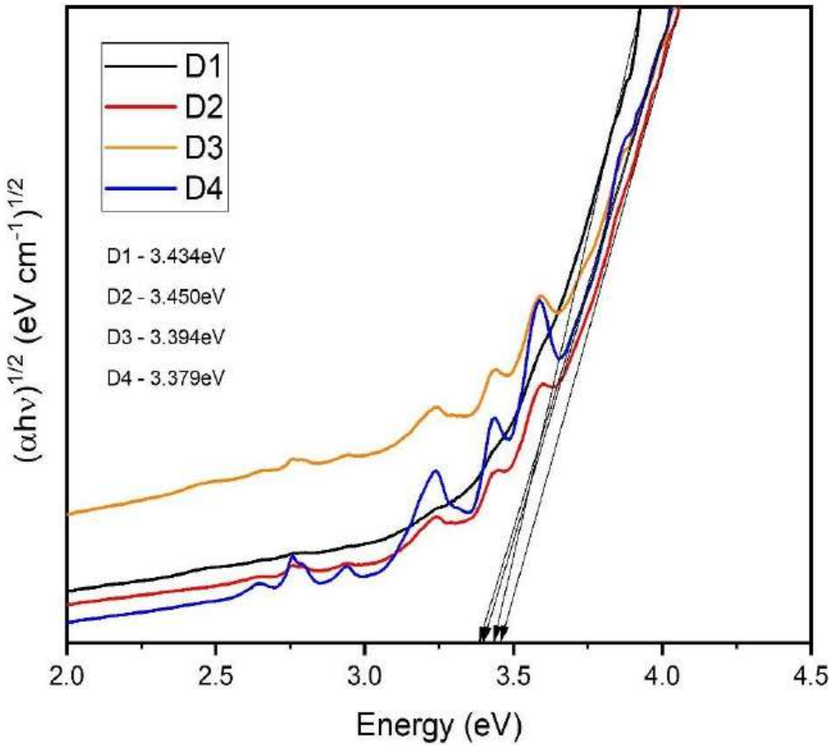

Fig.5A.7. Indirect Energy Band Gap of CaAlBBaNaDy glasses

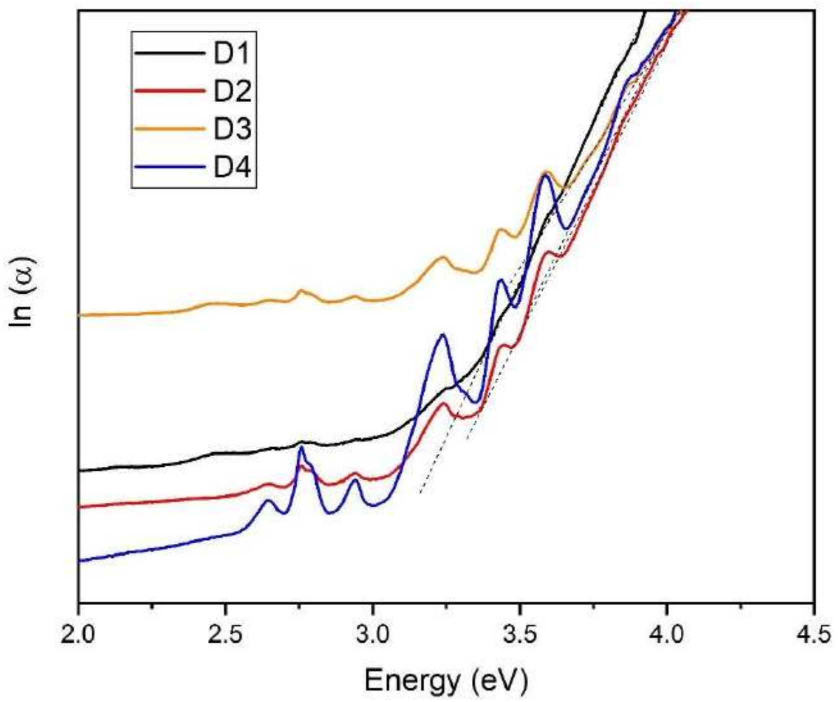

Fig.5A.8. Urbach energy of CaAlBBaNaDy glasses

Table. 3. Direct / Indirect band gap energy (optical) and Urbach energy EU of the prepared glass samples.

Sl. No.	Glasses	Direct band gap (in ev)	Indirect band gap (in ev)	Urbach Energy (EU, ev)
01	(D1) CaAlBBaNaDy0.1	3.7060	3.085	0.53
02	(D2) CaAlBBaNaDy0.3	3.8717	3.589	0.58
03	(D3) CaAlBBaNaDy0.5	3.8664	3.500	0.54
04	(D4) CaAlBBaNaDy1.0	3.8672	3.450	0.50

5A.3.3 Luminescence studies:

5A.3.3.1 Photo Excitation spectra:

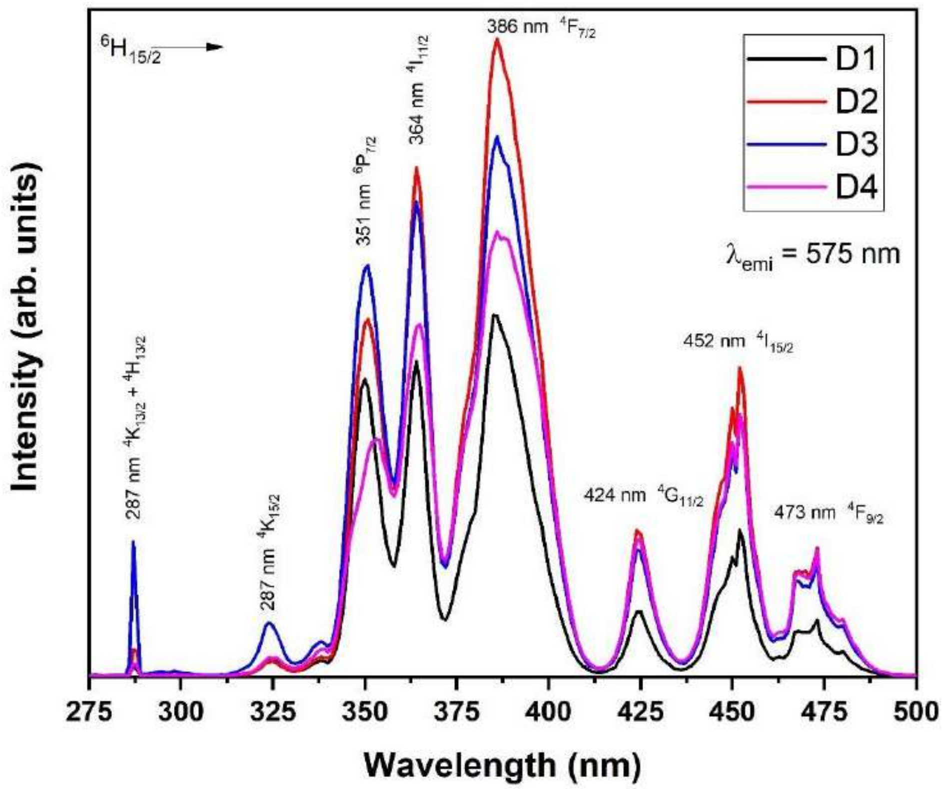

Fig.5A.9. Photoluminescence Spectra of Excitation of CaAlBBaNaDy glasses

By keeping track of emission wavelengths at 575 nm and the excitation spectrum of CaAlBBaNaDy glasses as shown in fig5A.9. The excitation spectra of the Dy^{3+} ions doped CaAlBBaNaDy series glasses have been recorded over the wavelength range 250-550 nm **[13-16].** The CaAlBBaNaDy glasses excitation spectrum which was captured at 575 nm for emission showed eight distinct peaks that ranged from the initial state ($^6H_{15/2}$) to several excited states $^6P_{3/2}$, ($^6F_{5/2}$, $^4D_{5/2}$), $^6P_{7/2}$ $^4M_{19/2}$+($^4P_{3/2}$, $^4D_{3/2}$), $^5P_{5/2}$, $^4F_{7/2}$+$^4I_{13/2}$, $^4I_{11/2}$ $^4I_{15/2}$and $^4F_{9/2}$

Since the excitation spectra of the glasses showed that the most powerful peak was at 386 nm reports represents that effective excitation might be initiated by blue or near UV wavelength which are characteristics of white light generations [13-16].

5A.3.3.2 Photo Emission spectra:

Fig.10. shows the emission spectra of the examined glasses at the excitation wavelength of 386 nm and it is made up of three observable peaks due to the transitions from the $^4F_{9/2}$ to $^6H_{15/2}$ state,$^6H_{13/2}$ and $^6H_{11/2}$ state [13-16].

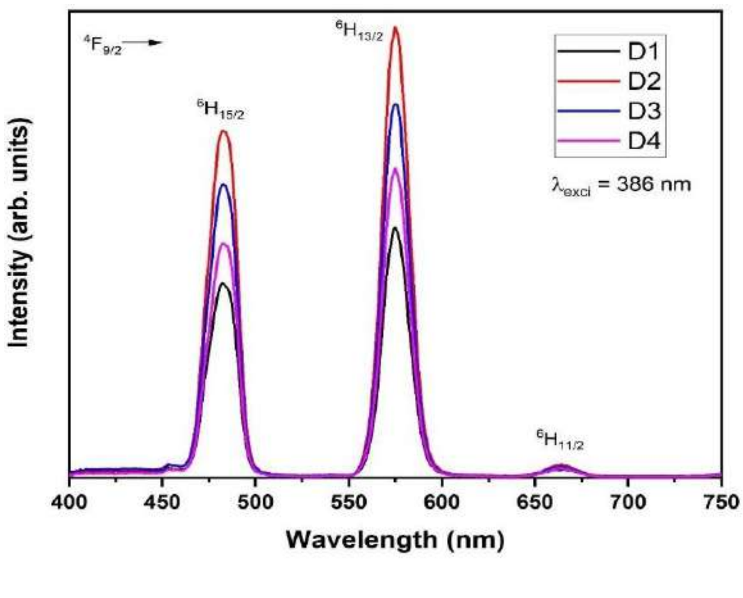

Fig.5A.10. Photoluminescence Spectra of Emission of CaAlBBaNaDy glasses

Two strong bands in the blue and yellow region with a maximum at 485 nm and 575 nm as well as a minor red band at 645 nm were identified in the emission spectrum under 386nm excitation for $^4F_{9/2}$ to $^6H_{15/2}$ transitions which are connected magnetic dipole transitions of Dy^{3+} are responsible for 485 nm (blue) emission. While the transition which is connected to an electric dipole transition of Dy^{3+} is $^4F_{9/2}$ to $^6H_{13/2}$ responsible for the 575 nm (yellow) emission. Hypersensitive and reliant on local symmetry and the electric field surrounding Dy^{3+} ions is the ED transition $^4F_{9/2}$ $^6H_{13/2}$ that follows the selection rule (L=2,J=2) . In the Dy^{3+} doped CaAlBBaNaDy glasses according to the PL emission spectrum. The yellow emission stronger than the blue emission. This represents that the rare earth ion Dy^{3+} is present in the current glass at a low symmetry site **[16-17].** Beyond 0.3 mol% Dy_20_3 level, concentration quenching effect was seen the intensity of the luminescence dropped RET phenomenon and the activation of cross relaxation pathways are to responsible for this CRC as shown in Fig.5A.11.

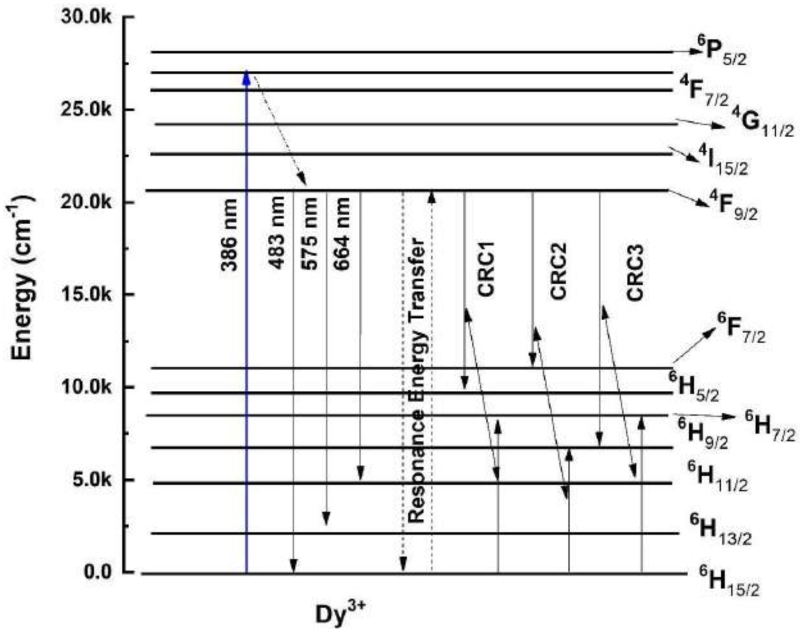

Fig.5A.11 Partial energy level diagram of CaAlBBaNaDy glasses

5A.3.4 Judd-Ofelt Analysis:

The absorption spectra synthesized Dy^{3+} doped CaAlBBaNaDy glasses have been used to evaluate the J-O intensity parameters ($\Omega\lambda$, where λ=2,4,6), and the results are shown in table 5 and it shows that the J-O parameters constituently follow the trend of $\Omega 2 > \Omega 4 > \Omega 6$ for all the current glass samples. Among the J-O intensity characteristics $\Omega 2$ is most dependent on the hypersensitive transition and is more sensitive to the local structure around the rare- earth ions (Dy^{3+}). The larger $\Omega 2$ value results from the hypersensitive transitions with higher relative oscillator strength value. The $\Omega 4$ and $\Omega 6$ parameters are connected to the bulk characteristics of the glasses such as viscosity, rigidity and a considerably higher value of the $\Omega 4$ parameters implies more stiffness in the glass network which were compared to documented literature **[11-13].** The J-O intensity characteristics of subjected glasses are observed to be equivalent to those previously known Dy^{3+} doped glasses **[14-16].**

Table.4. Judd-Ofelt parameters of the prepared CaAlBBaNaDy glasses

Wavelength	(D1)		(D2)		(D3)		(D4)	
	fexp	fcal	fexp	fcal	fexp	fcal	fexp	fcal
346			0.30	0.04	0.33	0.04	0.56	0.03
361			1.45	0.52	1.05	0.35	1.30	0.26
383	0.18	0.52	2.59	1.16	1.65	0.85	2.11	0.66
422	1.03	0.19	0.46	0.09	0.25	0.14	0.28	0.08
450	2.86	0.28	0.75	0.69	0.50	0.49	0.54	0.38
468	1.78	0.11	0.30	0.27	0.11	0.20	0.13	0.14
745	0.41	0.08	0.84	0.31	0.85	0.20	0.43	0.15
796	0.63	0.42	1.89	1.65	1.93	1.10	1.21	0.82
883	1.98	1.63	4.00	3.59	2.53	2.74	2.02	1.95
1077	3.36	3.45	3.80	3.89	3.83	3.80	2.50	2.53
1252	0.90	9.00	8.57	8.52	8.14	8.12	6.68	6.65
1657	0.63	0.95	1.59	1.94	1.27	1.45	0.91	1.13
N	10		12		12		12	
RI	1.58		1.58		1.57		1.58	
δrms	0.988		0.556		0.447		0.548	
Ω2 (×1020)	8.382		7.183		6.793		6.219	
Ω4 (×1020)	5.461		2.611		4.108		2.453	
Ω6 (×1020)	1.011		3.965		2.666		1.969	
JO Trend	Ω2> Ω4> Ω6		Ω2> Ω6> Ω4		Ω2> Ω4> Ω6		Ω2> Ω4> Ω6	

Table.5. Comparison of J-O parameters (x1020) with other Dy doped glasses.

Sl.No.	Glass	Ω2 (×10^{20})	Ω4 (×10^{20})	Ω6 (×10^{20})	J-O Trend	References
1	CaAlBBaNaDy0.1	8.382	5.461	1.011	Ω2> Ω4> Ω6	Present Glass
2	CaAlBBaNaDy 0.3	7.183	2.611	3.965	Ω2> Ω6> Ω4	Present Glass
3	CaAlBBaNaDy 0.5	6.793	4.108	2.666	Ω2> Ω4> Ω6	Present Glass
4	CaAlBBaNaDy 1.0	6.219	2.453	1.969	Ω2> Ω4> Ω6	Present Glass
5	Borate (0.8 mol%)	16.09	3.67	2.61	Ω2> Ω4> Ω6	[13]
6	BaPbAlFBDy0.5	2.48	1.55	0.98	Ω2> Ω4> Ω6	[14]
7	0.05LBTPD	8.64	4.43	3.46	Ω2> Ω4> Ω6	[15]
8	LMgBDy05	9.60	5.83	5.82	Ω2> Ω4> Ω6	[16]
9	L4BD	9.85	4.35	2.47	Ω2> Ω4> Ω6	[17]
10	0.5Dy	10.69	4.81	5.17	Ω2> Ω6> Ω4	[18]
11	0.1DyBBCZFB	6.747	2.389	2.202	Ω2> Ω4> Ω6	[19]
12	Glass A	6.02	1.73	0.82	Ω2> Ω6> Ω4	[20]
13	NBaBiBDy1.0	13.60	07.73	02.01	Ω2> Ω4> Ω6	[21]
14	BPAPbLiDy0.1	5.0624	2.1889	2.5195	Ω2> Ω6> Ω4	[22]
15	Dy_0.5	19.85	6.66	8.64	Ω2> Ω6> Ω4	[23]
16	BGGD	3.11	0.84	1.87	Ω2> Ω6> Ω4	[24]
17	Dy01	6.1242	1.2689	1.2299	Ω2> Ω4> Ω6	[25]
18	MgB2O3Dy0.2	17.62	12.36	10.84	Ω2> Ω4> Ω6	[9]

5A.3.5 Radiative transition Properties:

Radiative features such as stimulated emission cross-section (σ), radiative transition probability (AR), experimental and calculated branching ratio (β) were determined using J-O parameters emission spectra and refractive index **[30].** Table 6 shows the results of D series glasses for said transitions $^4F_{9/2} \rightarrow {}^6H_J$ (J = 15/2, 13/2, and 11/2). The stimulated emission cross-section (σ) is an important metric in the use of low threshold high gain lasers. According to table.6 the D2 glass sample has highest stimulated emission cross-section value for the highest emission peak 575 nm. This values was agreeable with experimental as well as reference values listed shown in table.7. The values observed for D2 glass sample is higher than DyNaGdP series **[26].**

Table.6. Radiative properties of prepared glass samples

Radiative Properties	D1	D2	D3	D4
482nm				
Δλeff (nm)	16.95	18.66	13.83	17.19
AR (s-1)	139.81	323.02	240.38	174.29
σ (cm2)×1020	0.337	0.859	0.4738	0.4268
βexp	0.46	0.45	0.37	0.45
βCal	0.11	0.22	0.19	0.17
575nm				
Δλeff (nm)	15.08	16.62	17.88	14.83
AR (s-1)	769.9	29.14	767.54	849.31
σ (cm2)×1020	3.467	4.207	3.960	3.635
βexp	0.52	0.53	0.61	0.52
βCal	0.65	0.60	0.61	0.62
664nm				
Δλeff (nm)	16.73	13.86	13.86	14.82
AR (s-1)	97.43	91.39	114.72	276.41
σ (cm2)×1020	0.836	0.6501	0.816	2.10
βexp	0.02	0.01	0.01	0.01
βCal	0.08	0.06	0.07	0.07

Table.7. Radiative properties of present glasses and compared with other Dy3+ doped glasses.

λ = 482nm						
Glass	Δλeff (nm)	AR (s-1)	σ (cm2)×1020	βexp	βCal	References
CaAlBBaNaDy0.1	16.95	139.81	0.337	0.46	0.11	Present work
CaAlBBaNaDy0.3	18.66	223.02	0.859	0.45	0.22	Present work
CaAlBBaNaDy0.5	13.83	240.38	0.4738	0.37	0.19	Present work
CaAlBBaNaDy1.0	17.19	174.29	0.4268	0.45	0.17	Present work
BLCFDy3	16.536	165.55	0.0448	0.0692	0.1058	[5]
0.05LBTPD	9.38	350.8	8.71	0.610	0.635	[15]
LMgBDy05	18.67	419.14	6.49	0.40	0.24	[16]
BGGD1.00	19.77	253.53	3.10	0.320	0.213	[24]
C2	16.29	440.31	1.1176	0.49	0.20	[26]
D	16.39	489.11	0.5837	0.48	0.21	[26]
BLND	16	337	6.09	0.290	0.171	[27]
LFB-Dy07	16.54	114.19	0.28	0.45	0.10	[28]
BTKA0.05D	6±1	70.77	2.84	0.126±0.0007	0.109	[29]
λ =575 nm						
CaAlBBaNaDy0.1	15.08	769.9	3.467	0.52	0.65	Present work
CaAlBBaNaDy0.3	16.62	29.14	4.207	0.53	0.60	Present work
CaAlBBaNaDy0.5	17.88	767.54	3.960	0.61	0.61	Present work
CaAlBBaNaDy1.0	14.83	849.31	3.635	0.52	0.62	Present

						work
BLCFDy3	15.006	492.31	0.2973	0.5841	0.8941	[5]
0.05LBTPD	6.68	1193.1	84.04	0.357	0.213	[15]
LMgBDy05	17.76	1031.26	33.98	0.56	0.60	[16]
BGGD1.00	19.51	835.56	20.93	0.723	0.703	[24]
C2	16.44	1425.3	6.869	0.50	0.70	[26]
D	18.91	1412.81	4.8265	0.50	0.69	[26]
BLND	16	1278	46.71	0.636	0.649	[27]
LFB-Dy07	14.26	124.11	5.29	0.53	0.70	[28]
BTKA0.05D	5±1	395.08	38.56	0.850±0.0017	0.609	[29]
λ = 664 nm						
CaAlBBaNaDy0.1	16.73	97.43	0.836	0.02	0.08	Present work
CaAlBBaNaDy0.3	13.86	91.39	0.650	0.01	0.06	Present work
CaAlBBaNaDy0.5	13.86	14.72	0.816	0.01	0.07	Present work
CaAlBBaNaDy1.0	14.82	276.41	2.10	0.01	0.07	Present work
BLCFDy3	14.799	58.3	0.0634	0.1964	0.3006	[5]
0.05LBTPD	13.23	208.9	13.27	0.033	0.063	[15]
LMgBDy05	15.37	96.45	6.53	0.02	0.06	[16]
BGGD1.00	21.00	80.03	3.27	0.069	0.067	[24]
C2	9.35	149.82	0.721	0.01	0.06	[26]
D	15.71	144.13	0.789	0.01	0.06	[26]
BLND	21	137	7.65	0.071	0.070	[27]
LFB-Dy07	17.27	154.96	1.39	0.02	0.09	[28]
BTKA0.05D	8±1	57.99	6.17	0.019±0.0007	0.089	[29]

5A.3.6 Asymmetry (Y/B) Ratio:

The asymmetry values was calculated using the Yellow to blue (Y/B) emission peak ratios for the current values to be in the range of 1.257 to 1.316 as shown in the table.8these values agreed with literature values. The created glass samples are in the same range as the other glasses and provided in the table.8. Such Y/B values variations might be utilized to tailor pure white emission.

Glass	Y/B ratio	References
CaAlBBaNaDy0.1	1.316	Present Work
CaAlBBaNaDy0.3	1.299	Present Work
CaAlBBaNaDy0.5	1.267	Present Work
CaAlBBaNaDy1.0	1.315	Present Work
NCB0	1.54	[30]
NPABSDy5	1.063	[31]
LZBSDy0.1	2.35	[32]
BiBTDy0.1	1.642	[33]
DY0.1	1.66	[34]

5.3.7 CIE Color Chromaticity Diagram:

The CIE 1931 chromaticity diagram is a color coordinate study of the glass samples under consideration. The luminescence color of the studied materials stimulated at 386 nm has a distinctive feature based on the doped rare-earth ions in the present instance Dy^{3+} ions have been analysed and the values were to be around x=0.34-0.35; y=0.38-0.39 as shown in the Table.9. The co-related color temperature (CCT) value is calculated by using these color co-ordinates (x, y) from the CIE diagram using formula **[35-36].**

CCT = -449n3 + 3535n2 - 6823n + 5520.33

where n = (x-0.332)/(y-0.186). The CCT values showed 4957 K, 4894 K, 4970 K, and 4824 K for D1, D2, D3, and D4 glasses respectively. From these results it is suggested that the studied glasses emit white emission under 386 nm excitation wavelength. The prepared glass samples show the ability to withstand high temperatures which is a basic requirement for solid-state lighting device applications.

Table.9. CIE Chromatically coordinates, and CCT(K) for CaAlBBaNaDy glasses

Glass	X	Y	CCT (K)	DUV	References
CaAlBBaNaDy0.1	0.3493	0.3828	4957	0.0133	Present Work
CaAlBBaNaDy0.3	0.3518	0.3882	4894	0.0148	Present Work
CaAlBBaNaDy0.5	0.3490	0.3846	4970	0.0142	Present Work
CaAlBBaNaDy1.0	0.3546	0.3922	4824	0.0156	Present Work
NCB0	0.371	0.400	4394	-	[32]
NPABSDy5	0.34	0.38	5107	-	[33]
LZBSDy0.1	0.321	0.347	6002	-	[34]
BiBTDy0.1	0.382	0.425	4237	-	[35]

DY0.1	0.376	0.402	4247	-	[36]
KD	0.386	0.401	4022	0.009	[37]
NaD	0.397	0.427	3928	0.017	[37]
CaD	0.391	0.421	4022	0.016	[37]
SrD	0.351	0.415	4978	0.027	[37]
BaD	0.333	0.383	5485	0.056	[37]
L15(Oxyfluoride)	0.347	0.380	5016	0.013	[38]

Delta u,v (Duv) is a significant number that displays the separation of a light color point from the black body radiation curve and is usually associated to CCT values in revealing the black body curves to a specific light source **[39].** Duv is like CCT is an important metric that provides combine scale and orientation information about a color sensitive lighting applications such as film and photography. This number is in the range ± 0.003. Duv values were calculated using the expressions found in the literature **[38, 40].** In the current glasses, Duv values are positive indicating that the color emitted photons of the glasses deviates out from the black body profile but is more situated in the yellow region of CIE 1931 diagram.

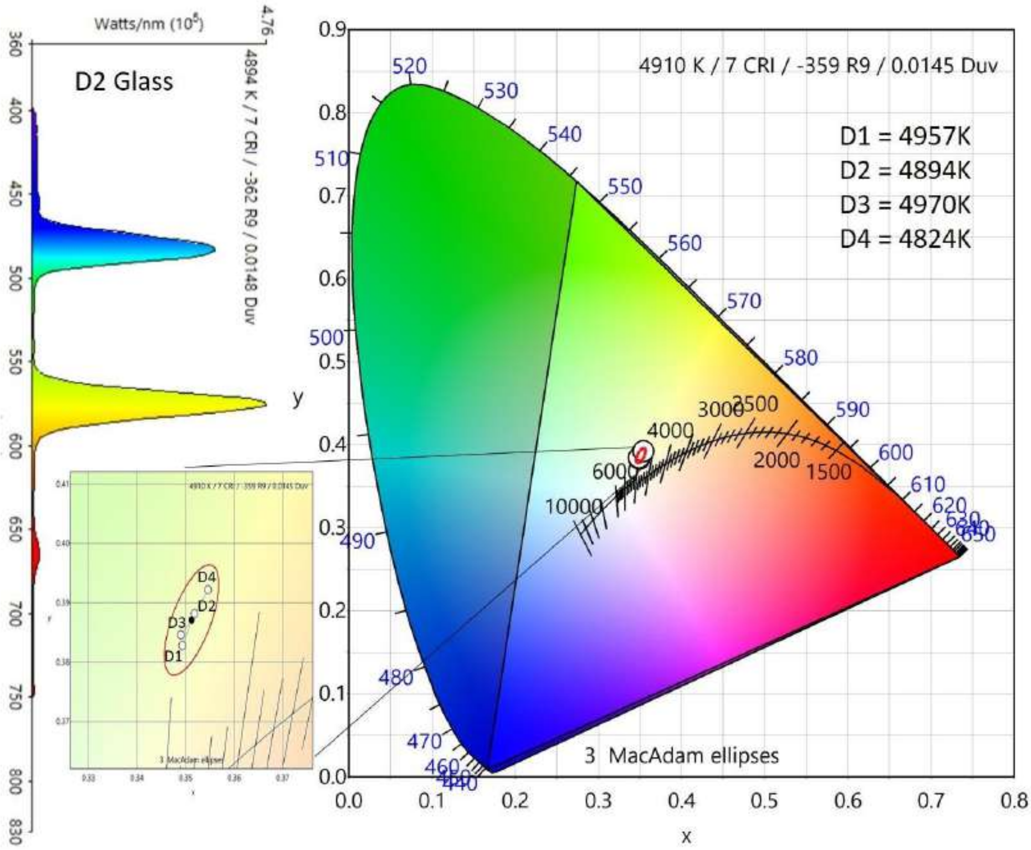

Fig.5A 11. Representation of D series glasses using CIE diagram.

Conclusions:

Glasses doped with Dy^{3+} ions were prepared by conventional melt-quenching technique. Density and molar volume of the glasses show opposite trend indicating that the glasses show a greater number of non-bridging oxygen with increase in Dy_2O_3 concentration. Average boron-boron distance increases with increase in Dy_2O_3 content suggesting that the bonding of Dy^{3+} atom with neighboring boron increases the distance between them. D2 glass show higher NBO's and oxide polarizability in the present glass system. Metallization criteria depicts these prepared glasses exhibits the insulating behavior of the samples. The basicity proves that the D2 glasses show decrease in covalency than other glasses. FTIR show presence of B-O bond stretching of BO_4- structural unit from a di borate group and stretching vibrations of NBOs of trigonal units of BO_3.Urbach energy revealed more disorderness for D2 glass sample. Judd-Ofelt theory was employed to bring out the significance of $\Omega\lambda$ (λ=2,4,6) and found that they follow $\Omega2> \Omega4> \Omega6$ trend whereas D2 follows $\Omega2> \Omega6> \Omega4$. Stimulated emission cross-section showed higher values at 575 nm and compared. The variation in asymmetry (Yellow / blue) emission peak ratio could be used to tune pure white emission. The CCT values show in the range of 4824 – 4970K and the values are comparable. The Color coordinates (x,y) and DUV also show values which are comparable suggesting that these prepared glasses can be used for white light emitting (w-LED's) solid state device applications.

References

[1] S. Ravangvomg, N. Chantima, R. Rajaramakrishna, H.J. Kim, N. Sangawaranatee, J. Kae wkhao.Dy^{3+} ions doped (Na_2O/NaF)-Gd_2O_3-P_2O_5 glasses for solid state lighting ssmaterial applications. Solid state sciences 97 (2019) 105972.

[2] D. Kothandan, R. Jeevan Kumar, Optical Properties of Rare Earth Doped Borate Glasses, International Journal of Chem Tech Research. Vol. 8, No. 6 (2015) 310-314.

[3] M. Vijayakumar, K. Maheswaran, Dinesh. K. Patel, S. Arunkumar, K. Marimuttu, Structural and optical properties of Dy^{3+}doped Aluminofluoroborophosphate glasses for White light applications. Optical materials, Vol. 37 (2014) 695- 705

[4] P.P. Pawar, S.R. Munishwar, S. Gautam, R.S Gedam. Physical, thermal, structural and optical properties of Dy^{3+} doped lithium alumino- borate glasses for bright W- LED. Journalof luminescence 183 (2017) 79 – 88.

[5] A. R. Venugopal, R. Rajaramakrishna, K.M. Rajashekhara, J. Rajaguguk, N.H. Ayachit,

S. Kothan, J. Kaewkhao. Dy^{3+} doped B_2O_3-Li_2O_3-CaO-CaF_2 glass for efficient white lightemitting sources. Journal of non-crystalline solids 554 (2021) 120604.

[6] Simranpreet Kaur, Deepawali Arora, Sunil Kumar, Gurinderpal Singh, Shaweata Mohan, Puneet Kaur, Kriti, puneet Kaur, D.P. Singh. Blue – yellow emission adjustability with aluminium incorporation for cool to warm white light generation in dysprosium doped borate glasses. Journal of Luminescence 202 (2018) 168 - 175

[7] S. Kaewjaeng, S. Kothan, W. Chiphaksa, N. Chantima, R. Rajaramakrishna,

H.J. Kim, J. Kaewkhao High transparency La2O3-CaO-B2O3-SiO2 glass for diagnosis x-rays shielding material applications. Radiation Physics and Chemistry 160 (2019) 41-47.

[8] V. Dimitrov, T. Lomatsu, An interpretation of optical properties of oxides and oxide glasses interms of the electronic ion polarizability and average single bond strength. Journal of university of chemical technology and metallurgy, 453 (2010) 219-250.

[9] A. Ichoja, S. Hashim, S. K. Ghoshal, I. H. Hashim, R. S. Omar, Physical, Structural and Optical studies on Magnesium Borate Glasses Doped with Dysprosium Ion. Journal of Rare Earths Vol. 36, Issue 12, (2018) 1264-1271.

[10] Rupesh A. Talewar, Sk. Mahamuda, K. Swapna, A.S. Rao. Near UV based Dy^{3+} ions doped alkaline - earth chloro borate glasses for white – LED's and visible lasers. Optics andLaser Technology 119 (2019) 105646.

[11] N. Luewarasirikul, J. Kaewkhao, Dy^{3+} doped Ba-Na-B white light-emitting glass for W-LED applications, Science Direct, Materials today proceeding 5, 2018, 13963-13970.

[12] M. Veeramohan Rao, B. Shanmugavelu, V.V. Ravi Kanth Kumar, Optical Absorption and Photoluminescence studies of Dy^{3+} Doped Alkaline earth Bismuth Borate Glasses. Journal of Luminescence 181 (2017) 291-298.

[13] K. Venkata Rao, S. Babu, G. Venkatayya, Y.C. Ratnakaran, Optical spectroscopy of Dy^{3+} doped borate glasses for luminescence applications, J. Mol. Structure. 1094, 2015, 274-280.

[14] P. Rekharani, M. Venkateswarlu, Sk Mahamuda, K. Swapna, Nisha Deopa, A.S. Rao, Spectroscopic studies of Dy3+ ions doped barium lead alumino fluoro borate glasses. Journalof Alloys and Compounds. 787 (2019) 503-518.

[15] S. Selvi, Venkataiah, G. Arunkumar, S. Muralidharan, G. K. Marimuthu, Structural and l uminescence studies on Dy^{3+} doped lead boro- telluro-phosphate- glasses, Physica B.Vol. 454 (2014) 72-81.

[16] L. Shamshad, G. Rooh, K. Kirdsiri, N. Srisittipokakum, B. Damdee, H.J. Kim, J. Kaewkhao, Effect of alkaline earth oxides on the physical and spectroscopic properties of Dy3+ doped Li2O-B2O3 glasses for white emitting material application. Optical Materials 64 (2017)268-275.

[17] P. Babu, C.K. Jayashankar, Spectroscopic properties of Dy^{3+} ions in lithium borate andlithium fluoro -borate glasses, Optical materials, volume 15, (2000), 65-79.

[18] L. Yuliantini, R. Hidayat, M. Djamal, P. Yasaka, K. Boonin, J. Kaewkhao, White Emission from Dy^{3+} doped borate glasses and their Judd-Ofelt analysis, 2017 5th international conference on instrumentation, communications, Information technology and biomedical engineering, Bandung, 6-7 nov.2017.

[19] K. Mariselvam, Juncheng Liu, Spectroscopic and radiative properties of Dy^{3+}: BBCZFB glass suitable for solid state yellow laser and W-LEDs applications. Optics and Laser Technology 140 (2021) 106944.

[20] K. Swapna, Sk. Mahamuda, A. Srinivasa Rao, M. Jayasimhadri, T. Sasikala, L. Rama Moorthy, Visible fluorescence characteristics of Dy3+ doped zinc alumino bismuth borate glasses for optoelectronic devices. Ceramics International 39 (2013) 8459-8465.

[21] F. Zaman, N. Srisittipokakun, G. Rooh, S.A. Khattak, J. Kaewkhao, M. Rani, H.J. Kim, Comparative study of Dy3+ doped borate glasses on the basis of luminescence and lasing properties for white light generation. Optical Materials 119 (2021) 111308.

[22] P. Arun Jegannatha Joseph, K. Maheshvaran, I. Arul Rayappan, Structural and optical studies Dy^{3+} ions doped alkali lead borophospate glasses for white light applications. Journal of Non-Crystalline Solids 557 (2021) 120652.

[23] Juniastel Rajagukguk, Lia Yulintini, Fitrilawati, Mitra Djamal and Jakrapong Kaewkhao, Investigation of Dy3+ ion doped borate glasses and their potential for WLED and Laser application. J. Eng. Technol. Sci. Vol. 52, No. 6, 2020, 891-906.

[24] Melis Gokce, Deniz Kocyigit, Spectroscopic investigations of Dy^{3+} doped borogermanate glasses for laser and w-LED applications. Optical Materials 89 (2019) 568-575.

[25] Yasha Tayal, A.S. Rao, Spectroscopic analysis of Dy3+ ions activated borosilicate glasses for photonic device applications. Optical Materials 117 (2021) 111-112.

[26] R. Rajaramakrishna, Y. Ruangtaweep, S. Sattyaporn, P. Kidkhunthod, S. Kothan,

J. Kaewkhao, Structural analysis and Luminescence studies of Ce^{3+}: Dy^{3+} co-doped calcium zinc gadolinium borate glasses using EXAFS. Radiation Physics and Chemistry 171 (2020) 108695.

[27] R.T. Karunakaran, K. Marimuthu, S. Surendra Babu, A. Arumugam, Dysprosium doped alkali fluoroborate glasses-Thermal, Structural and optical investigations. Journal of Luminescence 130 (2010) 1067-1072.

[28] F. Zaman, I. Khan, S.A. Khattak, J. Kaewkhao, Ataullah, M. Shoaib, A. Shah, G. Rooh, Investigation of luminescence and lasing properties of Dy^{3+}-doped-borate glasses for white light generation. Solid State Sciences Vol.90 (2019) 68-75.

[29] K. Annapoorani, P. Karthikeyan, Ch. Basavapoornima, K. Marimuthu, Investigations on the optical properties of Dy3+ ions doped potassium aluminiumtelluroborate glasses for white light applications. Journal of Non-Crystalline Solids Vol.476 (2017) 128-136.

[30] Pinki Narwal, Manjeet S. Dahiya, Ashish Agarwal, Ashima Hooda, Satish Khasa, Compositional Dependence of White Light Emission in Dy^{3+} Doped NaCl-BaO BismuthBorate Glasses. Vol. 209 (2019) 121-128.

[31] K. Vijay Babu, Sandhya Cole, Luminescence properties of Dy^{3+} doped alkali lead alumino borosilicate glasses, Ceramics International Vol, 44 Issue 8, (2018) 9080-9090.

[32] N. Jaidass, C. Krishna Moorthi, A. Mohan Babu, M. Reddi Babu, Luminescence properties of Dy^{3+} doped lithium zinc borosilicate glasses for photonic applications. Heliyon,Vol. 4 (2018) e00555.

[33] Y. Ananta Lakshmi, K. Swapna, K.S. Ramakrishna Reddy, Sk. Mahamuda, M. Venkateswarulu, A.S. Rao, Concentration dependent photoluminescence studies of Dy^{3+} dopedBismuth Boro-Tellurite glasses for lasers and wLEDs. Optical Materials Vol. 409 (2020)110328.

[34] M. Monisha, Nirmal Mazumder, G. Laxminarayana, Soumen Mandal, Sudha D. Kamath, Energy transfer and luminescence study of Dy^{3+} doped zinc-aluminoborosilicate glasses for white light emission. Ceramic International Vol.47 Issue 1 (2021) 598-610.

[35] L. Mishra, A. Sharma, A.K. Vishkarma, K. ha, M. Jayasimhadri, B.V. Ratman, K. Jang,A. S. Rao, R.K. Simha, J. Lumin. 169 (2019) 121-127.

[36] L. R. Moorthy, S. N. Rasool, C.K. Jayasankar, Solid State Sci. 22 (2013) 89-90.

[37] R. Divina, P. Evangelin Teresa, K. Marimuthu, Dy^{3+} ion as optical probe to study the luminescence behavior of Alkali lead bismuth borate glasses for w-LED application, Journal of Alloys and Compounds. 883 (2021) 160845.

[38] G. Lakshminarayana, K.R. Vighnesh, N.S. Prabhu, D.-E. Lee, J. Yoon, T. Park, S.D. Kamath, Dy^{3+}:B2O3−Al2O3−ZnF2−NaF/LiF oxyfluoride glasses for cool white or day white light-emitting applications, Opt. Mater. 108 (2020) 110186.

[39] Y. Ohno, Practical use and calculation of CCT and Duv, LEUKOS, J. Illum. Eng. Soc.North Am. 10 (1) (2014) 47–55.

[40] K.A. Naseer, S. Arunkumar, K. Marimuthu, The impact of Er3+ ions on the spectroscopic scrutiny of Bismuth bariumtelluroborate glasses for display devices and 1.53 μm amplification,J. Non-Cryst. Solids 520 (2019) 119463.

Chapter 5(B)

Barium oxide and oxyfluoride glasses doped with Dy^{3+} ions for WLED's applications.

The present chapter reports the systematic analysis of Dysprosium doped in aluminium calcium sodium barium borate glass synthesized and characterized properties of physical, optical, structural and photo-luminescence. The characterized glasses were analysed the results are agrees with literature values which are use in solid state in white light emitting device applications. The density and molar volume were evaluated at room temperature. optical absorption studies were carried out and has been determined variation in optical band gap for oxide and oxy-fluoride glasses in this work. The possible radiative transitions probabilities, branching ratio, stimulated emission cross -section for 575 nm emission has been evaluated for oxide and oxy-fluoride glasses and compared with other reported literatures. The asymmetry ratio (Y/B) of oxide and oxy-fluoride glasses has been evaluated. Physical, optical, structural and photoluminescence properties studies were analysed for oxide and oxy-fluoride glasses for the use in solid state white light emitting device applications.

5B.1 INTRODUCTION

The investigation of rare-earth (RE) ions doped glass has recently received a lot of attention due to its potential use in the design of a variety of optical devices, including optical memory devices, wave-guide devices, display devices, solid state lasers, Q-switching of lasers, fibre amplifiers, fluorescent lamps solar concentrator white LEDs, and sensors **[1].** Borate glasses are fascinating materials because they include rare-earth ions for structural and optical investigations **[2].** Calcium oxide is frequently used to change the structure of glasses, improving their strength and chemical stability **[3].** Hence, many academics have focused on the glass matrix of composite components to address the problem of insufficient performance of one element of glass. The oxyfluoride glass is ideal for application in the field of luminescence because to its excellent properties, which include low phonon energy and high strength **[4].** Among the rare earth ions dysprosium ($Dy^{3+)}$ ions have intriguing emission spectra. Their visible luminescence is mostly composed of two strong bands in the blue (481 nm $^4F_{9/2}\rightarrow{}^6H_{13/2}$) and yellow (575 nm $^4F_{3/2}\rightarrow{}^6H1_{5/2}$) wavelength regions **[5].** The CIE (commission international illumination) 1931 chromaticity diagram also shows that the line joining the wavelengths of yellow and blue typically passes through the region of white light. By changing a suitable yellow to blue ratio (Y/B), the glass containing Dy^{3+}ions can adapt to the white light zone and be used for solid-state lighting applications **[6].** This host glasses enhanced Dy^{3+} ions concentration and comprehend the viability of using it for solid state white light emitting device applications.

5B.1 .1 Materials and methods

2.1. Glass preparation

The glass samples with composition of oxide and oxifluoride glasses 23CaO +$10Al_2O_3$+ (51-X) B_2O_3+ 6Bao +10NaF+ XDy_2O_3 Where X=0.5, and 1.0, (coded as CaAlBBaNaFDy0.5),(CaAlBBaNaFDy1.0) 23CaO; $10Al_2O_3$; (51-X) B_2O_3; 6BaF; 1 0NaF; XDy_2O_3 where X=0.5, and 1.0, (CaAlBBaFNaFDy0.5), (CaAlBBaFNaFDy1. 0) mol% concentrations prepared by conventional melt quenching technique. The oxide chemicals with the high purity of $CaCO_3$, Al_2O_3, H_3BO_3, $BaCO_2$, Na_2CO_3, BaF_2, NaF and Dy_2O_3 were well mixed on pestle mortar and ground to fine powder till it obtained a homogeneous mixture and weighed to 15 gm. a porcelain crucible with well grinded oxides was used to place the uniform mixture in electrical muffle furnace. The prepared mixture was then heated at 1150^0C for 3hours.the homogeneous oxides melt remained and then swifty dispensed on the brass plate that had been pre heated and it was quenched to create uniform thick glass samples. The glass was annealed at 550^0 C for an entire day to diminish thermal stress and it was allowed to cool gradually to room temperature. The acquired glass sample were shaped for characterization. by being cut and polished. Using Perkin Elmer lambda 950 UV/VIS/NIR spectrophotometer, the optical absorption spectra of present glass were measured in UV/VIS/NIR region of 250-2500nm.

5B.2. Resulst and Discussion

5B.2.1 Physical properties

Table 1. Glass samples with different compositions

Samples	Glass composition (mol%)
(A1 CaAlBBaNaFDy (0.5)	23CaO-10Al_2O_3-50.5B_2O_3.6Bao-10NaF—0.5Dy_2O_3
(A2) CaAlBBaNaFDy (1.0)	23CaO-10Al_2O_3-50B_2O_3.6Bao-10NaF—1.0Dy_2O_3
(R3) CaAlBBaFNaFDy(0.5)	23CaO-10Al_2O_3-50.5B_2O_3.6BaF-10NaF—0.5Dy_2O_3
(R2) CaAlBBaFNaFDy (1.0)	23CaO-10Al_2O_3-50B_2O_3.6BaF-10NaF—1.0Dy_2O_3

Table2. Physical Properties of Dy series with different Dy_2O_3 Concentration.

Physical properties	A1	A2	R3	R2
Density(g/cm^3)	2.39367	2.91064	2.5691	2.777
Molar volume(cm^3/mol)	30.7	25.8	29.1659	27.013
Refractive index (n)	1.58	1.58	1.56	1.57
Dielectric constant(Ɛ)	2.4964	2.4964	2.433	2.464
Dy^{3+}ionconcentration (x10^{21}ions/cm^3)	2.1497	7.6831	1.1318	7.331
Poloran radius r_p(A°)	5.6747	3.7116	3.262	3.77
Interionic distance r_i(A°)	7.7483	5.0678	4.453	5.147
Field Strength (Fx10^{20}cm^{-2}	9.315	2.177	2.8194	2.1108
Average boron-boron separation (d_{B-B})(A°)	2.2919	2.1621	2.252	2.2919
Molar refraction (R)(cm^3/mol)	10.220	8.5791	9.430	8.862
Molar cation polarizability (α_{cat})	0.233387	0.233387	0.233387	0.233387
No. of oxides in chemical formula (N_{O2}^-)	2.22	2.22	2.22	2.22
Electronic oxide polarizability (α_{o2-}n)	1.7215	1.4281	1.5804	1.4789
Optical basicity(Λ)	0.6999	0.50679	0.6133	0.540
Metallization Criteria(M)	0.8679	0.8679	0.8716	0.8698
Theoretical Basicity(Λ_{theo})	0.69132	0.69132	0.69132	0.69132

5B.2.2 Analysis of physical properties (Density, Molar volumeV_m and dielectric constant)

The density measurements were done in air and toluene by using a 3 -digit sensitive microbalance (WENSAR Co Ltd) by using Archimedes 'principle, the mass density (ρ) of prepared glass measured applying by $\rho=\{W_a/(W_a-W_l)\}$ where w_a-the weight of glass sample in air, w_l the weight of glass sample in liquid and density of toluene (0.866 g/cm3). The V_m calculations were using the relation $V_m=Mw/\rho_g$ where M_w-weight mole% of glasses and ρ_g-mass density of glasses **[7].** The mass density of glass samples has been listed in table along with the physical properties of Dysprosium doped Calcium Aluminium Barium Sodium Barium Fluoride Sodium Fluoride- Borate glasses. From these result it found that mass density and Molar volume (V_m) rises from 2.39367 (kg/m^3) to 2.91064 (kg/m^3) and 2.58(cm^3/mol) to 30.7(cm^3/mol) in accordance with the increase in mol concentration of Dy_2O_3 composition. In the glass sample Dy_2O_3 concentration rises at the expense of B_2O_3 concentration. The increase molar weight of Dy_2O_3 (372.998g/mol) which is greater than the molecular weight of the constituents in the glass sample accounts for the rise in glass density as (molecular weight of Cao, Al_2O_3, B_2O_3, BaO, Na_2O, BaF_2, and NaF are 56.08, 101.96, 69.6203, 153.33, 61.9789, 175.34, 41.998 g/mol respectively). Therefore, glass network turns denser when Dy^{3+}ions are exchange internally along by B_2O3. Whereas A1 glass show lower density and higher volume compared with other glasses suggesting a greater number of non-bridging oxygen's in the glass. The creation of non-bridging oxygen (NBO) and the expansion of Calcium Aluminium Barium Sodium Barium Fluoride Sodium Fluoride- Borate glass network may be the causes of the rises in molar volume in the glass sample. The dielectric constant somewhat increased by increasing Dy_2O_3 content in the glass sample **[8].**

5B.3 X-Ray Diffraction Studies:

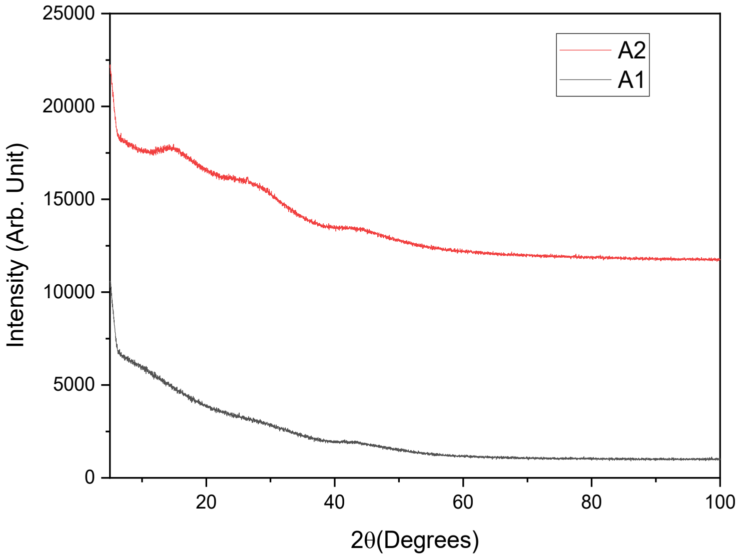

Fig. 5B.1.X-Ray diffraction pattern of CaAlBBaFNaFDy glasses

Fig 1 Represents the CaAlBBaFNaFDy glasses X-ray diffraction profile, supporting their amorphous structural nature and lack of diffraction peaks **[9].**

5B.3.1. Optical Absorption studies:

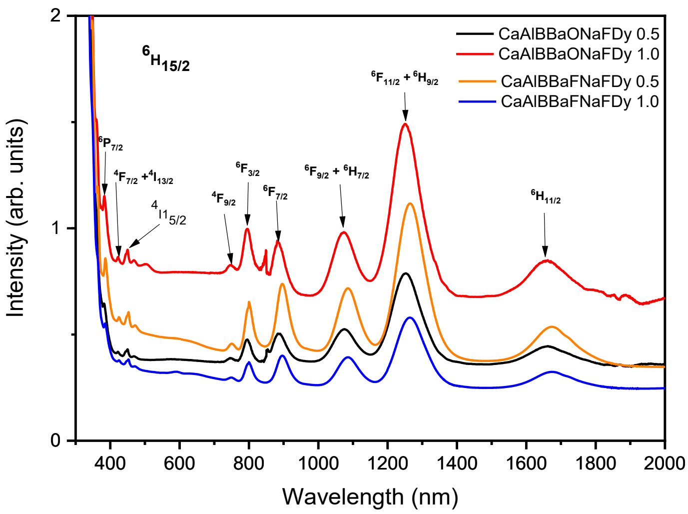

Fig.5B.2.UV-Vis-NIR absorbance of CaAlBBaFNaFDy glasses

The absorption studies of 23Cao-10Al_2O_3-(51-X) B_2O_3-6Bao-10NaF,xDy_2O_3 where x=0.5and1.0 23Cao-10Al_2o_3-(51-x) B_2o_3-6BaF -10NaF-Xdy_2O_3 where x=0.5 and 1.0 doped with various concentration of Dy_2O_3 are calculated UV-Vis-NIR region are shown in the **Fig.2.**The absorption spectra comprise of ten transition bands located at 383, 422, 451, 747, 795, 885, 1074, 1252, 1658nm and their corresponding bands are ascribed at $^6P_{7/2,}$ $^4I_{13/2}$,+$^4F_{7/2}$$^4I_{15/2}$, $^4F_{9/2,}$ $^6F_{3/2}$, $^6F_{7/2}$, $^6F_{9/2}$+ $^6H_{7/2}$, $^6F_{11/2}$+ $^6H_{9/2}$ and , $^6H_{11/2}$ transitions respectively these transitions are originating from ground state ($^6H_{15/2}$)to related excited states. The absorption bands of the as-quenched glasses are identical with the exception of variations in intensities; all band assignments have been made in accordance with the steps outlined by Carnal. In the near - infrared region of the absorption spectrum at a wavelength of 1260 nm ($^6F_{11/2}$+, $^6H_{9/2}$) and among the absorption bands, there is an electric dipole transition that is extremely intense, sharp, and broad in nature. This particular transition is hypersensitive in nature and is highly responsive to its environment by following the selection rules. $I_{\Delta S}I=0$ $I_{\Delta <}I \leq 2$, $I_{\Delta}JI \leq 2$ **[10].**

5B.3.2 Luminescence studies:

5B3.2.1 Photo-Excitationspectra:

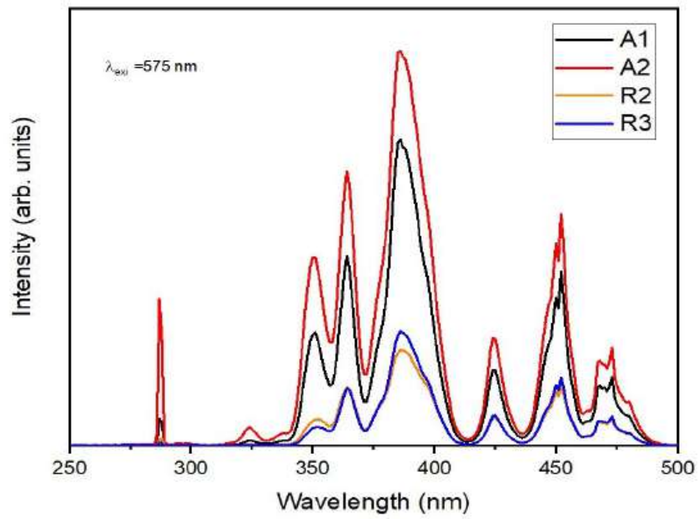

Fig.5B.3.Photoluminescence Spectra of Excitation of CaAlBBaBaFNaFdy glasses

The excitation spectra of prepared dy^{3+} ions doped CaAlBBaBaFNaFdy glasses have been recorded wavelength range 250-500nm by monitoring of emission wavelength at 575 nm and the excitation spectrum CaAlBBaFNaFdy glasses as shown in fig.3.The excitation spectra of the sample monitoring at 575 nm the excitation spectra shows peaked at 282,325,352,364,386,423,451,472nm corresponding to the transitions from ground state energy level $^6H_{15/2}$ to excited state $^6P_{3/2}$ ($^6F_{5/2}$,$^4D_{5/2}$) $^6P_{7/2}$ $^4M_{19/2}$ + ($^4P_{3/2}$, $^4D_{3/2}$), $^5P_{5/2}$, $^4F_{7/2}$+$^4I_{13/2}$, $^4G_{11/2}$,$^4I_{15/2}$, and $^4F_{9/2}$) transitions in Dy^{3+} respectively. The present work white light emission under ultraviolet light was studied and the strong excitation peak at 386 nm was chosen to generate intense powerful emission. **[11].**

5B.3.2.2 Photo emission spectra

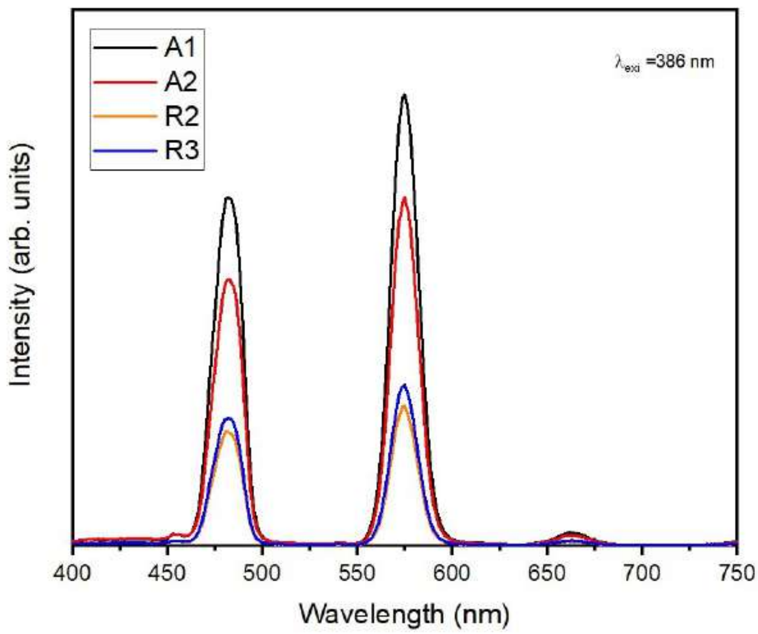

Fig.5B.4.Photoluminescence Spectra of Emission of CaAlBBaBaFNaFdy glasses

The emission spectrum ranges from 400-750 nm by monitoring excitation wavelength at 386 nm as shown in the fig.4. The two bands of emission consist of from the transitions $^4F_{9/2}\rightarrow^6H_{13/2}$ at 484 nm forms the blue (B) emission . Transition $^4F_{9/2}\rightarrow^6H_{13/2}$ at 575 nm forms the yellow(y) emission the transitions $^4F_{9/2}\rightarrow^6H_{13/2}$ is assigned to magnetic dipole (MD) and transitions $^4F_{9/2}\rightarrow^6H_{13/2}$ is assigned to electric dipole (ED) and also hypersensitive transitions **[11].**

Conclusions:

The glasses $23CaO+10Al_2O_3+(51\text{-}x)B_2O_3+6BaO/BaF_2+10NaF+xDy_2O_3$ Where x = 0.5, and 1.0 mol% were synthesised using melt-quench technique. In this work the effect of Dy_2O_3 with different concentrations on physical and optical properties in borate oxide and oxyfluoride glasses were investigated. The results show that density and molar volume tend to increase with increasing of Dy_2O_3 concentration. The absorption spectra of all glass sample reveal six intense bands at 754, 801, 898, 1,089, 1,269, and 1,676 nm were observed .The Judd-Ofelt analysis were performed and compared with other reported literatures. The excitation bands were identified at 325, 351, 364, 387, 425, 452, and 472 nm while the emission spectra exhibit three intense emission bands at 483 (blue), 575 (yellow) and 664 (red) nm. Radiative properties were evaluated and compared with oxide and oxyfluoride glasses values with other reported glasses. The Y/B values for the present have been evaluated with increasing in Dy^{3+} ions and brought the significance of Dy^{3+}- O^{2-} bond covalence. The CIE color coordinates (x,y) is found to be (0.3,0.4) for all glasses which was fall on white region. The obtained Dy^{3+} ions doped glasses can be applied as potential for the solid-state white lighting material applications.

References

[1] B. Munisudhakar, C. Nageswara Raju, M. Reddy Babu, A. Mohan Babu, L. Rama Moorthy and N. Manohar Reddy Investigation on structural and Luminescence Properties of $Dy3^{+}$-ions Doped Bismuth Borate Glasses for Optoelectronic devices International Journal of Advanced Scientific Research management, Vol 4. 2019.

[2] Joanna Pisarska, Lidia Zur, and Wojciech A. Pisarski Structural and Optical Characterization of Dy-doped heavy metal oxide and oxyhalide borate glasses phys. Status solidi, Vol 209 (2012) 1134-1140

[3] N. Luewarasirikul, H.J. kim, P. Meejitpaisan, J. Kaewkhao white light emission of Dysprosium doped lanthanum calcium phosphate oxide and oxyfluoride glasses optical materials Vol. 66 (2017) 599-566

[4] Jingxi An, Shuang Zhang, Ruiwang Liu, Guagnxu Hu, Zhiwei Zhang, YiyuQiu, Yanyan Zhou, Fanming Zeng, ZhongminSu Luminescent properties of $Dy3^{+}$ /$Eu3^{+}$ doped fluorescent glass for white LED based on oxyfluoride matrix journal of rare earths Vol. 39 Issue1, (2021), 26-32

[5] G. Sharma, R. Bagga, A. Cemmi, M. Falconieri, S. Baccaro spectroscopic investigation on γ-irradiated $Eu3^{+}$ and $Dy3^{+}$ oxyfluoride glasses radiation physics and chemistry vol. 108, 2015, 48-53

[6] S. Babu, V. Reddy prasad, D. Rajesh, Y.C. Ratnakaram, Luminescent properties of Dy^{3+} doped different fluoro-phosphate glasses for solid-state lighting applications journal of molecular structure 1080, 2015, 153-161

[7] S. Kaewjaeng, S. Kothan, W. Chiphaksa, N. Chantima, R. Rajaramakrishna, H. J. Kim, J. Kaewkhao, High transparency La_2O_3-CaO-B_2O_3-SiO_2 glass for diagnosis x-rays shielding material applications. Radiation Physics and Chemistry 160 (2019)41-47.

[8] V. Dimitrov, T. Lomatsu, An interpretation of optical properties of oxides and oxide glasses in terms of the electronic ion polarizability and average single bond strength. Journal of university of chemical technology andmetallurgy,453 (2010) 219-250.

[9] G. Lakshminarayana, Hucheng Yang, JianrongQiu, white light emission from Tm^{3+} / Dy^{3+} co-doped oxyfluoride germanate glasses under UV light excitation journal of solid state chemistry 182, 2009, 669-676

[10] Poonam, Shivani, Anu, A. Kumar, M. K. Sahu, P.R. Rani, Nisha Deopa, R. Punia, Judd-Ofelt Parameterization and Luminescence characterization of Dy^{3+} doped oxyfluoride Lithium zinc Borosilicate glasses for Lasers and w-LEDs journal of non-crystalline solids 544, 2020, 120-187

[11] C.S. Sarumaha, J. Rajagukguk , N. Wantana, N. Chanthima, R. Rajaramakrishna, and J. Kaewkhao white light emission of Dy^{3+}doped Oxy-fluoride phosphate glass system for active laser medium journal of integrated ferroelectrics vol. 224, 2022, 1-12

CHAPTER-6

CONCLUSION

The absorbance studies of 23CaO- 10Al_2O_3- (51-x) B_2O_3- 6BaO- 10Na2O- X$Nd_2O_3$where x=0.1,0.3,0.5 glass doped with various concentrations of Nd_2O_3 are evaluated using UV-VIS-NIR. Excitation of 582 nm was used as source to excite Nd^{3+} ions in CaAlBBaNaNd glass from $^4I_{9/2}$ ground state to $^4F_{3/2}$ excited state the peaks corresponding to $^4F_{3/2}$ to $^4I_{9/2}$ and $^4F_{3/2}$ to $^4I_{13/2}$ are absorbed at 1074 and 1341 nm respectively. Among two bands a transitions corresponds to $^4F_{3/2}$ to $^4I_{11/2}$ (1074nm) is a potential laser transitions having high intensity than the remaining transitions for all the prepared glasses. These glasses are potential for NIR emitting solid state device applications.

The absorbance studies of 23CaO- 10Al_2O_3- (51-x) B_2O_3- 6BaF_2-10Na_2O- XNd_2O_3 where x= 0.5 and 1.0 and 23CaO- 10Al_2O_3- (51-x) B_2O_3- 6BaO-10NaF- XNd_2O_3 where x= 0.5 and 23CaO- 10Al_2O_3- (51-x) B_2O_3- 6BaO-10NaF-XNd_2O_3 1.0 glasses doped with various concentrations of Nd_2O_3. The UV-VIS-NIR absorption spectrum of prepared glasses. Judd-Ofelt analysis were employed to evaluate the J-O parameters and fallows the trend $\Omega_2>\Omega_6>\Omega_4$ and $\Omega_4>\Omega_6>\Omega_2$. It was found that higher intensity peak 1.06 μm for higher fluorine content than the compare to oxygen content. It was also noted that the oxyfluoride glasses show higher stimulated emission cross section than compared to oxide glasses. The present glasses show quantum efficiency around 28 to 47% .The data clearly suggest that addition of higher fluorine content In the glasses are suitable for NIR solid state device applications.

Using the JO theory, spontaneous emission probabilities and radiative lifetimes of Dy^{3+} ions in title glasses are determined. It is found that 23CaO + $10Al_2O_3$ + (51x) B_2O_3 + 6BaO + $10Na_2O$ + xDy_2O_3 (where x = 0.1, 0.3, 0.5, 1.0) glass possess high emission cross-section and figure of merit. The high stimulated emission cross-section and branching ratio for the $^4F_{9/2}$ to $^6H_{13/2}$ transition can be useful for laser action in yellow region. Yellow-to-blue intensity ratios are varied with activator (Dy^{3+}) concentration. The yellowish white luminescence from the glasses consists of mainly 486 nm (blue) and 576 nm (yellow) emission bands. Chromaticity color coordinates are calculated and are found to be in the white-light region. The decay rates of the $^4F_{9/2}$ level of Dy^{3+} ions change from single exponential to non-exponential nature associated with decrease in lifetimes with increase in Dy^{3+} ion concentrations.

The glasses 23CaO+$10Al_2O_3$ + (51-x)B_2O_3+6BaO/BaF_2+10NaF+xDy_2O_3 Where x = 0.5, and 1.0 mol% were synthesised using melt-quench technique. In this work, the effect of Dy_2O_3 with different concentrations on physical and optical properties in borate oxide and oxy-fluoride glasses were investigated. The results show that the density and molar volume tend to increase with increasing of Dy_2O_3 concentration. The absorption spectra of all glass sample reveal six intense bands at 754, 801, 898, 1,089, 1,269, and 1,676 nm. Judd-Ofelt analysis were performed and compared with other reported literatures. The excitation bands were identified at 325, 351, 364, 387, 425, 452, and 472 nm while the emission spectra exhibit three intense emission bands at 483 (blue), 575 (yellow) and 664 (red) nm. The radiative properties were evaluated and compared with oxide and oxyfluoride glasses and also compared with other reported glasses. The Y/B values for the present have been evaluated with increasing in Dy^{3+} ions and brought the significance of Dy^{3+}- O^{2-}

bond covalence. The CIE color coordinates (x,y) is found to be (0.3, 0.4) for all glasses which was fall on white region. The obtained Dy^{3+} ions doped glasses can be applied as potential candidate for the solid-state white lighting material applications.

Scope of work

1. The glasses synthesized with Nd^{3+} doped borate glasses will be used for 1.06μm NIR solid state emitting material applications
2. The prepared Dy^{3+} glasses can be used for white light emitting (W-LED's) solid state device applications.

List of publication

1. Photoluminescence interaction of alkali fluoride over alkali oxide in Nd^{3+} doped glasses for NIR solid state device applications

   Basavaraj Gurav, Devidas G B., Ashok Dinkar, Shreekant Biradar, R. Rajaramkrishna

   Indian journal of science and technology Vol 16 Issue 3 (2023) 230-238 DOI: 10.17485/IJST/v16i3.2367

2. Neodymium doped Borate glasses for NIR-Emitting solid state device applications. Indian journal of science and technology

   Basavaraj Gurav, Devidas G B., Ashok Dinkar, Shreekant Biradar

   Indian journal of science and technology Vol 16 Issue 6 (2023) 435-441 DOI: 10.17485/IJST/v16i6.2295

3. Optical properties of Sm3+ doped in CaO-Al_2O_3-Na_2O-BaO-B_2O_3 glasses for under-sea optical device applications.

   Hebbar, Deepak, **Basavaraj Gurav**, J. Kaewkhao, N. Intachai, S. Kothan, and R. Rajaramakrishna.

   Optik 262(2022):169366. https://doi.org/10.1016/j.ijleo.2022.169366

4. Dy3+ ion doped borate glasses for solid state lighting WLED's applications. (2023) communicated. **Basavaraj Gurav**, Devidas G B., Ashok Dinkar, J. Kaewkhao, S Kothan, R. Rajaramakrishna

B. PAPERS PRESENTED IN NATIONAL / INTERNATIONAL CONFERENCES

1) **Poster presentation** on Effect of Dy_2O_3 composition on energy band gap in borate glasses in the two days national conference on "Impact of Chemistry and Biology to the society and Industry (ICBSI) held on 20th and 21st May 2022 at dept. of Industrial Chemistry, Kuvempu University, Shankarghatta, shimogga, Karnataka 577451

2) **Oral presentation** on "Neodymium doped Oxyfluoride glasses for solid-state device applications, National conference on science, technology and applications of Rare-Earth ions (STAR -2022) jointly organized by Rare Earth Association of India, and department of physics and chemistry, Sri Venkateshwara University, Tirupati, 517502 September 22-23(2022)

3) **Conference participated on** Optical properties of Sm^{3+} doped in CaO-Al_2O_3-Na_2O-BaO- B_2O_3 glasses of under -sea optical device applications conference on applied physics and material applications and applied magnetism and ferroelectrics **(ICAPMA-JMAG)** December 1st -4th 2021 **conference participated.**

INDIAN JOURNAL OF SCIENCE AND TECHNOLOGY

RESEARCH ARTICLE

Neodymium Doped Borate Glasses for NIR Emitting Solid State Device Applications

Basavaraj Gurav[1], **G B Devidas**[1]*, **Ashok Dinkar**[1], **Shrikant Biradar**[1]

1 Department Of Physics, Jnana Sahyadri, Kuvempu University, Shankarghatta, Shimoga, 577451, India

OPEN ACCESS

Received: 30-11-2022

Accepted: 17-01-2023

Published: 15-02-2023

Citation: Gurav B, Devidas GB, Dinkar A, Biradar S (2023) Neodymium Doped Borate Glasses for NIR Emitting Solid State Device Applications. Indian Journal of Science and Technology 16(6): 435-441. https://doi.org/10.17485/IJST/v16i6.2295

* **Corresponding author**.

devidasgb02@gmail.com

Funding: None

Competing Interests: None

Published By Indian Society for Education and Environment (iSee)

ISSN
Print: 0974-6846
Electronic: 0974-5645

Abstract

Objectives: To investigate the effect of B_2O_3 replaced by Nd_2O_3 studies on the spectroscopic characteristics of trivalent neodymium (Nd^{3+})-doped glasses using XRD, FTIR, absorption, and emission spectroscopy. **Methods:** The glasses were synthesized using the conventional melt quenching technique at 1150^0 C. The amorphous nature of the samples was confirmed by x-ray diffraction studies. **Findings:** The addition of Nd_2O_3 concentration affects the absorption and emission properties of the Nd^{3+} ion measured in the near-infrared luminescence range from 0.9μm, 1.06 μm, and 1.36μm associated with the $^4F_{3/2}\rightarrow{}^4I_J$ (J = 9/2, 11/2, 13/2) transitions. **Novelty:** The novelty of the present work is to fully understand and characterize the luminescence of Nd^{3+} doped borate bulk glasses with different doping concentrations. So as to gain an insight of 1.06 μm corresponding to $^4F_{3/2}\rightarrow{}^4F_{11/2}$ transition, these glasses are highly potential one which is an applicable to NIR emitting solid state device.

Keywords: Nd3+ ions; FTIR; UV; Photoluminescence; Borate glasses

1 Introduction

Glasses are the most advanced material in terms of technology and are utilized in a wide range of applications. They are notable for being optically transparent and brittle. Due to their wide range of prospective uses and applications in the design and development of photonic devices, the rare-earth (RE) doped glass materials have attracted a lot of attention [1,2].

Due to their high transparency, low melting point, great thermal stability, and potent solubilities in rare earth ions, borate-based glass hosts have been demonstrated to be capable of lasing in the NIR range. A particularly good optical medium are borate glasses [3]. The addition of alkaline element improves the chemical stability by modifying the glass network due to their charge transfer with the neighbor host element [4].

Optical material activated by Nd^{3+} ions are very interesting for emitting devices. Especially Nd^{3+} ions are very attractive active media for powerful solid-state laser working in the NIR spectral region [5]. Dinesh Kumar et.al (2019) had studied Nd^{3+} doped sodium strontium borate glasses their results shows that their prepared glasses are suitable for thermoluminescence device materials [6].

INDIAN JOURNAL OF SCIENCE AND TECHNOLOGY

RESEARCH ARTICLE

OPEN ACCESS

Received: 08-12-2022

Accepted: 22-12-2022

Published: 24-01-2023

Citation: Gurav B, Devidas GB, Dinkar A, Biradar S, Rajaramakrishna R (2023) Photoluminescence Interaction of Alkali Fluoride Over Alkali Oxide in Nd^{3+} Doped Glasses for NIR Applications . Indian Journal of Science and Technology 16(3): 230-238. https://doi.org/10.17485/IJST/v16i3.2367

* **Corresponding author**.

devidasgb02@gmail.com

Funding: None

Competing Interests: None

Published By Indian Society for Education and Environment (iSee)

ISSN
Print: 0974-6846
Electronic: 0974-5645

Photoluminescence Interaction of Alkali Fluoride Over Alkali Oxide in Nd^{3+} Doped Glasses for NIR Applications

Basavaraj Gurav[1], G B Devidas[1]*, Ashok Dinkar[1], Shrikant Biradar[1], R Rajaramakrishna[2,3]

1 Department of Physics, Jnana Sahyadri, Kuvempu University, Shankarghatta, Shimoga, 577451, Karnataka, India
2 Center of Excellence in Glass Technology and Materials Science (CEGM), Nakhon Pathom Rajabhat University, 73000, Nakhon Pathom, Thailand
3 Department of Post Graduate Studies and Research in Physics, The National College, Jayanagar, Bengaluru, 560070, Karnataka, India

Abstract

Background/Objectives: $23CaO + 10Al_2O_3 + (51 - x)B_2O_3 + 6BaF_2 + 10Na_2O + xNd_2O_3$ glasses were designed for understanding the optical properties of the emission, such as absorption, lifetime, and quantum efficiencies (QEs) of the glasses. **Methods:** The glasses were synthesized using the conventional melt-quenching technique at 1150^{0}C. The amorphous nature of the samples was confirmed by x-ray diffraction studies. **Findings:** The radiative QE (η) obtained from the radiative lifetime by Judd-Ofelt analysis, as well as directly measured lifetime using a 582 nm were measured and compared with other reported literature. **Novelty:** The present work focuses on the replacement of fluorine ions to their alkali content and studied their stimulated emission cross section. The stimulated emission cross-section shows σ_{emi}=25.3x10^{-21}cm^2 and σ_{emi}=18.5x10^{-21}cm^2 for oxide (R1) and oxy-fluoride glasses (F2) with 0.5mol% Nd_20_3 content respectively. The stimulated emission cross section σ_{emi}=29.9x10^{-21}cm^2 and σ_{emi}=32.5x10^{-21}cm^2 for oxide (F1) and oxy-fluoride (A3) glasses with 1.0mol% Nd_20_3 content respectively. The data clearly suggests that addition of higher fluorine content in the glasses are suitable for NIR solid state device applications.

Keywords: Nd 3+ ions; JOtheory; Radiative properties; photoluminescence; Borate glass

1 Introduction

The use of Nd^{3+} glasses in the realm of technology has increased especially for applications involving photonic and solid-state devices. For lasers, amplifiers, etc., rare-earth ions-doped glass is more appropriate. Among all the rare-earth ions, Nd^{3+} finds in the field of infrared

KUVEMPU UNIVERSITY

"SYNTHESIS AND CHARACTERIZATION OF CERTAIN OXIDE AND OXYFLUORIDE GLASSES DOPED WITH RARE-EARTH IONS"

A Thesis Submitted to the Kuvempu University for the award of degree of

DOCTOR OF PHILOSOPHY

IN

PHYSICS

By

Mr. Basavaraj Gurav. M.Sc.,

Research Guide

Dr. Devidas G B.
M.Sc., M.Phil. Ph.D.
Associate Professor
Department of PG Studies and Research in Physics,
Kuvempu University

Department of PG Studies and Research in Physics,
Kuvempu University,
Jnana Sahyadri, Shankarghatta, - 577451,
Shivamogga District, Karnataka, INDIA.

2023

CHAPTER-6

CONCLUSION

The absorbance studies of 23CaO- 10Al_2O_3- (51-x) B_2O_3- 6BaO- 10Na2O- X$Nd_2O_3$where x=0.1,0.3,0.5 glass doped with various concentrations of Nd_2O_3 are evaluated using UV-VIS-NIR. Excitation of 582 nm was used as source to excite Nd^{3+} ions in CaAlBBaNaNd glass from $^4I_{9/2}$ ground state to $^4F_{3/2}$ excited state the peaks corresponding to $^4F_{3/2}$ to $^4I_{9/2}$ and $^4F_{3/2}$ to $^4I_{13/2}$ are absorbed at 1074 and 1341 nm respectively. Among two bands a transitions corresponds to $^4F_{3/2}$ to $^4I_{11/2}$ (1074nm) is a potential laser transitions having high intensity than the remaining transitions for all the prepared glasses. These glasses are potential for NIR emitting solid state device applications.

The absorbance studies of 23CaO- 10Al_2O_3- (51-x) B_2O_3- 6BaF_2-10Na_2O-XNd_2O_3 where x= 0.5 and 1.0 and 23CaO- 10Al_2O_3- (51-x) B_2O_3- 6BaO-10NaF-XNd_2O_3 where x= 0.5 and 23CaO- 10Al_2O_3- (51-x) B_2O_3- 6BaO-10NaF-XNd_2O_3 1.0 glasses doped with various concentrations of Nd_2O_3. The UV-VIS-NIR absorption spectrum of prepared glasses. Judd-Ofelt analysis were employed to evaluate the J-O parameters and fallows the trend $\Omega_2>\Omega_6>\Omega_4$ and $\Omega_4>\Omega_6>\Omega_2$. It was found that higher intensity peak 1.06 μm for higher fluorine content than the compare to oxygen content. It was also noted that the oxyfluoride glasses show higher stimulated emission cross section than compared to oxide glasses. The present glasses show quantum efficiency around 28 to 47% .The data clearly suggest that addition of higher fluorine content In the glasses are suitable for NIR solid state device applications.

Using the JO theory, spontaneous emission probabilities and radiative lifetimes of Dy^{3+} ions in title glasses are determined. It is found that 23CaO + $10Al_2O_3$ + (51x) B_2O_3 + 6BaO + $10Na_2O$ + xDy_2O_3 (where x = 0.1, 0.3, 0.5, 1.0) glass possess high emission cross-section and figure of merit. The high stimulated emission cross-section and branching ratio for the $^4F_{9/2}$ to $^6H_{13/2}$ transition can be useful for laser action in yellow region. Yellow-to-blue intensity ratios are varied with activator (Dy^{3+}) concentration. The yellowish white luminescence from the glasses consists of mainly 486 nm (blue) and 576 nm (yellow) emission bands. Chromaticity color coordinates are calculated and are found to be in the white-light region. The decay rates of the $^4F_{9/2}$ level of Dy^{3+} ions change from single exponential to non-exponential nature associated with decrease in lifetimes with increase in Dy^{3+} ion concentrations.

The glasses 23CaO+$10Al_2O_3$ + (51-x)B_2O_3+6BaO/BaF_2+10NaF+xDy_2O_3 Where x = 0.5, and 1.0 mol% were synthesised using melt-quench technique. In this work, the effect of Dy_2O_3 with different concentrations on physical and optical properties in borate oxide and oxy-fluoride glasses were investigated. The results show that the density and molar volume tend to increase with increasing of Dy_2O_3 concentration. The absorption spectra of all glass sample reveal six intense bands at 754, 801, 898, 1,089, 1,269, and 1,676 nm. Judd-Ofelt analysis were performed and compared with other reported literatures. The excitation bands were identified at 325, 351, 364, 387, 425, 452, and 472 nm while the emission spectra exhibit three intense emission bands at 483 (blue), 575 (yellow) and 664 (red) nm. The radiative properties were evaluated and compared with oxide and oxyfluoride glasses and also compared with other reported glasses. The Y/B values for the present have been evaluated with increasing in Dy^{3+} ions and brought the significance of Dy^{3+}- O^{2-}

bond covalence. The CIE color coordinates (x,y) is found to be (0.3, 0.4) for all glasses which was fall on white region. The obtained Dy^{3+} ions doped glasses can be applied as potential candidate for the solid-state white lighting material applications.

Scope of work

1. The glasses synthesized with Nd^{3+} doped borate glasses will be used for 1.06µm NIR solid state emitting material applications
2. The prepared Dy^{3+} glasses can be used for white light emitting (W-LED's) solid state device applications.